1

Aircraft Engines – A Review

1.1 Introduction

A brief review of aircraft gas turbine propulsion is presented in Chapter 1. Most topics are fundamental to undergraduate propulsion education and thus serve as a refresher before we embark on more advanced propulsion concepts. *Aircraft Propulsion, 2nd edition,* by the author, provides the bulk of the material presented in this review chapter.

1.2 Aerothermodynamics of Working Fluid

In gas turbine (GT) engines the working fluid is treated as perfect gas, often air, which behaves as *continuum* rather than individual molecules. The density of the gas, ρ, is a fluid property that is defined on the basis of continuum. The perfect gas law that relates the pressure, density, and the absolute temperature of the gas may be derived rigorously from the kinetic theory of gases. It is stated here without proof:

$$p = \rho RT \tag{1.1}$$

Where R is known as the *gas constant*, which is inversely proportional to the molecular mass of the gas, i.e.

$$R \equiv \frac{\overline{R}}{MW} \tag{1.2a}$$

where $\overline{R}$ is the *universal gas constant* expressed in two systems of units:

$$\overline{R} = 8{,}314 \frac{J}{kmol.K} \quad \text{or} \quad \overline{R} = 4.97\,x10^4 \frac{ft.lbf}{slug.mol.^{\circ}R} \tag{1.2b}$$

The thermodynamic relations for a perfect gas in terms of specific heats at constant pressure and volume are:

$$dh \equiv c_p dT \tag{1.3}$$

$$de \equiv c_v dT \tag{1.4}$$

Future Propulsion Systems and Energy Sources in Sustainable Aviation, First Edition. Saeed Farokhi.

Companion website: www.wiley.com/go/farokhi/power

In aircraft engines, the specific heats at constant pressure and volume are often functions of gas temperature only:

$$c_p = c_p(T) \quad \text{and} \quad c_v = c_v(T) \tag{1.5}$$

The gas is then called *thermally perfect* gas. There is a simplifying assumption of constant specific heats, which is a valid approximation to gas behavior in a narrow temperature range. In this case,

$$c_p = \text{Constant} \quad \text{and} \quad c_v = \text{Constant} \tag{1.6}$$

The gas is referred to as *calorically perfect* gas.

The first law of thermodynamics is the statement of conservation of energy for a system of fixed mass, m, namely,

$$\delta q = de + \delta w \tag{1.7}$$

where the element of heat transferred to the system from the surrounding is considered positive and on a per-unit-mass basis is δq with a unit of energy/mass, e.g. $\mathrm{J\,kg^{-1}}$. The element of work done by the gas on the surrounding is considered positive and per-unit-mass of the gas is depicted by δw. The net energy interaction with the system results in a change of energy of the system, which again on a per-unit-mass basis is referred to as de. The three terms of the first law of thermodynamics have dimensions of energy per mass, e.g. $\mathrm{J\,kg^{-1}}$. The elemental heat and work exchange are shown by delta, δ, instead of an exact differential, d, as in de. This is in recognition of *path dependent* nature of heat and work exchange.

The application of the first law to a closed cycle is of importance to engineering and represents a balance between the heat and work exchange in a cyclic process, i.e.

$$\oint \delta q = \oint \delta w \tag{1.8}$$

Also, for an adiabatic process, i.e. $\delta q = 0$ with no mechanical exchange of work, i.e. $\delta w = 0$ the energy of a system remains constant, namely $e_1 = e_2 =$ constant. We shall use this principle in conjunction with a control volume approach in the study of aircraft engine inlets and exhaust systems.

The second law of thermodynamics introduces the absolute temperature scale and a new thermodynamic property, s, the entropy. It is in fact a statement of impossibility of a heat engine exchanging heat with a single reservoir and producing mechanical work continuously. It calls for a second reservoir at a lower temperature where heat is rejected by the heat engine. In this sense, the second law of thermodynamics distinguishes between heat and work. It asserts that all mechanical work may be converted into system energy, whereas not all heat transfer to a system may be converted into system energy continuously. A corollary to the second law incorporates the new thermodynamic property, s, and the absolute temperature, T, into an inequality, known as the Clausius inequality,

$$T ds \geq \delta q \tag{1.9}$$

where the equal sign holds for a *reversible* process. The concept of irreversibility ties in closely with frictional losses, viscous dissipation and the appearance of shock waves in supersonic flow. The pressure forces within the fluid perform reversible work and the viscous stresses account for dissipated energy of the system (into heat). Hence, the reversible work done by a system per unit mass is the work done by pressure

$$\delta w_{rev.} = p dv \tag{1.10}$$

where v is the specific volume, which is the inverse of fluid density, ρ. A combined first and second law of thermodynamics is known as the *Gibbs equation*, which relates fluid property, entropy, to other thermodynamic properties, namely

$$Tds = de + pdv \tag{1.11}$$

Although it appears that we have substituted the reversible forms of heat and work into the first law to obtain the Gibbs equation, it is applicable to irreversible processes as well (see Farokhi 2014). We introduce a derived thermodynamic property known as *enthalpy*, h, as

$$h \equiv e + pv \tag{1.12}$$

This derived property, i.e. h, combines two forms of fluid energy, namely internal energy (or thermal energy) and what is known as the flow work, pv, or the pressure work. The other forms of energy such as kinetic energy and potential energy are still unaccounted by the enthalpy, h. We shall account for the other forms of energy by a new variable called the *total enthalpy* in Section 1.2.7.

We take the differential of Eq. (1.12) and substitute it in the Gibbs equation, to get:

$$Tds = dh - vdp \tag{1.13}$$

By expressing enthalpy in terms of specific heat at constant pressure, via Eq. (1.3), and dividing both sides of Eq. (1.13) by temperature, T, we get:

$$ds = c_p \frac{dT}{T} - \frac{v}{T}dp = c_p \frac{dT}{T} - R\frac{dp}{p} \tag{1.14}$$

We incorporated the perfect gas law in the last term of Eq. (1.14). We may now integrate this equation between states 1 and 2, in a perfect gas, to arrive at:

$$s_2 - s_1 \equiv \Delta s = \int_1^2 c_p \frac{dT}{T} - R\ln\frac{p_2}{p_1} \tag{1.15}$$

An assumption of calorically perfect gas (i.e. c_p = constant) will enable us to integrate the first term on the right-hand side of Eq. (1.15):

$$\Delta s = c_p \ln\frac{T_2}{T_1} - R\ln\frac{p_2}{p_1} \tag{1.16}$$

Otherwise, we need to use a tabulated thermodynamic function, ϕ, defined as:

$$\int_1^2 c_p \frac{dT}{T} \equiv \phi_2 - \phi_1 \tag{1.17}$$

From the definition of enthalpy, let us replace the flow work, pv, term by its equivalent from the perfect gas law, i.e. RT, and then take the differential of the equation as

$$dh \equiv c_p dT = de + RdT = c_v dT + RdT \tag{1.18}$$

Dividing through by the temperature differential, dT, we get

$$c_p = c_v + R \quad \text{Or} \quad \frac{c_p}{R} = \frac{c_v}{R} + 1 \tag{1.19}$$

This provides valuable relations among the gas constant and the specific heats at constant pressure and volume. The ratio of specific heats is given a special symbol, γ, due to its frequency of appearance in compressible flow analysis, i.e.

$$\gamma \equiv \frac{c_p}{c_v} = \frac{c_v + R}{c_v} = 1 + \frac{1}{c_v / R} \tag{1.20}$$

In terms of the ratio of specific heats, γ, and R, we express c_p and c_v as

$$c_p = \frac{\gamma}{\gamma - 1} R \quad \text{and} \quad c_v = \frac{1}{\gamma - 1} R \tag{1.21}$$

The ratio of specific heats is related to the degrees of freedom of the gas molecules, n, via

$$\gamma = \frac{n+2}{n} \tag{1.22}$$

The degrees of freedom of a molecule are represented by the sum of the energy states that a molecule possesses. For example, atoms or molecules possess kinetic energy in three spatial directions. If they rotate as well, they have kinetic energy associated with their rotation. In a molecule, the atoms may vibrate with respect to each other, which then create kinetic energy of vibration as well as the potential energy of intermolecular forces. Finally, the electrons in an atom or molecule are described by their own energy levels (both kinetic energy and potential) that depend on their position around the nucleus. As the temperature of the gas increases, the successively higher *energy states* are excited; thus, the degrees of freedom increases. A monatomic gas, which may be modeled as a sphere, has at least three degrees of freedom, which represent translational motion in three spatial directions. Hence, for a monatomic gas, under "normal" temperatures, the ratio of specific heats is

$$\gamma = \frac{5}{3} \cong 1.667 \quad \text{Monatomic gas at "normal" temperatures} \tag{1.23}$$

A monatomic gas has negligible rotational energy about the axes that pass through the atom due to its negligible moment of inertia. A monatomic gas will not experience a vibrational energy, as vibrational mode requires at least two atoms. At higher temperatures the electronic energy state of the gas is affected, which eventually leads to ionization of the gas.

For a diatomic gas, which may be modeled as a dumbbell, there are five degrees of freedom, under "normal" temperature conditions, three of which are in translational motion and two are in rotational direction. The third rotational motion along the intermolecular axis of the dumbbell is negligibly small. Hence, for a diatomic gas such as air (near room temperature), hydrogen, nitrogen etc., the ratio of specific heats is

$$\gamma = \frac{7}{5} = 1.4 \quad \text{Diatomic gas at "normal" temperatures} \tag{1.24a}$$

At high temperatures, molecular vibrational modes and the excitation of electrons add to the degrees of freedom and that lowers γ. For example, at ~600 K (i.e. typical of HPC, high-pressure compressor, environment in a GT engine) vibrational modes in air are excited; thus, the degrees of freedom of diatomic gases are initially increased by one, i.e. it becomes 5 + 1 = 6, when the vibrational mode is excited. Therefore, the ratio of specific heats for diatomic gases at elevated temperatures becomes:

$$\gamma = \frac{8}{6} \approx 1.33 \quad \text{Diatomic gas at elevated temperatures} \tag{1.24b}$$

The vibrational mode represents two energy states corresponding to the kinetic energy of vibration and the potential energy associated with the intermolecular forces. When fully excited, the vibrational mode in a diatomic gas, such as air, adds two to the degrees of freedom; namely, it becomes 7. Therefore the ratio of specific heats becomes

$$\gamma = \frac{9}{7} \approx 1.29 \quad \text{Diatomic gas at higher temperatures} \tag{1.24c}$$

For example, air at 2000 K has its translational, rotational, and vibrational energy states fully excited. This temperature level describes the combustor, turbine, or afterburner environment. Gases with a more complex structure than a diatomic gas have higher degrees of freedom and thus their ratio of specific heats is less than 1.4. Figure 1.1 (from Anderson 2003) shows the behavior of a diatomic gas from 0 to 2000 K. The nearly constant specific heat ratio in 3–600 K range represents the calorically perfect gas behavior of a diatomic gas such as air with $\gamma = 1.4$. Note that near absolute zero (0 K), $c_v/R \rightarrow 3/2$, therefore, a diatomic gas ceases to rotate and thus behaves like a monatomic gas, i.e. it exhibits the same degrees of freedom as a monatomic gas, i.e. $n = 3$, $\gamma = 5/3$.

The composition of *dry air* at normal temperatures is often approximated as the mixture of two diatomic gasses, i.e. 21% O_2 and 79% N_2, by volume. However, this description applies to zero humidity. Water vapor, i.e. $H_2O_{(g)}$, a triatomic gas, is present in humid air, with the subsequent change in mixture properties, molecular weight, c_p, c_v,

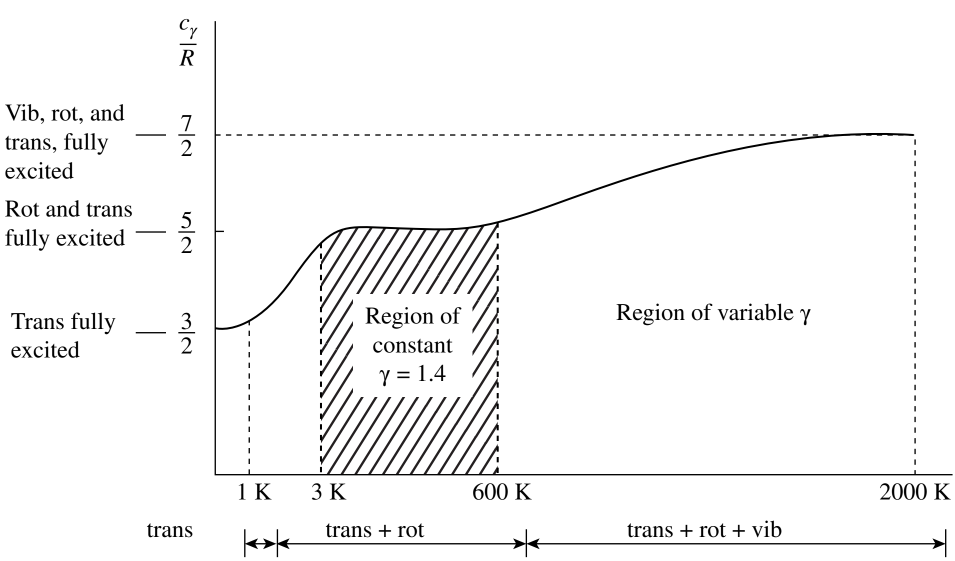

Figure 1.1 Temperature dependence of specific heats for a diatomic gas. *Source:* From Anderson 2003.

and γ. Also, air at elevated temperatures may dissociate to form oxygen and nitrogen atoms and other products such as O, OH, NO_2, N_2O, among others.

1.2.1 Isentropic Process and Isentropic Flow

For a reversible, adiabatic process, entropy remains constant, hence the designation: *isentropic process*. The Gibbs equation then may be used to relate the pressure and temperature ratios by an isentropic exponent, namely

$$\frac{p_2}{p_1} = \left(\frac{T_2}{T_1}\right)^{\frac{c_p}{R}} = \left(\frac{T_2}{T_1}\right)^{\frac{\gamma}{\gamma-1}} \quad \left[\text{Calorically perfect gas}\right] \tag{1.25}$$

Now, using the perfect gas law by replacing the temperature ratio by pressure and density ratios in Eq. (1.25) and simplifying the exponents, we get:

$$\frac{p_2}{p_1} = \left(\frac{\rho_2}{\rho_1}\right)^{\gamma} \quad \left[\text{Calorically perfect gas}\right] \tag{1.26}$$

1.2.2 Conservation of Mass

One of the pillars of the *great conservation laws* (the term coined by Richard Feynman) in Newtonian mechanics is the conservation of mass. The integral form is derived in elementary fluids/propulsion books (e.g. see Farokhi 2014) and is repeated here for reference:

$$\oiiint_{C.V.} \frac{\partial \rho}{\partial t} dV + \oiint_{C.S.} \rho \vec{V}.\hat{n} dS = 0 \tag{1.27}$$

$\vec{V}$ is the local fluid velocity vector, dV is the element of volume in the volume integral, dS is the element of surface in the surface integral and $\hat{n}$ is the unit vector normal to the control surface and pointing out. The integrals in Eq. (1.27) are thus performed over the control volume (C.V.) and the control surface (C.S.). The first integral represents the mass accumulation/depletion with time within the control volume. For steady flows (i.e. when $\frac{\partial}{\partial t} \to 0$), the first integral vanishes. The second integral represents the net mass flux through the control surface, surrounding the control volume. For steady flows, the second integral suggests that the mass flow rate into a control volume is balanced by the same mass flow rate out of the control volume. We can write the law of conservation of mass as the *continuity equation* as:

$$\dot{m}_{\text{out}} = \dot{m}_{\text{in}} \tag{1.28}$$

For steady uniform flows, the continuity equation may be integrated and written as:

$$\sum(\rho VA)_{\text{out}} = \sum(\rho VA)_{\text{in}} \tag{1.29}$$

where the summation is performed over all the "inlets" and "exits" of the control surface, e.g. in an aircraft engine, we have air and fuel inlets and one or more nozzle exits.

1.2.3 Conservation of Linear Momentum

Newton's secondnd law of motion, in vector form, written for a control volume is:

$$\oiiint_{C.V.} \frac{\partial}{\partial t}\left(\rho \vec{V}\right) dV + \oiint_{C.S.} \rho \vec{V}\left(\vec{V}.\hat{n}\right) dS = \vec{F}_{\text{net}} \tag{1.30}$$

Here, $\vec{F}_{\text{net}}$ represents the net external forces acting on the fluid. These external forces are divided into *body forces* that acts over the fluid volume and the *surface forces* that act on the surface. Gravitational force or electromagnetic force are examples of the body force and the pressure and shear are the examples of the surface force. The first integral in Eq. (1.30) measures the unsteady momentum within the control volume and vanishes identically for a *steady flow*. The second integral is the net flux of momentum in and out of the control surface. Assuming uniform flow at the boundaries of the control surface inlets and outlets, we may simplify the momentum equation to a very useful engineering form, namely

$$\left(\dot{m}\vec{V}\right)_{\text{out}} - \left(\dot{m}\vec{V}\right)_{\text{in}} = \vec{F}_{\text{net}} \tag{1.31}$$

Since Eq. (1.34) is a vector equation, it is satisfied at the component level, namely:

$$\left(\dot{m}V_x\right)_{\text{out}} - \left(\dot{m}V_x\right)_{\text{in}} = F_{\text{net},x} \tag{1.32a}$$

$$\left(\dot{m}V_y\right)_{\text{out}} - \left(\dot{m}V_y\right)_{\text{in}} = F_{\text{net},y} \tag{1.32b}$$

$$\left(\dot{m}V_z\right)_{\text{out}} - \left(\dot{m}V_z\right)_{\text{in}} = F_{\text{net},z} \tag{1.32c}$$

In cylindrical coordinates (r, θ, z), we may write the momentum equation as:

$$\left(\dot{m}V_r\right)_{\text{out}} - \left(\dot{m}V_r\right)_{\text{in}} = F_{\text{net},r} \tag{1.33a}$$

$$\left(\dot{m}V_\theta\right)_{\text{out}} - \left(\dot{m}V_\theta\right)_{\text{in}} = F_{\text{net},\theta} \tag{1.33b}$$

$$\left(\dot{m}V_z\right)_{\text{out}} - \left(\dot{m}V_z\right)_{\text{in}} = F_{\text{net},z} \tag{1.33c}$$

Note that the cylindrical coordinate system best suits the turbomachinery environment and is thus of particular interest in gas turbine propulsion.

1.2.4 Conservation of Angular Momentum

By taking the moment of Newton's second law of motion (Eq. (1.30)) about an arbitrary point O in the fluid, we arrive at the law of conservation of angular momentum about the point O (in vector form), according to

$$\oiiint_{C.V.} \frac{\partial}{\partial t}\left(\rho \vec{V} x \vec{r}\right) dV + \oiint_{C.S.} \rho \vec{V} x \vec{r}\left(\vec{V}.\hat{n}\right) dS = \vec{F}_{\text{net}} x \vec{r} \tag{1.34}$$

In turbomachinery, the fluid angular momentum undergoes a change interacting with the rotating (rotor) and stationary (stator) blade rows. The arbitrary point O is on the axis of turbomachinery. In cylindrical coordinates [r, θ, z], the angular momentum equation for *uniform steady flows* is simplified to:

$$\left(\dot{m}rV_\theta\right)_{\text{out}} - \left(\dot{m}rV_\theta\right)_{\text{in}} = rF_{\text{net},\theta} \tag{1.35}$$

More discussions are included in the compressor section.

1.2.5 Conservation of Energy

The law of conservation of energy for a control volume starts with the first law of thermodynamics written for a system. On a per unit time basis, we get the *rate* of energy transfer to the fluid, namely:

$$\dot{Q} = \frac{dE}{dt} + \dot{W} \tag{1.36}$$

where the Eq. (1.36) is written for the entire mass of the system. The energy E is now represented by the internal energy, e, times mass, as well as the kinetic energy of the gas in the system and the potential energy of the system. Internal energy, e, is a fluid property that is revealed through the first law of thermodynamics. The contribution of potential energy change in gas turbine engines or most other aerodynamic applications is negligibly small and often ignored. We write the energy term, dE/dt, in Eq. (1.36) as the mass integral of specific energy, e, over the volume of the system, and apply *Leibnitz's rule of integration* to get the control volume version, namely,

$$\frac{dE}{dt} = \frac{d}{dt}\oiiint_{V(t)} \rho\left(e + \frac{V^2}{2}\right)dV = \oiiint_{C.V.} \frac{\partial}{\partial t}\left[\rho\left(e + \frac{V^2}{2}\right)\right]dV + \oiint_{C.S.} \rho\left(e + \frac{V^2}{2}\right)\vec{V}.\hat{n}dS \tag{1.37}$$

The first term on the right-hand side (RHS) of Eq. (1.37) is the time rate of change of energy within the control volume, which identically vanishes for a steady flow. The second integral represents the net flux of fluid power (i.e. the *rate* of energy) crossing the boundaries of the control surface. The rates of heat transfer to the control volume and the rate of mechanical energy transfer by the gases inside the control volume on the surrounding are represented by $\dot{Q}$ and $\dot{W}$ terms in the energy Eq. (1.37). Now, let us examine the forces at the boundary that contribute to the rate of energy transfer. These surface forces are due to pressure and shear acting on the boundary, as noted earlier. The pressure forces act normal to the boundary and point inward, i.e. opposite to the convention on $\hat{n}$,

$$-p\hat{n}dS \tag{1.38}$$

To calculate the rate of work done by a force, we take the scalar product of the force and the velocity vector, namely

$$-p\vec{V}.\hat{n}dS \tag{1.39}$$

Now, we need to sum this elemental rate of energy transfer by pressure forces over the surface, via a closed surface integral, i.e.

$$\oiint_{C.S.} -p\vec{V}.\hat{n}dS \tag{1.40}$$

Since the convention on the rate of work done in the first law is positive when it is performed "on" the surroundings, and Eq. (1.40) represents the rate of work done "by" the surroundings on the control volume, we need to incorporate an additional negative factor for this term in the energy equation. The rate of energy transfer by the shear forces is divided into a shaft power, $\wp_s$ that crosses the control surface in the form of shaft torque (due to moment of shear stresses in a rotating shaft) multiplied by the shaft angular speed and the viscous shear stresses on the boundary of the control volume. Hence,

$$\dot{W} = \oint\!\!\oint_{C.S.} p\vec{V}.\hat{n}dS + \wp_s + \dot{W}_{\text{viscous-shear}} \tag{1.41}$$

We arrive at a useful form of the energy equation for a control volume when we combine Eq. (1.41) with Eqs. (1.37) and (1.36), i.e.

$$\oint\!\!\oint\!\!\oint_{C.V.} \frac{\partial}{\partial t}\left[\rho\left(e+\frac{V^2}{2}\right)\right]dV + \oint\!\!\oint_{C.S.} \rho\left(e+\frac{V^2}{2}\right)\vec{V}.\hat{n}dS + \oint\!\!\oint_{C.S.} p\vec{V}.\hat{n}dS = \dot{Q} - \wp_s - \dot{W}_{\text{visc}} \tag{1.42}$$

The closed surface integrals on the LHS may be combined and simplified to:

$$\oint\!\!\oint\!\!\oint_{C.V.} \frac{\partial}{\partial t}\left[\rho\left(e+\frac{V^2}{2}\right)\right]dV + \oint\!\!\oint_{C.S.} \rho\left(e+\frac{V^2}{2}+\frac{p}{\rho}\right)\vec{V}.\hat{n}dS = \dot{Q} - \wp_s - \dot{W}_{visc} \tag{1.43}$$

We may replace the internal energy and the flow work terms in Eq. (1.43) by enthalpy, *h*, and define the sum of the enthalpy and the kinetic energy as the total or stagnation enthalpy, to get:

$$\oint\!\!\oint\!\!\oint_{C.V.} \frac{\partial}{\partial t}\left[\rho\left(e+\frac{V^2}{2}\right)\right]dV + \oint\!\!\oint_{C.S.} \rho h_t\vec{V}.\hat{n}dS = \dot{Q} - \wp_s - \dot{W}_{\text{visc.}} \tag{1.44}$$

Where the *total or stagnation enthalpy*, h_t, is defined as:

$$h_t \equiv h + \frac{V^2}{2} \tag{1.45}$$

In *steady flows* the volume integral that involves a time derivative vanishes. The second integral represents the net flux of fluid power across the control volume. The terms on the RHS are the external energy interaction terms, which serve as the *drivers* of the energy flow through the control volume. In adiabatic flows, the rate of heat transfer through the walls of the control volume vanishes. In the absence of shaft work, as in inlets and nozzles of a jet engine, the second term on the RHS of Eq. (1.44) vanishes. The rate of energy transfer via the viscous shear stresses is zero on solid boundaries (since velocity on solid walls obeys the no slip boundary condition) and nonzero at the inlet and exit planes. The contribution of this term over the inlet and exit planes is, however, small compared to the net energy flow in the fluid, hence neglected.

The integrated form of the energy equation for a control volume, assuming uniform flow over the inlets and outlets, yields a practical solution for quick engineering calculations,

$$\sum\left(\dot{m}h_t\right)_{\text{out}} - \sum\left(\dot{m}h_t\right)_{\text{in}} = \dot{Q} - \wp_s \tag{1.46}$$

The summations in Eq. (1.46) account for multiple inlets and outlets of a general control volume. In flows that are adiabatic and involve no shaft work, the energy equation simplifies to:

$$\sum\left(\dot{m}h_t\right)_{\text{out}} = \sum\left(\dot{m}h_t\right)_{\text{in}} \tag{1.47}$$

For a single inlet and a single outlet the energy equation is even further simplified, as the mass flow rate also cancels out in Eq. (1.47), to yield:

$$h_{t\text{-exit}} = h_{t\text{-inlet}} \tag{1.48}$$

Total or stagnation enthalpy then remains constant for adiabatic flows that involve no shaft power, such as inlets and nozzles or across shock waves.

1.2.6 Speed of Sound and Mach Number

Sound waves are infinitesimal pressure waves propagating in a medium. The propagation of sound waves, or acoustic waves, is *reversible and adiabatic*, hence *isentropic*. Since sound propagates through collision of fluid molecules, the speed of sound is higher in liquids than gas. Written for a gas, speed of sound, a, is related to pressure, density via

$$a^2 = \frac{dp}{d\rho} = \left(\frac{\partial p}{\partial \rho}\right)_s \tag{1.49}$$

In a perfect gas, Eq. (1.49) may be written as:

$$a = \sqrt{\frac{\gamma p}{\rho}} = \sqrt{\gamma RT} = \sqrt{(\gamma - 1)c_p T} \tag{1.50}$$

The speed of sound is a *local* parameter, which depends on *local* absolute temperature of the gas. Its value changes with gas temperature, hence it drops when fluid accelerates (or *expands*) and increases when the gas decelerates (or *compresses*). The speed of sound in air at standard sea level conditions is ~340 m s^{-1} or ~1100 ft s^{-1}. The molecular structure of gas also affects the speed of propagation of sound through its molecular mass. We may observe this behavior by the following substitution for gas constant, R,

$$a = \sqrt{\gamma RT} = \sqrt{\gamma\left(\frac{\bar{R}}{MW}\right)T} \tag{1.51}$$

A light gas, like hydrogen (H_2) with a molecular mass of 2 (kg kmol^{-1}, or g mol^{-1}), causes an acoustic wave to propagate *faster* than a heavier gas, such as air with (a mean) molecular weight of 29 (kg kmol^{-1}, or g mol^{-1}). If we substitute these molecular weights in Eq. (1.51) we note that sound propagates in gaseous hydrogen *nearly four times faster* than air. Since both hydrogen, H_2, and air (mixture of N_2 and O_2) are diatomic gases, the ratio of specific heats, γ, remains (nearly) the same for both gases at the same temperature.

The ratio of local gas speed to the speed of sound is called *Mach number*, M:

$$M \equiv \frac{V}{a} \tag{1.52}$$

Mach number is often used as a measure of the compressibility in a gas.

1.2.7 Stagnation State

We define the stagnation state of a gas as the state reached by decelerating a flow to rest reversibly and adiabatically and without any external work. Thus, the stagnation state is reached *isentropically*. This state is also referred to as the *total* state of the gas. The symbols for stagnation state in this book use a subscript t for total. The total pressure is p_t, the total temperature is T_t and the total density is ρ_t. Since the stagnation state is reached isentropically, the static and total entropy of the gas remain the same, i.e. $s_t = s$. Based on the definition of stagnation state, the total energy of the gas does not change in the deceleration or acceleration process; hence, the stagnation enthalpy, h_t, takes on the form:

$$h_t \equiv h + \frac{V^2}{2} \tag{1.53}$$

which we defined earlier in this chapter. Assuming a *calorically perfect gas*, we may simplify the total enthalpy relation (1.53) by dividing through by c_p to get an expression for total temperature according to:

$$T_t = T + \frac{V^2}{2c_p} \quad \left[\text{Calorically perfect gas}\right] \tag{1.54}$$

This equation is very useful in converting the local static temperature and gas speed into the local stagnation temperature. To nondimensionalize Eq. (1.54), we divide both sides by the static temperature, i.e.

$$\frac{T_t}{T} = 1 + \frac{V^2}{2c_p T} \tag{1.55}$$

The denominator of the kinetic energy term on the RHS is proportional to the square of the local speed of sound, a^2, according to Eq. (1.50), which simplifies to:

$$\frac{T_t}{T} = 1 + \left(\frac{\gamma - 1}{2}\right)\frac{V^2}{a^2} = 1 + \left(\frac{\gamma - 1}{2}\right)M^2 \tag{1.56}$$

The ratio of stagnation to static temperature of a (calorically perfect) gas is a unique function of local Mach number, according to Eq. (1.56). From isentropic relations between the pressure and temperature ratio that we derived earlier based on Gibbs equation of thermodynamics, we relate the ratio of stagnation to static pressure to local Mach number:

$$\frac{p_t}{p} = \left(\frac{T_t}{T}\right)^{\frac{\gamma}{\gamma-1}} = \left[1 + \left(\frac{\gamma - 1}{2}\right)M^2\right]^{\frac{\gamma}{\gamma-1}} \quad \left[\text{Calorically perfect gas}\right] \tag{1.57}$$

Also the stagnation density is higher than the static density according to:

$$\frac{\rho_t}{\rho} = \left(\frac{p_t}{P}\right)^{\frac{1}{\gamma}} = \left[1 + \left(\frac{\gamma - 1}{2}\right)M^2\right]^{\frac{1}{\gamma-1}} \quad \left[\text{Calorically perfect gas}\right] \tag{1.58}$$

1.3 Thrust and Specific Fuel Consumption

An aircraft engine is designed to produce thrust, F (or sometimes lift in VTOL/STOL aircraft, e.g. the lift fan in the Joint Strike Fighter, F-35). In air-breathing engines, mass flow rate of air, $\dot{m}_0$, and fuel, $\dot{m}_f$, are responsible for creating that thrust. In a liquid rocket engine, the air is replaced with an on-board oxidizer, $\dot{m}_{ox}$, which then reacts with an on-board fuel, $\dot{m}_f$, to produce thrust. Figure 1.2 is a schematic drawing of a two-spool afterburning turbojet (TJ-AB) engine. The air is brought in through the air intake, or inlet, system, where station 0 designates the unperturbed flight condition, station 1 is at the inlet (or cowl) lip, and station 2 is at the exit of the air intake system, which corresponds to the inlet of the compressor (or fan). The compression process from stations 2 to 3 is divided into a low-pressure compressor (LPC) spool and a HPC spool. The exit of LPC is designated by station 2.5 and the exit of the HPC is station 3. The HPC is designed to operate at a higher shaft rotational speed than the LPC spool. The compressed gas enters the main or primary burner at 3 and is combusted with the fuel to produce hot, high-pressure gas at 4 to enter the high-pressure turbine (HPT). Flow expansion through the HPT and the low-pressure turbine (LPT) produces the shaft power for the HPC and LPC, respectively. An afterburner is designated between stations 5 and 7, where an additional fuel is combusted with the turbine discharge flow before it expands in the exhaust nozzle. Station 8 is at the throat of the nozzle and station 9 designates the nozzle exit.

To derive an expression for the engine thrust, it is most convenient to describe a control volume surrounding the engine and apply momentum principles to the fluid flow crossing the boundaries of the control volume. From a variety of choices that we have in describing the control volume, we may choose one that shares the same exit plane as the engine nozzle and its inlet is far removed from the engine inlet so as not to be disturbed by the nacelle lip. These choices are made for convenience.

As for the sides of the control volume, we may either choose stream surfaces, with the advantage of no flow crossing the sides, or a constant-area box, which has a simple geometry but fluid flow crosses the sides. Figure 1.3 depicts a control volume in the shape of a box, with cross-sectional area, A.

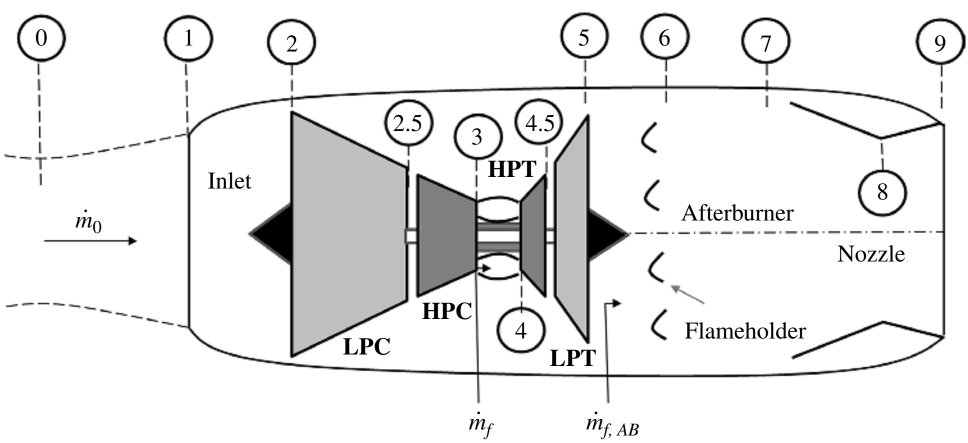

Figure 1.2 Station numbers for a turbojet with afterburner (TJ-AB) engine.

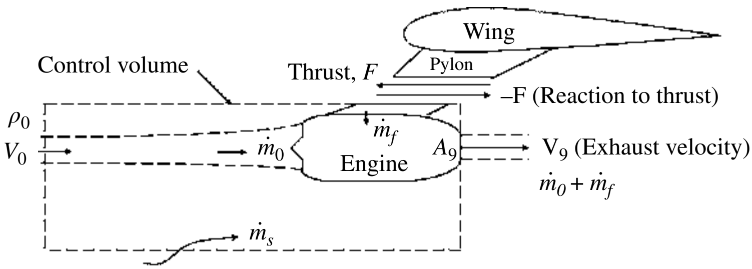

Figure 1.3 Schematic drawing of an air-breathing engine with a box-like control volume positioned around the engine (Note the flow of air to the engine, $\dot{m}_0$, through the sides, $\dot{m}_s$ and the fuel flow rate, $\dot{m}_f$).

The pylon that transmits the engine force to the aircraft, by necessity is cut by the control volume, which is enclosing the engine. The thrust force, F, and its reaction are shown in Figure 1.3. We may assume the sides of the control volume are not affected by the flowfield around the nacelle, i.e. the static pressure distribution on the sides is nearly the same as the ambient static pressure, p_0. In the same spirit, we may assume that the exit plane also sees an ambient pressure of p_0 with an exception of the plane of the jet exhaust, where a different static pressure, namely p_9, may prevail.

Application of continuity to the control volume for steady uniform flow, gives:

$$\rho_0 V_0 A + \dot{m}_s + \dot{m}_f = \left(\dot{m}_0 + \dot{m}_f\right) + \rho_0 V_0 \left(A - A_9\right) \tag{1.59}$$

which simplifies to:

$$\dot{m}_s = \dot{m}_0 - \rho_0 V_0 A_9 \tag{1.60}$$

The x-momentum balance on the control volume, assuming steady uniform flow, gives

$$\sum\left(\dot{m}V_x\right)_{\text{out}} - \sum\left(\dot{m}V_x\right)_{\text{in}} = \sum\left(F_x\right)_{\text{fluid}} \tag{1.61}$$

Equation (1.61) states that the difference between the fluid (time rate of change of) momentum out of the box and into the box is equal to the net forces acting on the fluid in the x-direction on the boundaries and within the box. These are:

$$\sum\left(\dot{m}V_x\right)_{\text{out}} = \left(\dot{m}_0 + \dot{m}_f\right)V_9 + \left[\rho_0 V_0\left(A - A_9\right)\right]V_0 \tag{1.62}$$

$$\sum\left(\dot{m}V_x\right)_{\text{in}} = \left(\rho_0 V_0 A\right)V_0 + \dot{m}_s V_0 \tag{1.63}$$

$$\sum\left(F_x\right)_{\text{fluid}} = \left(-F_x\right)_{\text{fluid}} - \left(p_9 - p_0\right)A_9 \tag{1.64}$$

Substituting Eqs. (1.62), (1.63), and (1.64) into (1.61) and for $\dot{m}_s$ from Eq. (1.60), we get:

$$\begin{aligned}&\left(\dot{m}_0 + \dot{m}_f\right)V_9 + \rho_0 V_0\left(A - A_9\right)V_0 - \rho_0 V_0 A V_0 - \left(\dot{m}_0 - \rho_0 V_0 A_9\right)V_0 = \\ &= \left(-F_x\right)_{\text{fluid}} - \left(p_9 - p_0\right)A_9\end{aligned} \tag{1.65}$$

which simplifies to:

$$\left(\dot{m}_0 + \dot{m}_f\right)V_9 - \dot{m}_0 V_0 = \left(-F_x\right)_{\text{fluid}} - \left(p_9 - p_0\right)A_9 \tag{1.66}$$

Now, through the action-reaction principle of Newtonian mechanics, we know that an equal and opposite axial force is exerted on the engine, by the fluid, i.e.

$$\left(-F_x\right)_{\text{fluid}} = \left(F_x\right)_{\text{pylon}} = \left(F_x\right)_{\text{engine}} \tag{1.67}$$

Therefore, calling the axial force of the engine "thrust," or simply F, we get the following expression for the engine thrust:

$$F = \left(\dot{m}_0 + \dot{m}_f\right)V_9 - \dot{m}_0 V_0 + \left(p_9 - p_0\right)A_9 \tag{1.68}$$

This expression for the thrust is referred to as the *net uninstalled thrust* and sometimes a subscript n is placed on F to signify the "net" thrust. Therefore, the thrust expression of Eq. (1.68) is often written as:

$$\left.F_n\right)_{\text{uninstalled}} = \left(\dot{m}_0 + \dot{m}_f\right)V_9 - \dot{m}_0 V_0 + \left(p_9 - p_0\right)A_9 \tag{1.69}$$

We first note that the RHS of Eq. (1.69) is composed of two momentum terms and one pressure-area term. The first momentum term is the exhaust momentum through the nozzle, contributing positively to the engine thrust. The second momentum term is the inlet momentum, which contributes negatively to the engine thrust in effect it represents a drag term. This drag term is called *ram drag*. It is often given the symbol of D_{ram} or D_r, and expressed as:

$$D_{\text{ram}} = \dot{m}_0 V_0 \tag{1.70}$$

The last term in Eq. (1.69), is a pressure-area term, which acts over the nozzle exit plane, i.e. area A_9, and will only contribute to the engine thrust if there is an imbalance of static pressure between the ambient and the exhaust jet. As we remember from our aerodynamic studies, a nozzle with a subsonic jet will always expand the gases to the same static pressure as the ambient condition and a sonic or supersonic exhaust jet may or may not have the same static pressure in their exit plane as the ambient static pressure. Depending on the *mismatch* of the static pressures, we categorized the nozzle flow as follows:

If $p_9 < p_0$ the nozzle is *overexpanded,*
which can only happen in supersonic jets
(i.e. in convergent-divergent nozzles with area ratio *larger* than needed for perfect expansion).

If $p_9 = p_0$ the nozzle is *perfectly expanded,*
which is the case for *all subsonic jets* and sometimes in sonic or supersonic jets
(i.e. with the "right" nozzle area ratio).

If $p_9 > p_0$ the nozzle is *underexpanded,*
which can only happen in sonic or supersonic jets (i.e. with inadequate nozzle area ratio).

Examining the various contributions from Eq. (1.69) to the net engine (uninstalled) thrust, we note that the thrust is the difference between the nozzle contributions (both momentum and pressure-area terms) and the inlet contribution (the momentum term). The nozzle contribution to thrust is called *gross thrust* and is given a symbol F_g, i.e.

$$F_g \equiv \left(\dot{m}_0 + \dot{m}_f\right)V_9 + \left(p_9 - p_0\right)A_9 \tag{1.71}$$

and, as explained earlier, the inlet contribution was negative and was called *ram drag*, D_{ram}:

$$F_n)_{\text{uninstalled}} = F_g - D_{\text{ram}} \tag{1.72}$$

We may generalize the result expressed in Eq. (1.72) to aircraft engines with more than a single stream, as for example the turbofan engine with separate exhausts. This task is very simple as we account for all gross thrusts produced by all the exhaust nozzles and subtract all the ram drag produced by all the air inlets to arrive at the engine uninstalled thrust, i.e.

$$F_n)_{\text{uninstalled}} = \sum \left(F_g\right)_{\text{nozzles}} - \sum \left(D_{\text{ram}}\right)_{\text{inlets}} \tag{1.73}$$

Equation (1.73) is the balance the momentum of the exhaust stream and the inlet momentum with the pressure thrust at the nozzle exit planes and the net uninstalled thrust of the engine. In a turbofan engine, the captured airflow is typically divided into a *core* flow, where the combustion takes place, and a fan flow, where the so-called *bypass* stream of air is compressed through a fan and later expelled through a fan exhaust nozzle. This type of arrangement (i.e. bypass configuration) leads to a higher overall efficiency of the engine and lower fuel consumption. A schematic drawing of the engine is shown in Figure 1.4.

In this example, the inlet consists of a single stream and the exhaust streams are split into a primary and a fan nozzle. We may readily write the uninstalled thrust produced by the engine following the momentum principle, namely;

$$F_n)_{\text{uninstalled}} = \dot{m}_9 V_9 + \dot{m}_{19} V_{19} + \left(p_9 - p_0\right) A_9 + \left(p_{19} - p_0\right) A_{19} - \dot{m}_0 V_0 \tag{1.74}$$

The first four terms account for the momentum and pressure thrusts of the two nozzles (what is known as gross thrust) and the last term represents the inlet ram drag.

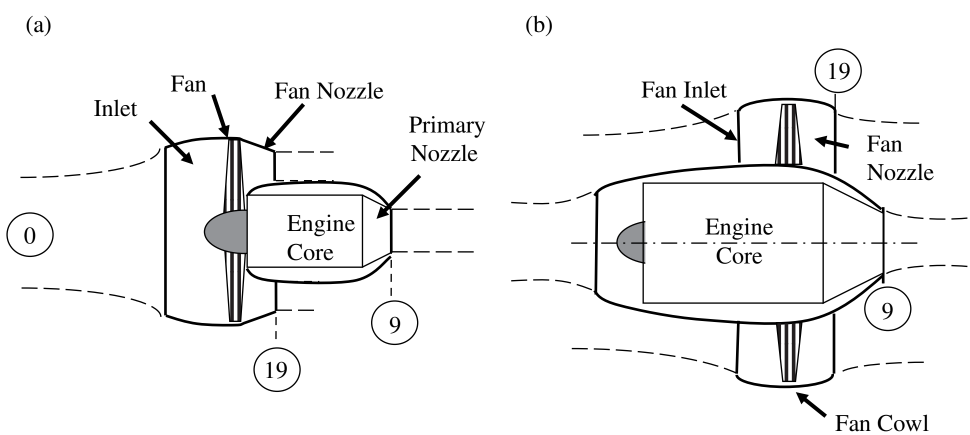

Figure 1.4 Schematic drawing of a turbofan engine with separate exhausts: (a) front-fan configuration; (b) aft-fan configuration.

1.3.1 Takeoff Thrust

At takeoff, the air speed V_0 ("flight" speed) is often ignored in the thrust calculation, therefore the ram drag contribution to engine thrust is neglected:

$$F_{\text{takeoff}} \approx F_g = \left(\dot{m}_0 + \dot{m}_f\right)V_9 + \left(p_9 - p_0\right)A_9 \tag{1.75}$$

For a perfectly expanded nozzle, the pressure thrust term vanishes to give:

$$F_{\text{takeoff}} \approx \left(\dot{m}_0 + \dot{m}_f\right)V_9 \approx \dot{m}_0 V_9 \tag{1.76}$$

Therefore, the takeoff thrust is proportional to the captured airflow.

1.3.2 Installed Thrust – Some Bookkeeping Issues on Thrust and Drag

As indicated by the description of the terms *installed thrust* and *uninstalled thrust*, they refer to the *actual propulsive force* transmitted to the aircraft by the engine and the thrust produced by the engine if it had zero external losses, respectively. Therefore, for the installed thrust, we need to account for the installation losses to the thrust such as the nacelle skin friction and pressure drags, which are to be included in the propulsion-side of the drag bookkeeping. On the other hand, the pylon and the engine installation, which affects the wing aerodynamics (in podded nacelle, wing-mounted configurations), namely by altering its "clean" drag polar characteristics, causes an "interference" drag that is accounted for in the aircraft drag polar. In the study of propulsion, we often concentrate on the engine's "internal" performance, i.e. the uninstalled characteristics, rather than the installed performance because the external drag of the engine installation depends not only on the engine nacelle geometry but also on the engine-airframe integration. Therefore, accurate installation drag accounting will require CFD analysis and wind tunnel testing at various flight Mach numbers and engine *throttle settings*. In its simplest form, we can relate the installed and uninstalled thrust according to:

$$F_{\text{installed}} = F_{\text{uninstalled}} - D_{\text{nacelle}} \tag{1.77}$$

In our choice of the control volume, as depicted in Figure 1.3, we made certain assumptions about the exit boundary condition imposed on the aft surface of the control volume. We made assumptions about the pressure boundary condition as well as the velocity boundary condition. About the pressure boundary condition, we stipulated the static pressure of flight, p_0, imposed on the exit plane, except at the nozzle exit area of A_9; therefore, we allowed for an under- or overexpanded nozzle. With regard to the velocity boundary condition at the exit plane, we stipulated that the flight velocity, V_0, is prevailed, except at the nozzle exit, where the jet velocity of V_9 prevails. In reality, the aft surface of the control volume is by necessity downstream of the nacelle and pylon, and therefore it is in the middle of the wake generated by the nacelle and the pylon. This implies that there would be a momentum deficit in the wake and the static pressure nearly equals the free stream pressure.

On the other hand, the force transmitted through the pylon to the aircraft is not the *uninstalled* thrust, as we called it in our earlier derivation, rather the *installed* thrust and pylon drag. But the integral of momentum deficit and the pressure imbalance in the wake is exactly equal to the nacelle and pylon drag contributions, i.e. we have

$$D_{\text{nacelle}} + D_{\text{pylon}} = \iint \rho V\left(V_0 - V\right)dA + \iint \left(p_0 - p\right)dA \tag{1.78}$$

where the surface integral is taken over the exit plane downstream of the nacelle and pylon.

Further breakdown of Eq. (1.78) separates the installation effects as:

$$F_{\text{uninstalled}} - D_{\text{nacelle}} - D_{\text{pylon}} = \left(\dot{m}_0 + \dot{m}_f\right)V_9 - \dot{m}_0 V_0 + \left(p_9 - p_0\right)A_9 - \iint \rho V\left(V_0 - V\right)dA - \iint \left(p_0 - p\right)dA \tag{1.79}$$

After canceling the integrals on the RHS with the drag terms of the LHS in Eq. (1.79), we recover our Eq. (1.69), which we derived earlier for the *uninstalled thrust*, i.e.

$$\left(F_n\right)_{\text{uninistalled}} = \left(\dot{m}_0 + \dot{m}_f\right)V_9 - \dot{m}_0 V_0 + \left(p_9 - p_0\right)A_9$$

The pressure integral on the captured streamtube is called the inlet *additive drag:*

$$D_{\text{add}} \equiv \oiint_0^1 \left(p - p_0\right)dA_n \tag{1.80}$$

where dA_n is the element of flow cross-sectional area normal to the flow direction. For subsonic inlets, additive drag is, for the most part, balanced by the cowl lip thrust and the difference is called the *spillage drag*. Figure 1.5 shows a schematic drawing of the flow near a blunt cowl lip and the resultant force. In general, for well-rounded cowl lips of subsonic inlets, the spillage drag is rather small and it becomes significant only for supersonic, sharp-lipped inlets. The nacelle frictional drag also contributes to the external force as well as the aft-end pressure drag of the boattail, which may be written as the sum of six contributions:

$$\begin{aligned}\sum\left(F_{x\text{-external}}\right)_{\text{control-surface}} &= \underset{(I)}{D_{\text{spillage}}} + \underset{(II)}{\iint_{M-9} \left(p - p_0\right)dA_n} + \underset{(III)}{\iint_{1-9} \tau_w dA_x} \\ &\quad + \underset{(IV)}{D_{\text{pylon}}} - \underset{(V)}{F_{x,\text{fluid}}} - \underset{(VI)}{\left(p_9 - p_0\right)A_9}\end{aligned} \tag{1.81}$$

The first term on the RHS, i.e. (I), is the spillage drag that we discussed earlier, the second term (II) is the pressure drag on the nacelle aft end or boat tail pressure drag, the third term (III) is the nacelle viscous drag, the fourth term (IV) is the pylon drag, the

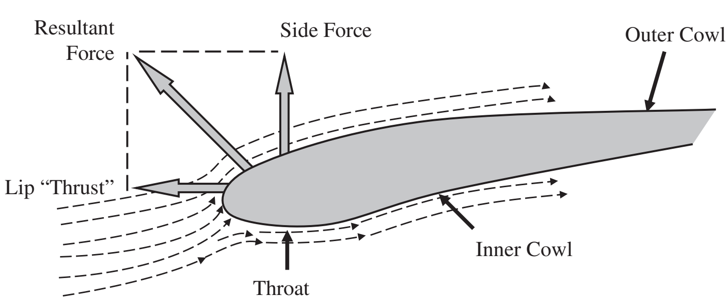

Figure 1.5 Flow detail near a blunt cowl lip showing lip thrust component and side force.

fifth term (V) is the reaction to the installed thrust force and pylon drag acting on the fluid, and the last term (VI) is the pressure thrust due to imperfect nozzle expansion. To summarize:

- Terms I + II + III are propulsion system installation drag losses.
- Term IV is accounted for in the aircraft drag polar.
- Terms V and VI combine with I, II, III, and IV to produce the uninstalled thrust.

Figure 1.6 (adapted from Lotter, 1977) shows the various contributions to net installed thrust in an air-breathing jet engine.

1.3.3 Air-Breathing Engine Performance Parameters

The engine thrust, mass flow rates of air and fuel, the rate of kinetic energy production across the engine or the mechanical power/shaft output, and engine dry weight, among other parameters, are combined to form a series of important performance parameters, known as the propulsion system figures of merit.

1.3.3.1 Specific Thrust

The size of the air intake system is a design parameter that establishes the flow rate of air, $\dot{m}_0$ Accordingly, the fuel pump is responsible for setting the fuel flow rate in the engine, $\dot{m}_f$. Therefore, in producing thrust in a "macro-engine," the engine size seems to be a "scalable" parameter. The only exception in scaling the jet engines is the "micro-engines" where the component losses do not scale. In general, the magnitude of the thrust

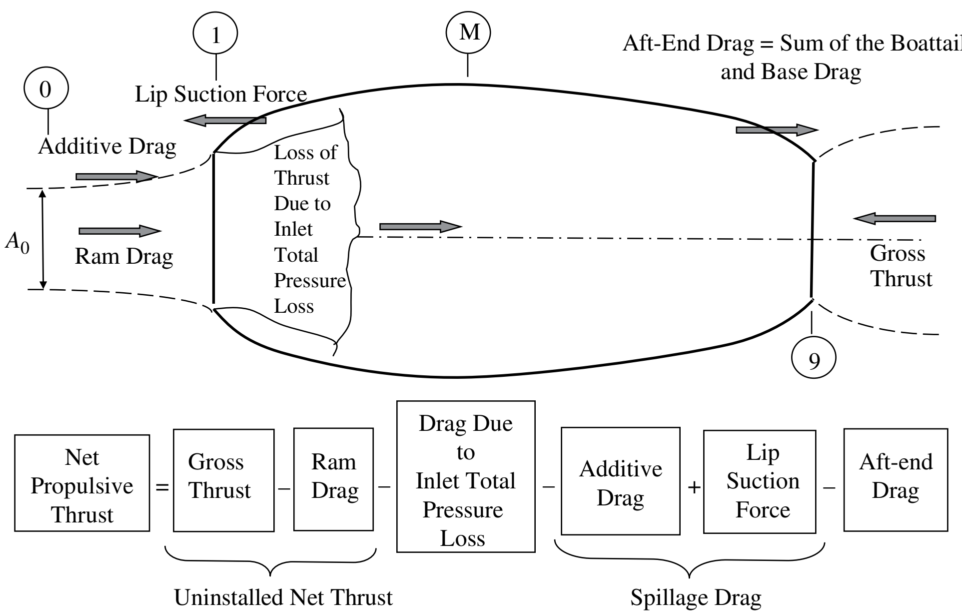

$$F_{n,inst.} = F_{gross} - D_{ram} - \Delta F_{inlet,\,pt} - D_{add} + F_{lip} - D_{aft-end}$$

Figure 1.6 Definition of *installed net thrust* in terms of internal and external parameters of an engine nacelle. *Source:* adapted from Lotter, K. 1977.

produced is directly proportional to the mass flow rates of the fluid flow through the engine. Then, it is logical to study thrust per unit mass flow rate as a *figure of merit* of a candidate propulsion system. In case of an air-breathing engine, the ratio of thrust to air mass flow rate is called *specific thrust* and is considered to be an engine performance parameter:

Air-breathing engine performance parameter #1: $\frac{F}{\dot{m}_0}$ "specific thrust"
With a metric unit of: [N.s/kg] and a British unit of: [lbf.s/lbm]

The target for this parameter, i.e. specific thrust, in a cycle analysis is usually to be maximized, i.e. to produce thrust with the least quantity of airflow rate, or equivalently to produce thrust with a minimum of engine frontal area. However, with subsonic cruise Mach numbers, the drag penalty for engine frontal area is far less severe than their counterparts in supersonic flight. Consequently, the specific thrust as a figure of merit in a commercial transport aircraft (e.g. Boeing 777 or Airbus A-340) takes a back seat to the lower fuel consumption achieved in a very large bypass ratio turbofan engine at subsonic speeds. As noted, specific thrust is a dimensional quantity with the unit of force per unit mass flow rate. A nondimensional form of the specific thrust, which is useful for graphing purposes and engine comparisons, is (following Kerrebrock 1992)

$$\text{Nondimensional specific thrust} \equiv \frac{F}{\dot{m}_0 a_0} \tag{1.82}$$

where a_0 is the ambient speed of sound taken as the reference velocity.

1.3.3.2 Specific Fuel Consumption and Specific Impulse

The ability to produce thrust with a minimum of fuel expenditure is another parameter, which is considered to be a performance parameter in an engine. In the commercial world, e.g. the airline business, specific fuel consumption represents perhaps the most important parameter of the engine. After all, the money spent on fuel is a major expenditure in operating an airline, for example. However, the reader is quickly reminded of the unspoken parameters of *reliability and maintainability* that have a direct impact on the cost of operating commercial engines and, therefore, they are at least as important, if not more important than, the engine specific fuel consumption. In the military world, the engine fuel consumption parameter takes a decidedly second role to other aircraft performance parameters, such as stealth, agility, maneuverability, and survivability. For an air-breathing engine, the ratio of fuel flow rate per unit thrust force produced is called thrust-specific fuel consumption, TSFC, or the specific fuel consumption, i.e. sfc, and is defined as:

Air-breathing engine performance parameter #2: $\frac{\dot{m}_f}{F}$ "thrust-specific fuel consumption,"

TSFC, with a metric unit of: [mg/s/N] and a British unit of: [lbm/h/lbf]

The target for this parameter, i.e. TSFC, in a cycle analysis is to be minimized, i.e. to produce thrust with a minimum of fuel expenditure. This parameter, too, is dimensional. For a rocket, on the other hand, the oxidizer as well as the fuel both contribute to the "expenditure" in the engine to produce thrust, and as such the oxidizer flow rate, $\dot{m}_{ox}$, needs to be accounted for as well.

The word *propellant* is used to reflect the combination of oxidizer and fuel in a liquid propellant rocket engine or a solid propellant rocket motor. It is customary to define a corresponding performance parameter in a rocket as thrust per unit propellant *weight flow rate*. This parameter is called *specific impulse*, I_s, i.e.

$$I_s \equiv \frac{F}{\dot{m}_p g_0} \tag{1.83}$$

$$\text{where} \quad \dot{m}_p \equiv \dot{m}_f + \dot{m}_{ox} \tag{1.84}$$

And g_0 is the gravitational acceleration on Earth's surface, i.e. $9.8\,\mathrm{m\,s^{-2}}$ or $32.2\,\mathrm{ft\,s^{-2}}$. The dimension of $\dot{m}_p g_0$ in denominator of Eq. (1.83) is then the *weight flow rate* of the propellant based on Earth's gravity, or force per unit time. Consequently, the dimension of specific impulse is "Force/Force/second," which simplifies to just the "second." All propulsors, rockets, and air breathers, then could be compared using a unifying figure of merit, namely their *specific impulse* in seconds. An added benefit of the specific impulse is that regardless of the units of measurement used in the analysis, i.e. either metric or the British on both sides of the Atlantic, specific impulse comes out as seconds in both systems. The use of specific impulse as a unifying figure of merit is further justified in the twenty-first century as we attempt to commercialize the space with potentially reusable rocket-based combined cycle (RBCC) powerplants in propelling a variety of single-stage-to-orbit (SSTO) vehicles. To study advanced propulsion concepts where the mission calls for multimode propulsion units, as in air-ducted rockets, ramjets, and scramjets, all combined into a single "package," the use of specific impulse becomes even more obvious.

In summary,

Specific impulse: $I_s \equiv \dfrac{F}{\dot{m}_f g_0}$ [sec] for an air-breathing engine

Specific impulse: $I_s \equiv \dfrac{F}{\dot{m}_p g_0}$ [sec] for a rocket

An important goal in an engine cycle design is to maximize specific impulse, i.e. the ability to produce thrust with the least amount of fuel or propellant consumption in the engine.

1.4 Thermal and Propulsive Efficiency

1.4.1 Thermal Efficiency

The ability of an engine to convert the thermal energy inherent in the fuel to net kinetic energy gain of the working medium, is called the engine *thermal efficiency*, η_{th}

$$\eta_{th} \equiv \frac{\Delta \dot{KE}}{\wp_{\text{thermal}}} = \frac{\dot{m}_9 \dfrac{V_9^2}{2} - \dot{m}_0 \dfrac{V_0^2}{2}}{\dot{m}_f Q_R} = \frac{\left(\dot{m}_0 + \dot{m}_f\right) V_9^2 - \dot{m}_0 V_0^2}{2 \dot{m}_f Q_R} \tag{1.85}$$

where $\dot{m}$ signifies mass flow rate corresponding to stations 0 and 9 and subscript f signifies fuel, and Q_R is the fuel heating value. The unit of Q_R is energy per unit mass of the fuel (e.g. kJ kg^{-1} or BTU lbm^{-1}) and is tabulated as a fuel property. Eq. (1.85) compares the *mechanical power* production in the engine to the *thermal power* investment in the engine. Figure 1.7 graphically depicts the energy sources in an air-breathing engine. The thermal energy production in an engine is not actually "lost," as it shows up in the hot jet exhaust stream, rather, this energy is "wasted" and we were unable to convert it to a *useful* power. It is important to know, i.e. to quantify, this inefficiency in our engine.

Equation (1.85), which defines thermal efficiency, is simply the ratio of "net mechanical output" to the "thermal input," as we learned in thermodynamics.

To lower the exhaust gas temperature, we can place an additional turbine wheel in the high-pressure, hot gas stream and produce shaft power. This shaft power can then be used to power a propeller, a fan, or a helicopter rotor, for example. The concept of additional turbine stages to extract thermal energy from the combustion gases and powering a fan in a jet engine has led to turbofan engines. Therefore, the mechanical output of these engines is enhanced by the additional shaft power. The thermal efficiency of a cycle that produces a shaft power can therefore be written as:

$$\eta_{th} = \frac{\wp_{\text{shaft}} + \Delta \dot{KE}}{\dot{m}_f Q_R} \tag{1.86}$$

A schematic drawing of an aircraft gas turbine engine, which is configured to produce shaft power, is shown in Figure 1.8. In part (a), the *power turbine* provides shaft power to a propeller, whereas in part (b) the power turbine provides the shaft power to a helicopter main rotor.

The gas generator in Figure 1.8 refers to the compressor, burner, and the turbine combination, i.e. the basic building block of a GT engine. In turboprops and turboshaft engines the mechanical output of the engine is dominated by the shaft power that in the definition of the thermal efficiency of such cycles the rate of kinetic energy increase is neglected, i.e.

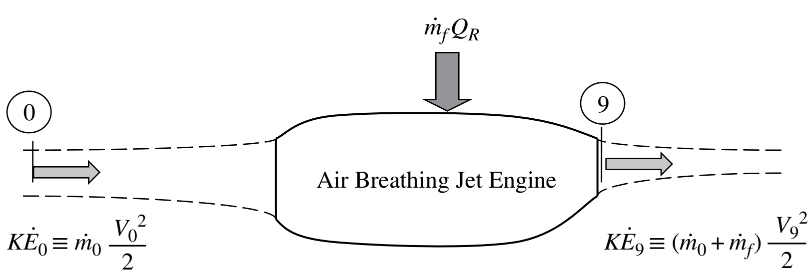

Figure 1.7 Thermal power input (by fuel) and the mechanical power production (output) by the engine.

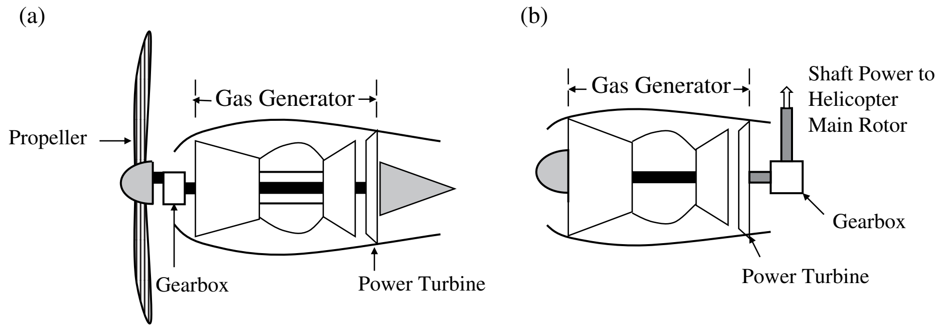

Figure 1.8 Schematic drawing of a power turbine placed in the exhaust of a gas turbine engine: (a) gas turbine engine with a power turbine providing shaft power to a propeller (turboprop); (b) power turbine providing shaft power to a helicopter rotor.

$$\eta_{th} \equiv \frac{\wp_s}{\dot{m}_f Q_R} \quad \text{In turboprop and turboshaft engines} \tag{1.87}$$

In addition to a shaft-power turbine concept, we can lower the exhaust gas temperatures by placing a heat exchanger in the exhaust stream to preheat the compressor air prior to combustion. The exhaust gas stream is cooled as it heats the cooler compressor gas and less fuel is needed to achieve a desired turbine entry temperature (TET). This scheme is referred to as *regenerative cycle* and is shown in Figure 1.9.

All of the cycles shown in Figures 1.8 and 1.9 produce less waste heat in the exhaust nozzle; consequently, they achieve a higher thermal efficiency than their counterparts without the extra shaft power or the heat exchanger.

We remember that the highest thermal efficiency attainable in a heat engine operating between two temperature limits was that of a Carnot cycle operating between those temperatures. Figure 1.10 shows the Carnot cycle on a T-s diagram.

As noted in Figure 1.10, both heat rejection at absolute zero ($T_1 = 0$) and heating to infinite temperatures ($T_2 = \infty$) are impossibilities; therefore, we are thermodynamically bound by the ideal Carnot thermal efficiency as the maximum, which for peak temperature of 2500 K corresponds to stoichiometric combustion of Jet-A, and the low temperature of 288 K, which corresponds to standard ambient condition, is 88%. Brayton cycle, which represents gas turbine engines, experiences a much lower thermal efficiency than the corresponding Carnot cycle., typically in the 30s.

1.4.2 Propulsive Efficiency

The fraction of the net mechanical output of the engine that is converted into thrust power is called the *propulsive efficiency*. The net mechanical output of the engine is $\Delta\dot{KE}$ for perfectly expanded nozzle and the thrust power is $F{\cdot}V_0$, therefore, the propulsive efficiency is defined as their ratio:

$$\eta_p \equiv \frac{F.V_0}{\Delta\dot{KE}} \tag{1.88}$$

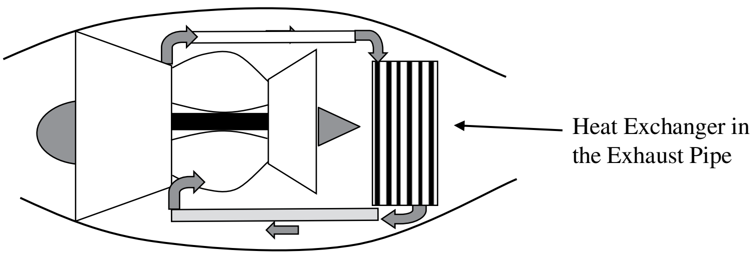

Figure 1.9 Schematic drawing of a gas turbine engine with a regenerative scheme.

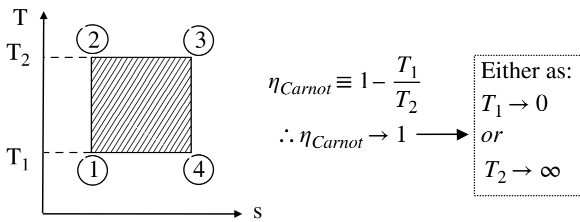

Figure 1.10 T-s diagram of a Carnot cycle.

A graphical depiction is shown in Figure 1.11 to help the reader to remember the definition of propulsive efficiency.

Although the thrust power represented by $F{\cdot}V_0$ in Eq. (1.88) is based on the *installed* thrust, for simplicity, it is often taken as the uninstalled thrust power to highlight a very important, and at first astonishing, result about the propulsive efficiency. Now, let us substitute the uninstalled thrust of a perfectly expanded jet in the above definition to get:

$$\eta_p \approx \frac{\left[\left(\dot{m}_0 + \dot{m}_f\right)V_9 - \dot{m}_0 V_0\right]V_0}{\left(\dot{m}_0 + \dot{m}_f\right)\frac{V_9^{\,2}}{2} - \dot{m}_0\frac{V_0^{\,2}}{2}} \tag{1.89}$$

We recognize that the fuel-flow rate is but a small fraction (~2–3%) of the airflow rate and thus may be ignored relative to the airflow rate so Eq. (1.89) may be simplified to

$$\eta_p \approx \frac{\left(V_9 - V_0\right)V_0}{\frac{1}{2}\left(V_9^{\,2} - V_0^{\,2}\right)} = \frac{2V_0}{V_9 + V_0} = \frac{2}{1 + \frac{V_9}{V_0}} \tag{1.90}$$

Equation (1.90) as an approximate expression for the propulsive efficiency of a jet engine is cast in terms of a single parameter, namely the jet-to-flight velocity ratio, V_9/V_0. We further note that 100% propulsive efficiency (within the context of approximation presented in the derivation) is mathematically possible and will be achieved by engines whose exhaust velocity is as fast as the flight velocity, i.e. V_9/V_0. Thrust production demands $V_9 > V_0$. To achieve a small velocity increment across a gas turbine engine for a given fuel-flow rate, we need to drain the thermal energy in the combustion gas further and convert it to additional shaft power. In turn, shaft power supplied to a fan

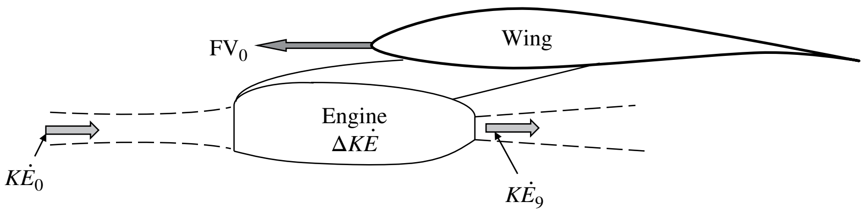

Figure 1.11 Schematic drawing of an aircraft engine installation showing the mechanical power produced by the engine and thrust power transmitted to aircraft.

(or propeller) impacts a larger mass flow rate of air, in a secondary or a bypass stream, which produce the desired level of thrust.

Propulsive efficiency of a turboprop engine is defined as the fraction of mechanical power, which is converted to the total thrust (i.e. the sum of propeller and engine nozzle thrust) power, namely;

$$\eta_p \equiv \frac{F.V_0}{\wp_s + \Delta\dot{KE}} \approx \frac{F.V_0}{\wp_s} \quad [\text{Turboprop}] \tag{1.91}$$

Again, this definition compares the propulsive *output* ($F{\cdot}V_0$) to the mechanical power *input* (shaft and change in jet kinetic power) in an aircraft engine. The fraction of shaft power delivered to the propeller, converted to the propeller thrust, is called *propeller efficiency*, η_{pr},

$$\eta_{pr} \equiv \frac{F_{\text{prop}}.V_0}{\wp_{s,\text{prop}}} \tag{1.92}$$

Due to large diameters of propellers as compared to power turbine, it is necessary to reduce their rotational speed to avoid severe tip shock-induced losses. Consequently, the power turbine rotational speed is mechanically reduced in a reduction gearbox and a small fraction of shaft power is lost in the gearbox, which is referred to as gearbox efficiency, i.e.

$$\eta_{gb} \equiv \frac{\wp_{s,\text{prop}}}{\wp_{s,\text{turbine}}} \tag{1.93}$$

1.4.3 Engine Overall Efficiency and Its Impact on Aircraft Range and Endurance

The product of the engine thermal and propulsive efficiency is called overall efficiency, η_0

$$\eta_0 \equiv \eta_{th}.\eta_p = \frac{\Delta\dot{KE}}{\dot{m}_f Q_R}\frac{F.V_0}{\Delta\dot{KE}} = \frac{F.V_0}{\dot{m}_f Q_R} \tag{1.94}$$

The overall efficiency of an aircraft engine is therefore the fraction of the fuel thermal power, which is converted into the thrust power of the aircraft. Again, a useful output is compared to the input investment in this efficiency definition. In an aircraft performance course that typically precedes the aircraft propulsion class, the engine overall

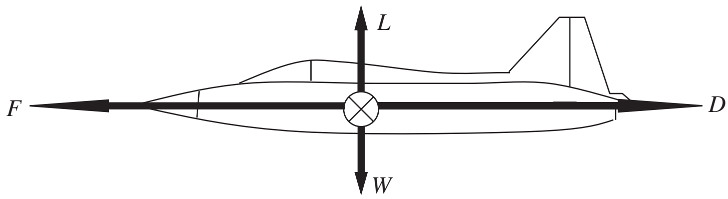

Figure 1.12 Aircraft in unaccelerated level flight showing a balance between thrust and drag forces and lift and weight forces.

efficiency is tied with the aircraft range, through the Breguet range equation. The derivation of the Breguet range equation is both fundamental to our studies and is surprisingly simple enough for us to repeat it here for review purposes. An aircraft in level flight cruising at the speed V_0 (see Figure 1.12) experiences a drag force that is entirely balanced by the engine installed thrust, i.e.

$$F_{\text{engine}} = D_{\text{aircraft}} \tag{1.95}$$

The aircraft lift, L, is also balanced by the aircraft weight to maintain level flight, i.e.

$$L = W \tag{1.96}$$

We can multiply Eq. (1.95) by the flight speed V_0 and then replace the resulting thrust power, $F{\cdot}V_0$, by $\eta_0\, \dot{m}_f\, Q_R$, via the definition of the engine overall efficiency, to get

$$F.V_0 = \eta_0\, \dot{m}_f\, Q_R = D.V_0 \tag{1.97}$$

Now, let us divide the RHS term in Eq. (1.97) by lift, L, and the middle term of Eq. (1.97) by aircraft weight (which is the same as lift), to get

$$\frac{\eta_0 \dot{m}_f Q_R}{W} = \frac{D}{L}.V_0 \tag{1.98}$$

Noting that the fuel-flow rate, $\dot{m}_f = -\frac{1}{g_0}\frac{dW}{dt}$, i.e. the rate at which the aircraft is losing mass (thus the negative sign), we can substitute this expression in Eq. (1.98) and rearrange to get

$$-\frac{\eta_0 Q_R}{g_0}\frac{dW}{W} = \frac{D}{L}.V_0 dt = \frac{dR}{L/D} \tag{1.99}$$

where g_0 is Earth's gravitational acceleration and $V_0 dt$ is interpreted as the aircraft elemental range, dR, which is the distance traveled in time dt by the aircraft flying at speed V_0. Now, we can proceed to integrate Eq. (1.99) by making the assumptions of constant lift-to-drag ratio and constant engine overall efficiency, over the cruise period, to derive the Breguet range equation as:

$$R = \eta_0.\frac{Q_R}{g_0}.\frac{L}{D}.\ell n\frac{W_i}{W_f} \tag{1.100}$$

where W_i is the aircraft initial weight and W_f is the aircraft final weight (note that the initial weight is larger than the final weight by the weight of the fuel burned in flight). As noted, Eq. (1.100) is known as the *Breguet range equation* that shows both aerodynamic efficiency (L/D) and overall propulsion efficiency, η_o, impact aircraft range. This equation owes its simplicity and elegance to our assumptions of (i) unaccelerated level flight and (ii) constant lift-to-drag ratio and engine overall efficiency. Also note that the range segment contributed by the takeoff and landing distances is not accounted for in the Breguet range equation. The direct proportionality of the engine overall efficiency and range is demonstrated by the Breguet range equation, i.e.

Aircraft range, $R \propto \eta_0$

By replacing the overall efficiency of the engine in the range equation by the ratio of thrust power to the thermal power in the fuel, we get:

$$R = \frac{F_n V_0}{\dot{m}_f Q_R} \frac{Q_R}{g_0} \frac{L}{D} \ell n \frac{W_i}{W_f} \tag{1.101}$$

We may express the flight speed in terms of a product of flight Mach number and the speed of sound; in addition, we may substitute the TSFC for the ratio of fuel flow rate to the engine net thrust, to get

$$R = \left(M_0 \frac{L}{D} \right) \frac{a_0 / g_0}{TSFC} \ell n \frac{W_i}{W_f} \tag{1.102}$$

The result of this representation of the aircraft range is the emergence of (ML/D) as the aerodynamic figure of merit for aircraft range optimization, known as the *range factor*, or *cruise efficiency:*

$$\text{Aircraft range}, R \propto M_0 \frac{L}{D} \tag{1.103}$$

$$\text{Aircraft range}, R \propto \frac{1}{TSFC} \tag{1.104}$$

By using a more energetic fuel than the current jet aviation fuel (e.g. hydrogen), we will be able to reduce the thrust-specific fuel consumption, or we can see the effect of fuel energy content on the range following Eq. (1.105), which shows

$$\text{Aircraft range}, R \propto Q_R \tag{1.105}$$

Equivalently, we may seek out the effect of engine overall efficiency, or the specific fuel consumption on aircraft endurance, which for our purposes is the ratio of aircraft range to the flight speed:

$$\text{Aircraft endurance} = \frac{R}{V_0} = \frac{\eta_0}{V_0} \frac{Q_R}{g_0} \frac{L}{D} \ell n \frac{W_i}{W_f} \tag{1.106}$$

This again points out the importance of engine overall efficiency on aircraft performance parameters such as endurance. In terms of TSFC, we get:

$$\text{Aircraft endurance} = \left(\frac{L}{D} \right) \frac{1/g_0}{TSFC} \ell n \frac{W_i}{W_f} \tag{1.107}$$

The engine thrust-specific-fuel consumption appears in the denominator as in the engine impact on the range equation, and this time the aerodynamic figure of merit is aerodynamic efficiency, L/D, instead of ML/D, as expected for the aircraft endurance.

$$\text{Aircraft endurance} \propto \frac{1}{TSFC} \tag{1.108}$$

$$\text{Aircraft endurance} \propto \frac{L}{D} \tag{1.109}$$

1.5 Gas Generator

At the heart of an aircraft gas turbine engine *is a gas generator*. It is composed of three major components, a compressor, a burner (sometimes referred to as combustor or combustion chamber) followed by a turbine. The schematics of a gas generator and station numbers are shown in Figure 1.13. The parameters that define the physical characteristics of a gas generator are noted in Table 1.1.

Compressor total pressure ratio, π_c, is a design parameter. An aircraft engine designer has the design choice of the compressor staging, i.e. the number and type of compressor stages. That choice is a strong function of flight Mach number, or what we will refer to as *ram pressure ratio*. As a rule of thumb, the higher the flight Mach number, the lower the compressor pressure ratio the cycle requires to operate efficiently. In fact, at the upper supersonic Mach numbers, i.e. $M_0 \geq 3$, an air-breathing engine will not even require *any* mechanical compression, i.e. the compressor is totally unneeded. Such engines work on the principle of ram compression and are called *ramjets*. We will refer to this later on in our analysis.

The compressor air mass flow rate is the sizing parameter, which basically scales the engine face diameter. The takeoff gross weight of the aircraft is the primary parameter that most often *sizes* the engine. Other parameters, which contribute to engine sizing, are the engine-out rate of climb requirements, the transonic acceleration and the allowable use of afterburner, among other mission specification parameters. The burner fuel flow rate is the fuel energy release rate parameter, which may be replaced by the TET, T_{t4}. Both of these parameters establish a *thermal limit* identity for the

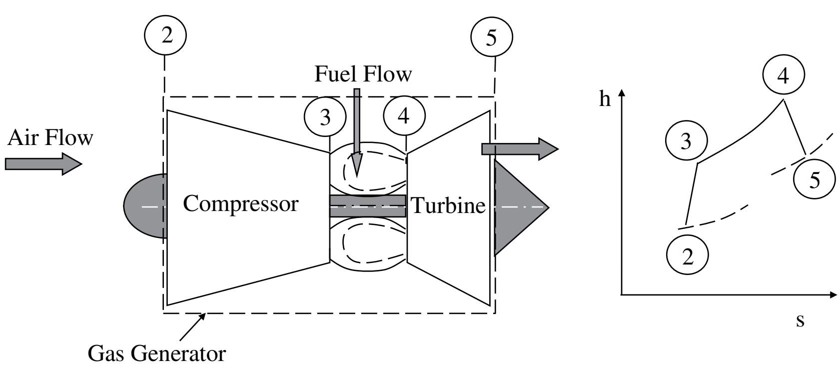

Figure 1.13 Schematic drawing of a gas generator.

Table 1.1 The parameters in a gas generator.

1.	Compressor pressure ratio, $\pi_c \equiv \dfrac{p_{t3}}{p_{t2}}$	[“design” parameter]
2.	Compressor air mass flow rate, $\dot{m}_0$	[“size” parameter]
3.	Combustor fuel flow rate, $\dot{m}_f$, or turbine entry temperature, T_{t4}	[“temperature limit” parameter]
4.	Fuel lower heating value, Q_R	[”ideal fuel energy” parameter]
5.	Component efficiency	[“irreversibility” or loss parameter]

engine, which dictates the material and the cooling technologies to be employed in the engine *hot section* (i.e. the turbine and nozzle) at the design stage. Fuel heating value, or heat of reaction, Q_R, represents the (ideal) fuel energy density, i.e. the fuel thermal energy per unit mass of fuel. Finally, the component efficiencies are needed to describe the extent of losses or stated in thermodynamic language “irreversibility” in each component.

1.6 Engine Components

1.6.1 The Inlet

The *basic* function of the inlet is to deliver the air to the fan/compressor at the *right* Mach number, M_2, and the *right* quality, i.e. low distortion. The subsonic compressors are designed for an axial Mach number of $M_2 = 0.5 - 0.6$. Therefore, if the flight Mach number is higher than 0.5 or 0.6, which includes all commercial (fixed-wing) transports and military (fixed-wing) aircraft, then the inlet is required to *decelerate* the air efficiently. Therefore the main function of an inlet is to *diffuse or decelerate* the flow, and hence it is also called a diffuser. Flow deceleration is accompanied by the static pressure rise, or what is known as the *adverse pressure gradient* in fluid dynamics.

As one of the first principles of fluid mechanics, we learned that the boundary layers, being of a low-energy and momentum deficit zone, facing an adverse pressure gradient environment tend to separate. Therefore, one of the challenges facing an inlet designer is to prevent inlet boundary layer separation. One can achieve this by tailoring the geometry of the inlet to avoid rapid diffusion or possibly through variable geometry inlet design. Now, it becomes obvious why an aircraft inlet designer faces a bigger challenge if the inlet has to decelerate a Mach 2 or 3 stream to the compressor face Mach number of 0.5 than an aircraft that flies at Mach 0.8 or 0.9.

Figure 1.14 shows the thermodynamic states of air in an inlet, where state 0 corresponds to flight or freestream condition, and station 2 is at the exit of the intake system, which corresponds to fan/compressor inlet in a GT engine and combustor inlet in a ramjet.

Irreversibility in an inlet stems from viscous effects and presence of shocks in supersonic flows. The real flow is assumed to be adiabatic. Consequently, total enthalpy remains constant in an inlet and total pressure suffers a loss.

$$\frac{p_{t2}}{p_{t0}} = e^{-\frac{s_2 - s_0}{R}} = e^{-\frac{\Delta s}{R}} \tag{1.110}$$

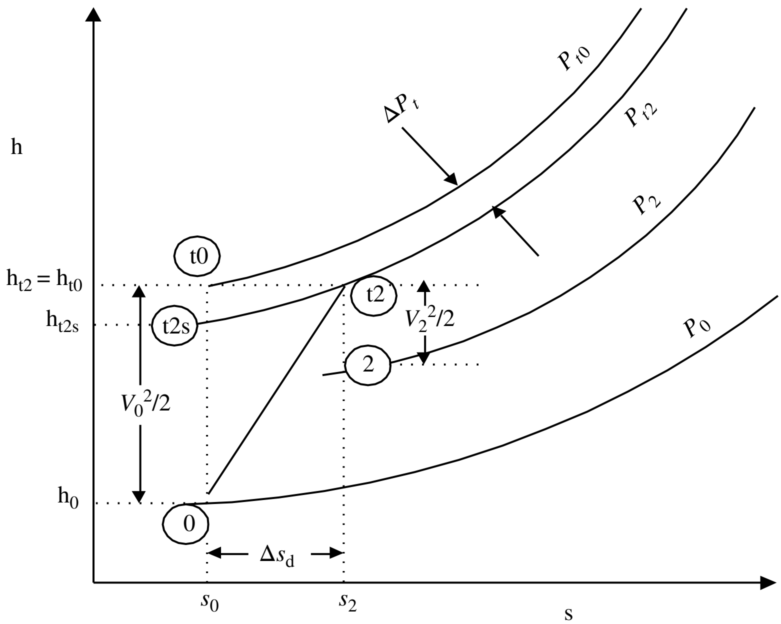

Figure 1.14 Enthalpy-entropy (h-s) diagram of an aircraft engine inlet flow under real and ideal conditions.

The ratio of p_{t2}/p_{t0} is the inlet total pressure ratio (often referred to as inlet recovery), π_d. We may define inlet adiabatic efficiency, η_d as

$$\eta_d \equiv \frac{h_{t2s} - h_0}{h_{t2} - h_0} = \frac{\left(V^2/2\right)_{\text{ideal}}}{V_0^2/2} \tag{1.111}$$

The practical form of the above definition is derived when we divide the numerator and denominator by h_0 to get:

$$\eta_d = \frac{\dfrac{h_{t2s}}{h_0} - 1}{\dfrac{h_{t2}}{h_0} - 1} = \frac{\dfrac{T_{t2s}}{T_0} - 1}{\dfrac{h_{t0}}{h_0} - 1} = \frac{\left(\dfrac{p_{t2}}{p_0}\right)^{\frac{\gamma-1}{\gamma}} - 1}{\dfrac{\gamma-1}{2} M_0^2} \tag{1.112}$$

where we have used the isentropic relation between the states ($t2s$) and (0). Note that the only unknown in Eq. (1.112) is p_{t2}, for a given flight altitude, p_0, flight Mach number, M_0 and an inlet adiabatic efficiency, η_d. We can separate the unknown term, p_{t2}, and write the following expression:

$$\frac{p_{t2}}{p_0} = \left\{1 + \eta_d \frac{\gamma-1}{2} M_0^2\right\}^{\frac{\gamma}{\gamma-1}} \tag{1.113}$$

It is interesting to note that Eq. (1.113) recovers the isentropic relation for a 100% efficient inlet, or $\eta_d = 1.0$. Another parameter, or a *figure of merit*, which describes the inlet performance is the total pressure ratio between the compressor face and the (total) flight condition. This is called π_d, and is often referred to as the *inlet total pressure recovery*:

$$\pi_d \equiv \frac{p_{t2}}{p_{t0}} \tag{1.114}$$

As expected, the two figures of merit for an inlet, i.e. η_d or $\pi_d$are not independent from each other and we can derive a relationship between $\eta_d$and π_d working the left-hand side of Eq. (1.113), as follows:

$$\frac{p_{t2}}{p_0} = \frac{p_{t2}}{p_{t0}}\frac{p_{t0}}{p_0} = \left\{1 + \eta_d \frac{\gamma - 1}{2} M_0{}^2\right\}^{\frac{\gamma}{\gamma-1}} \tag{1.115a}$$

$$\pi_d = \frac{\left\{1 + \eta_d \frac{\gamma - 1}{2} M_0{}^2\right\}^{\frac{\gamma}{\gamma-1}}}{\frac{p_{t0}}{p_0}} = \left\{\frac{1 + \eta_d \frac{\gamma - 1}{2} M_0{}^2}{1 + \frac{\gamma - 1}{2} M_0{}^2}\right\}^{\frac{\gamma}{\gamma-1}} \tag{1.115b}$$

Therefore, Eq. (1.115b) relates the inlet total pressure recovery, π_d, to the inlet adiabatic efficiency, η_d, at any flight Mach number, M_0. We note that in Eq. (1.115b) as $\eta_d \to 1$, then $\pi_d \to 1$ as well, as expected. Figure 1.14 also shows the static state 2, which shares the same entropy as the total state, $t2$, and lies below it by the kinetic energy at 2, namely, $V_2{}^2/2$.

1.6.2 The Nozzle

The primary function of an aircraft engine exhaust system is to accelerate the gas efficiently. The nozzle parameter that is of utmost importance in *propulsion* is the gross thrust, F_g. The expression we had earlier derived for the gross thrust was

$$F_g = \dot{m}_9 V_9 + \left(p_9 - 9_0\right) A_9 \tag{1.116}$$

In this equation, the first term on the RHS is called the momentum thrust and the second term is called the pressure thrust. It is interesting to note that the nozzles produce a "signature," typically composed of infrared radiation, thermal plume, smoke, and acoustic signatures, which are key design features of a stealth aircraft exhaust system *in addition* to the main propulsion requirement of the gross thrust.

As the fluid accelerates in a nozzle, the static pressure drops and hence a *favorable pressure gradient* environment is produced in the nozzle. This is in contrast to diffuser flows where an *adverse pressure gradient* environment prevails. Therefore, boundary layers are, by and large, well behaved in the nozzle and less cumbersome to treat than the inlet. For a subsonic exit Mach number, i.e. $M_9 < 1$, the nozzle expansion process will continue all the way to the ambient pressure, p_0. This important result means that in subsonic streams, the static pressure inside and outside of the jet are the same. In fact, there is no mechanism for a pressure jump in a subsonic flow, which is in contrast to the supersonic flows where shock waves and expansion fans allow for static pressure discontinuity. We have depicted a convergent nozzle in Figure 1.15 with its exhaust stream (i.e. a jet) emerging in the ambient gas of static state (0). The outer shape of the nozzle is called a boattail, which affects the *installed performance* of the exhaust system. The external aerodynamics of the nozzle installation belongs to the propulsion system integration studies and does not usually enter the discussions of the *internal performance*, i.e. the cycle analysis. However, we need to be aware that our decisions for the internal flow path optimization, e.g. the nozzle exit-to-throat area ratio, could have adverse effects on the installed performance, which may offset any gains that may have been accrued as a result of the internal optimization.

We have learned in aerodynamics that a convergent duct, as shown above, causes flow acceleration in a subsonic stream to a maximum Mach number of 1, which can only be reached at the minimum area of the duct, namely at its exit. So we stipulate that for all subsonic jets, i.e. $M_9 < 1$, there is a static pressure equilibrium in the exhaust stream and the ambient fluid, i.e. $p_9 = p_0$. Let us think of this as the *Rule 1* in nozzle flow.

$$\mathit{Rule}\,1: \mathit{If}\ M_{\text{jet}} < 1, \text{then}\ p_{\text{jet}} = p_{\text{ambient.}}$$

The expression "jet" in the above rule should not be confusing to the reader, as it relates to the flow that emerges from the nozzle. In that context, M_{jet} is the same as M_9 and p_{ambient} is the same as p_0. We recognize that not only it is entirely possible but also desirable for the sonic and supersonic jets to expand to the ambient static pressure as well. Such nozzle flows are called *perfectly expanded*. Actually the nozzle gross thrust can be maximized if the nozzle flow is perfectly expanded. We state this principle here without proof, but we will address it again, and actually prove it, in the next chapters. Let us think of this as the *Rule 2* in nozzle flow.

$$\mathit{Rule}\,2: \mathit{If}\ p_{\text{jet}} = p_{\text{ambient}}, \text{then we have a perfectly expanded nozzle which results in}\ F_{g,\max}.$$

Here, the stipulation is only on the *static pressure match* between the jet exit and the ambient static pressure and not *perfect flow* inside the nozzle. A real nozzle flow experiences total pressure loss due to viscous dissipation in the boundary layer as well as shock

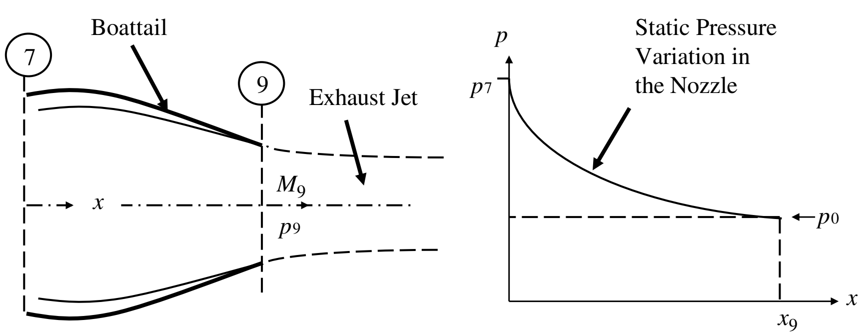

Figure 1.15 Schematic drawing of a subsonic nozzle with its static pressure distribution.

waves, and yet it is possible for it to *perfectly expand* the gas to the ambient condition. Remembering compressible duct flows in aerodynamics, we are reminded that the exit pressure, p_9, is a direct function of the nozzle area ratio, A_{exit}/A_{throat}, which in our notation, it becomes A_9/A_8, and the nozzle pressure ratio (NPR). Recalling the definition of NPR,

$$NPR \equiv \frac{p_{t7}}{p_0} \tag{1.117}$$

we will demonstrate a critical value of NPR that will result in the choking condition at the nozzle throat, i.e. $M_8 = 1.0$, when $NPR \geq (NPR)_{critical}$. Let us think of this as Rule 3 in convergent or convergent-divergent nozzle aerodynamics. These rules do not apply if the divergent section of a C-D nozzle becomes a subsonic a diffuser.

> $Rule\,3: If\ NPR \geq \left(NPR\right)_{\text{critical}}$, then the nozzle throat velocity is sonic $\left(\text{i.e. } choked\right), M_8 = 1.0.$

A schematic drawing of a convergent-divergent supersonic nozzle is shown in Figure 1.16.

The nozzle throat becomes choked at a static pressure of about 50% of the nozzle total pressure, i.e. $p_{throat} \sim ½\, p_{t7}$. This fact provides for an important *rule of thumb* in nozzle flows, which is definitely worth remembering. Let us consider this, as Rule 4.

> $Rule\,4: If\ \dfrac{p_{t7}}{p_0} \geq\sim 2$, then the nozzle throat can be choked, i.e. $M_8 = 1.0.$

The two possible solutions in static pressure distribution along the nozzle axis are shown in Figure 1.16. One is a subsonic solution downstream of the nozzle throat and the second is a supersonic flow solution downstream of the throat. The subsonic solution is clearly a result of high backpressure, i.e. p_0, and causes a flow deceleration in the divergent duct downstream of the throat. Therefore, the divergent portion of the duct is actually a *diffuser* and not a nozzle. The supersonic solution is a result of low backpressure and therefore the flow continues to expand (i.e. accelerates) beyond the throat to supersonic speeds at the exit. Also note that only a perfectly expanded nozzle flow is shown, as the supersonic branch of the nozzle flow in Figure 1.16. For ambient pressures in between the two pressures shown in Figure 1.16, there are a host of shock solutions, which occur as an oblique shock at the lip or normal shock inside the nozzle.

To examine the efficiency of a nozzle in expanding the gas to an exit (static) pressure, p_9, we create an enthalpy–entropy diagram, very similar to an inlet. In the inlet studies, we took the ambient static condition, 0, and compressed it to the total intake exit condition, $t2$. But since a nozzle may be treated as a reverse-flow diffuser (and vice versa), we take the nozzle inlet gas, at the total state $t7$, and expand it to the exit static condition, 9. This process is shown in Figure 1.17. A solid line connecting the gas total state $t7$ to the exit static state, 9, shows the actual nozzle expansion process. As the real nozzle flows may still be treated as adiabatic, the total enthalpy, h_t, remains constant in a nozzle, i.e

$$h_{t7} = h_{t9} \tag{1.118}$$

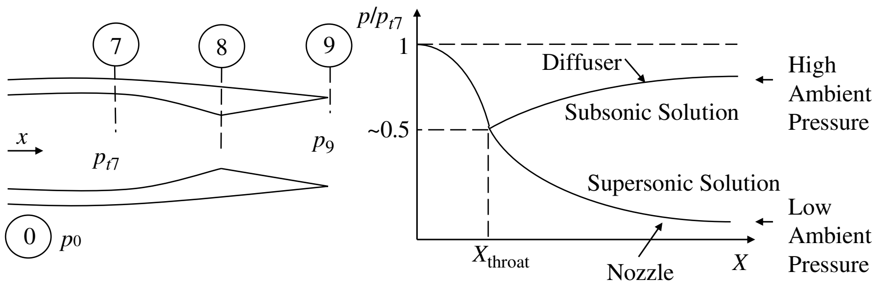

Figure 1.16 A choked C-D nozzle and the static pressure distribution along the nozzle axis.

An ideal exit state, 9s, is reached isentropically from the total state, $t7$, to the same exit pressure p_9, in Figure 1.17. The vertical gap between a total and static enthalpy states, in an h-s diagram, represents the kinetic energy of the gas, $V^2/2$, which is also shown in Figure 1.17. Due to frictional and shock losses in a nozzle, the flow will suffer a total pressure loss, i.e.

$$p_{t9} \prec p_{t7} \tag{1.119}$$

as depicted in Figure 1.17. We define the total pressure ratio across a nozzle as

$$\pi_n \equiv \frac{p_{t9}}{p_{t7}} \tag{1.120}$$

The entropy rise in an adiabatic nozzle is:

$$\frac{\Delta s_n}{R} = -\ln \pi_n \tag{1.121}$$

We define a nozzle adiabatic efficiency, η_n, very similar to the inlet adiabatic efficiency, as

$$\eta_n \equiv \frac{h_{t7} - h_9}{h_{t7} - h_{9s}} = \frac{V_9^2/2}{V_{9s}^2/2} \tag{1.122}$$

Let us interpret the above definition in physical terms. The fraction of an ideal nozzle exit kinetic energy, $V_{9s}^2/2$, which is realized in a real nozzle, $V_9^2/2$, is called the nozzle adiabatic efficiency. The loss in total pressure in a nozzle manifests itself as a loss of kinetic energy. Consequently, the adiabatic efficiency, η_n, which deals with the loss of kinetic energy in a nozzle, is related to the nozzle total pressure ratio, π_n, following:

$$\eta_n = \frac{1 - \dfrac{h_9}{h_{t7}}}{1 - \dfrac{h_{9s}}{h_{t7}}} = \frac{1 - \dfrac{h_9}{h_{t7}}}{1 - \left(\dfrac{p_9}{p_{t7}}\right)^{\frac{\gamma-1}{\gamma}}} = \frac{1 - \left(\dfrac{p_9}{p_{t9}}\right)^{\frac{\gamma-1}{\gamma}}}{1 - \left(\dfrac{p_9}{p_{t7}}\right)^{\frac{\gamma-1}{\gamma}}} \tag{1.123}$$

It is interesting to note that as the nozzle exit total pressure, p_{t9}, approaches the value of the nozzle inlet total pressure, p_{t7}, the nozzle adiabatic efficiency will approach 1. We

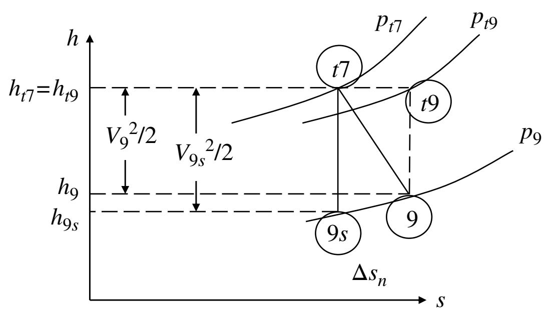

Figure 1.17 Enthalpy-entropy (h-s) diagram of nozzle flow expansion.

may treat Eq. (1.123) as an equation with one unknown, p_{t9}. Therefore, for a given nozzle exit static pressure, p_9, and the nozzle inlet total pressure, p_{t7}, the nozzle adiabatic efficiency, η_n, will result in a knowledge of the total pressure at the exit of the nozzle, p_{t9}. Now, if we multiply the numerator and denominator of the right-hand side of the Eq. (1.123) by $\left(p_{t7}/p_9\right)^{\frac{\gamma-1}{\gamma}}$, we will reach our goal of relating the two figures of merit in a nozzle, i.e.

$$\eta_n = \frac{\left(\dfrac{p_{t7}}{p_9}\right)^{\frac{\gamma-1}{\gamma}} - \pi_n^{-\frac{\gamma-1}{\gamma}}}{\left(\dfrac{p_{t7}}{p_9}\right)^{\frac{\gamma-1}{\gamma}} - 1} \tag{1.124}$$

There are three parameters in Eq. (1.124). The two figures of merit, η_n and π_n, and the ratio of nozzle inlet total pressure to the nozzle exit static pressure, p_{t7}/p_9. The last parameter is a known quantity, as we know the nozzle inlet total pressure, p_{t7}, from the upstream component analysis (in a turbojet, it is the turbine, $p_{t7} = p_{t5}$) and the nozzle exit pressure, p_9, is a direct function of the nozzle area ratio, A_9/A_8. To express the Eq. (1.124) in terms of the NPR, we may split p_{t7}/p_9 into

$$\frac{p_{t7}}{p_9} = \frac{p_{t7}}{p_0}\frac{p_0}{p_9} = NPR.\left(\frac{p_0}{p_9}\right) \tag{1.125}$$

Substituting the above expression in Eq. (1.124), yields:

$$\eta_n = \frac{\left\{NPR\left(\dfrac{p_0}{p_9}\right)\right\}^{\frac{\gamma-1}{\gamma}} - \pi_n^{-\frac{\gamma-1}{\gamma}}}{\left\{NPR\left(\dfrac{p_0}{p_9}\right)\right\}^{\frac{\gamma-1}{\gamma}} - 1} \tag{1.126}$$

A plot of Eq. (1.126) is shown in Figure 1.18 for a perfectly expanded nozzle, i.e. $p_9 = p_0$.

In Eq. (1.126), the nozzle adiabatic efficiency will approach 1, as the nozzle total pressure ratio approaches 1. The parameter p_0/p_9 represents a measure of mismatch between the nozzle exit static pressure and the ambient static pressure. For $p_9 > p_0$ the flow is considered to be *underexpanded*. For $p_9 < p_0$, the flow is defined as *overexpanded*. In the underexpanded scenario, the nozzle area ratio is not adequate, i.e. not large enough, to expand the gas to the desired ambient static pressure. In the overexpanded nozzle flow case, the nozzle area ratio is too large for the perfect expansion. As noted earlier, a perfectly expanded nozzle will have $p_0 = p_9$; therefore, Eq. (1.126) is further simplified to:

$$\eta_n = \frac{\{NPR\}^{\frac{\gamma-1}{\gamma}} - \pi_n^{-\frac{\gamma-1}{\gamma}}}{\{NPR\}^{\frac{\gamma-1}{\gamma}} - 1} \tag{1.127}$$

For a perfectly expanded nozzle. It is instructive to show the three cases of nozzle expansion, i.e. under-, over-, and perfectly expanded cases, on an h-s diagram (see Figure 1.19).

We note in Figure 1.19, that all nozzle expansions are depicted as irreversible processes with an associated entropy rise; therefore *perfect expansion* is not to be mistaken as *perfect (isentropic) flow*.

In summary, we learned that:

- The primary function of a nozzle is to accelerate the gas efficiently.
- The gross thrust parameter, F_g, signifies nozzle's contribution to the thrust production.
- The gross thrust reaches a maximum when the nozzle is perfectly expanded; i.e. $p_9 = p_0$.
- Real nozzle flows may still be considered as adiabatic.
- A NPR that causes a Mach-1 flow at the throat (i.e. choking condition) is called the *critical nozzle pressure ratio*, and as a rule of thumb, we may remember an $(NPR)_{crit}$ of ~2.
- There are two efficiency parameters that quantify losses or the degree of irreversibility in a nozzle, and they are related.
- Nozzle losses manifest themselves as the total pressure loss.
- All subsonic exhaust streams have $p_{jet} = p_{ambient}$.

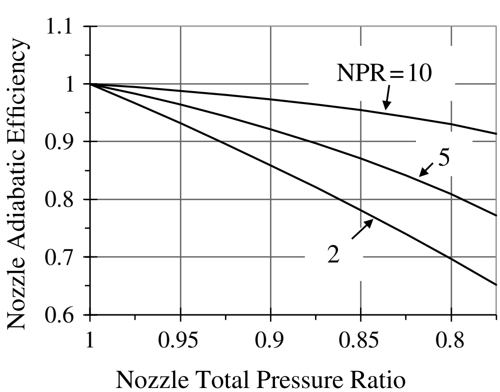

Figure 1.18 Two figures of merit in a nozzle plotted as a function of NPR ($\gamma = 1.33$).

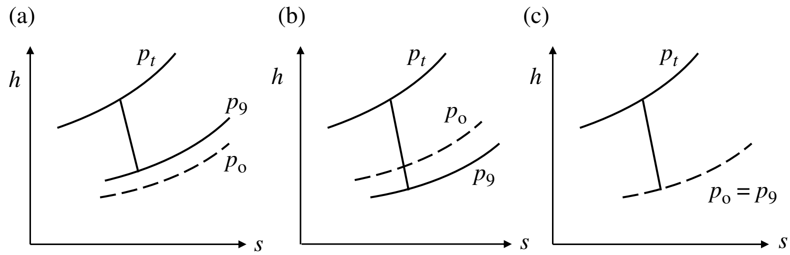

Figure 1.19 Enthalpy-entropy (h-s) diagram for the three possible nozzle expansions: (a) underexpanded; (b) overexpanded; (c) perfectly expanded.

- A perfect nozzle expansion means that the nozzle exit (static) pressure and the ambient pressure are equal.
- An imperfect nozzle expansion is caused by a mismatch between the nozzle area ratio and the altitude of operation.
- Underexpansion is caused by smaller-than-necessary nozzle area ratio, leading to $p_9 > p_0$.
- Overexpansion is caused by larger-than-necessary nozzle area ratio, leading to $p_9 < p_0$.

1.6.3 The Compressor

The thermodynamic process in a gas generator begins with the mechanical compression of air in the compressor. As the compressor discharge contains higher energy gas, i.e. the compressed air, it requires *external power* to operate. The power is delivered to compressor from the turbine via a shaft, as shown in Figure 1.2, in an operating gas turbine engine. Other sources of external power may be used to *start* the engine, which are in the form of electric motor, air-turbine, and hydraulic starters. The flow of air in a compressor is considered to be an essentially adiabatic process, which suggests that only a *negligible* amount of heat transfer takes place between the air inside and the ambient air outside the engine. Therefore, even in a real compressor analysis, we will still treat the flow as adiabatic.

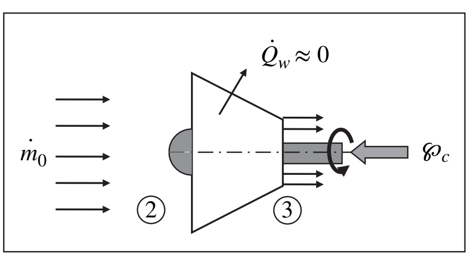

Perhaps a more physical argument in favor of neglecting the heat transfer in a compressor can be made by examining the order of magnitude of the energy transfer sources in a compressor. The power delivered to the medium in a compressor is achieved by one or more rows of rotating blades (called rotors) attached to one or more spinning shafts (typically referred to as *spools*). Each rotor blade, which changes the *spin* (or swirl) of a medium, will experience a countertorque as a reaction to its own action on the fluid.

If we denote the rotor torque as τ, then the power delivered to the medium by the rotor spinning at the angular speed, ω, follows Newtonian mechanics, namely

$$\wp = \tau . \omega \tag{1.128}$$

A typical axial-flow compressor contains hundreds of rotor blades (assembled in several stages), which interact with the medium according to Eq. (1.128). Therefore, the rate of mechanical energy transfer in a typical modern compressor is usually measured in megaWatt (MW) and is several orders of magnitude larger than heat transfer through the compressor wall. Symbolically, we may present this as:

$$\wp_c >>> \dot{Q}_w \tag{1.129}$$

As a real process, however, the presence of wall friction acting on the medium through the boundary layer and shock waves caused by the relative supersonic flow through compressor blades will render the process inside the compressor irreversible. The measure of irreversibility in a compressor may be thermodynamically defined through some form of compressor efficiency. There are two methods of compressor efficiency definitions:

- compressor adiabatic efficiency, η_c
- compressor polytropic efficiency, e_c

To define the compressor adiabatic efficiency, η_c, we depict a "real" compression process on an h-s diagram, as shown in Figure 1.20 and compare it to an ideal, i.e. isentropic, process. The state $t2$ represents the *total* (or stagnation) state of the gas entering the compressor, typically designated by p_{t2} and T_{t2}. An actual flow in a compressor will follow the solid line from $t2$ to $t3$ thereby experiencing an entropy rise in the process, Δs_c. The actual total state of the gas is designated by $t3$ in Figure 1.20. The ratio p_{t3}/p_{t2} is known as the compressor pressure ratio, with a shorthand notation, π_c. The compressor total temperature ratio is depicted by the shorthand notation, $\tau_c \equiv T_{t3}/T_{t2}$. Since the state $t3$ is the actual state of the gas at the exit of the compressor and is not achieved via an isentropic process, we cannot expect the isentropic relation between τ_c and π_c, to hold, i.e.

$$\tau_c \neq \pi_c^{\frac{\gamma-1}{\gamma}} \tag{1.130}$$

Figure 1.20 Enthalpy-entropy (h-s) diagram of an actual and ideal compression process.

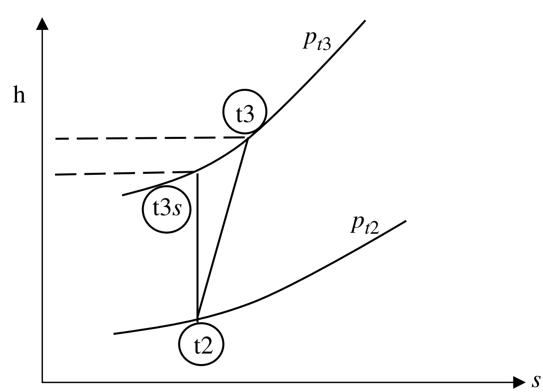

It can be seen from Figure 1.20 that the actual τ_c is higher than the ideal, i.e. isentropic, τ_c, which is denoted by the end state, T_{t3s}. This fact actually helps with the exponent memorization in a real compression process. The compressor adiabatic efficiency is the ratio of the ideal power required to the power consumed by the compressor, i.e.

$$\eta_c \equiv \frac{h_{t3s} - h_{t2}}{h_{t3} - h_{t2}} = \frac{\Delta h_{t,\text{isentropic}}}{\Delta h_{t,\text{actual}}} \tag{1.131}$$

The numerator in Eq. (1.131) is the power-per-unit mass flow rate in an *ideal compressor* and the denominator is the power-per-unit mass flow rate in the actual compressor. If we divide the numerator and denominator of Eq. (1.131) by h_{t2}, we get:

$$\eta_c = \frac{T_{t3s} / T_{t2} - 1}{T_{t3} / T_{t2} - 1} \tag{1.132}$$

Since the thermodynamic states $t3$s and $t2$ are on the same isentrope, the temperature and pressure ratios are then related via the isentropic formula:

$$\frac{T_{t3s}}{T_{t2}} = \left(\frac{p_{t3s}}{p_{t2}}\right)^{\frac{\gamma-1}{\gamma}} = \left(\frac{p_{t3}}{p_{t2}}\right)^{\frac{\gamma-1}{\gamma}} = \pi_c^{\frac{\gamma-1}{\gamma}} \tag{1.133}$$

Therefore, compressor adiabatic efficiency may be expressed in terms of compressor pressure and temperature ratios as:

$$\eta_c = \frac{\pi_c^{\frac{\gamma-1}{\gamma}} - 1}{\tau_c - 1} \tag{1.134}$$

Equation (1.134) involves three parameters, η_c, π_c, and τ_c. It can be used to calculate τ_c for a given compressor pressure ratio and adiabatic efficiency. As compressor pressure ratio and efficiency are typically known (π_c is a design parameter and η_c is assumed efficiency), the only unknown in Eq. (1.134) is τ_c.

A second efficiency parameter in a compressor is the *polytropic efficiency*, e_c. As might be expected, compressor adiabatic and polytropic efficiencies are related. The definition of compressor polytropic efficiency is:

$$e_c \equiv \frac{dh_{ts}}{dh_t} \tag{1.135}$$

It is interesting to compare the definition of compressor adiabatic efficiency, involving finite jumps (Δh_t), and the polytropic efficiency, which takes infinitesimal steps (dh_t). The conclusion can be reached that the polytropic efficiency is actually the adiabatic efficiency of a compressor with *small* pressure ratio. Consequently, compressor polytropic efficiency is also called *small-stage efficiency*. From the combined first and second law of thermodynamics, we have

$$T_t ds = dh_t - \frac{dp_t}{\rho_t} \tag{1.136}$$

We deduce that for an isentropic process, i.e. $ds = 0$, $dh_t = dh_{ts}$ and therefore

$$dh_{ts} = \frac{dp_t}{\rho_t} \tag{1.137}$$

If we substitute Eq. (1.137) in (1.135) and replace density with pressure and temperature from the perfect gas law, we get

$$e_c = \frac{\dfrac{dp_t}{p_t}}{\dfrac{dh_t}{RT_t}} = \frac{\dfrac{dp_t}{p_t}}{\dfrac{C_p dT_t}{RT_t}} = \frac{\dfrac{dp_t}{p_t}}{\dfrac{\gamma}{\gamma-1}\dfrac{dT_t}{T_t}} \tag{1.138}$$

$$\frac{dp_t}{p_t} = \frac{\gamma e_c}{\gamma-1}\frac{dT_t}{T_t} \tag{1.139}$$

which can now be integrated between the inlet and exit of the compressor to yield:

$$\frac{p_{t3}}{p_{t2}} = \pi_c = \left(\frac{T_{t3}}{T_{t2}}\right)^{\frac{\gamma e_c}{\gamma-1}} = \left(\tau_c\right)^{\frac{\gamma e_c}{\gamma-1}} \tag{1.140}$$

To express the compressor total temperature ratio in terms of compressor pressure ratio and polytropic efficiency, Eq. (1.140) can be rewritten as:

$$\tau_c = \pi_c^{\frac{\gamma-1}{\gamma e_c}} \tag{1.141}$$

The presence of e_c in the denominator of the above exponent (Eq. (1.141)) causes the exponent of π_c to be larger than its isentropic exponent (which is $\frac{\gamma-1}{\gamma}$), therefore

$$\tau_{c,\text{real}} \succ \tau_{c,\text{isentropic}} \quad \text{or} \quad T_{t3} > T_{t3s} \tag{1.142}$$

The physical argument for higher actual T_t than the isentropic T_t (to achieve the same compressor pressure ratio) can be made on the ground that *lost work* to overcome the irreversibility in the real process (friction, shock) is converted into heat therefore, a higher exit T_t is reached in a real machine due to dissipation. On the other hand, for a given compressor pressure ratio, π_c, an ideal compressor consumes less power than an actual compressor (the factor being η_c, as defined earlier). Again, the absence of dissipative mechanisms, leading to *lost work*, is cited as the reason for a reversible flow machine to require less power to run.

We relate the two types of compressor efficiency description, e_c and η_c, as

$$\eta_c = \frac{\pi_c^{\frac{\gamma-1}{\gamma}} - 1}{\tau_c - 1} = \frac{\pi_c^{\frac{\gamma-1}{\gamma}} - 1}{\pi_c^{\frac{\gamma-1}{\gamma . e_c}} - 1} \tag{1.143}$$

Equation (1.143) is plotted in Figure 1.21.

The compressor adiabatic efficiency, η_c, is a function of compressor pressure ratio, while the polytropic efficiency is independent of it. Consequently in a cycle analysis, we

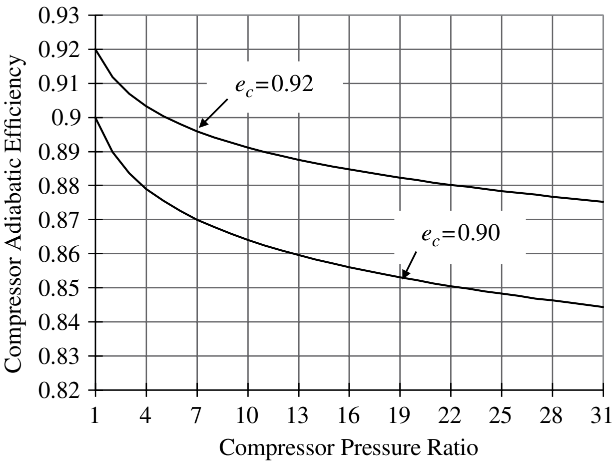

Figure 1.21 Variation of compressor adiabatic efficiency with the pressure ratio and polytropic efficiency.

usually assume the polytropic efficiency, e_c, as the figure of merit for a compressor (and turbine) and then we may keep e_c as constant in our engine off-design analysis. Typical values for the polytropic efficiency in modern compressors range in the 90–92%.

In summary, we have learned that:

- A real compressor flow may be considered adiabatic, i.e. $\dot{Q}_{\text{compressor}} \approx 0$.
- The energy transfer to the fluid due to shaft, in a compressor, is several orders of magnitude higher than any heat transfer that takes place through the casing; thus, heat transfer is neglected.
- Viscous dissipation in the wall boundary layer and shocks account for the sources of irreversibility in a compressor.
- Two figures of merit describe the compressor efficiency, the adiabatic compressor efficiency, η_c, and the polytropic or small-stage efficiency, e_c.
- The two compressor efficiencies are interrelated, i.e. $\eta_c = \eta_c(\pi_c, e_c)$.
- The compressor polytropic efficiency is independent of compressor pressure ratio, π_c.
- The compressor adiabatic efficiency is a function of π_c and decreases with increasing pressure ratio.
- To achieve a high pressure ratio in a compressor, multistaging and multispool configurations are needed.
- In a gas turbine engine, the compressor power is derived from a shaft that is connected to a turbine.

1.6.4 The Combustor

In the combustor, the air is mixed with the fuel and an *exothermic* chemical reaction ensues, resulting in a heat release. The ideal burner is considered to behave like a reversible heater, which means very slow burning, $M_b \approx 0$, and with no friction acting on its walls. Under such circumstances, the combustor total pressure remains constant.

In a real combustor, however, due to wall friction, turbulent mixing and chemical reaction at finite Mach number, the total pressure drops, i.e.

$$\pi_b = \frac{p_{t4}}{p_{t3}} \prec 1 \quad \text{“}\mathbf{Real}\text{ combustion chamber”} \tag{1.144}$$

$$\pi_b = 1 \quad \text{“}\mathbf{Ideal}\text{ combustion chamber”} \tag{1.145}$$

Kerrebrock (1992) gives an approximate expression for π_b in terms of the average Mach number of the gas in the burner, M_b, as

$$\pi_b \approx 1 - \varepsilon \frac{\gamma}{2} M_b{}^2 \quad \text{where} \quad 1 \prec \varepsilon \prec 2 \tag{1.146}$$

The total pressure loss in a burner is then proportional to the average dynamic pressure of the gases inside the burner, i.e. $\propto \frac{\gamma}{2} M_b{}^2$, where the proportionality coefficient is ε. Assuming an average Mach number of gases of 0.2 and $\varepsilon = 2$, we get $\pi_b \approx 0.95$ (for a $\gamma \approx 1.33$). This formula is obviously not valid for supersonic combustion throughflow; rather, it points out the merits of *slow* combustion in a conventional burner. A schematic diagram of a combustion chamber, and its essential components, is shown in Figure 1.22.

A preliminary discussion of the components of the combustion chamber is useful at this time. The inlet diffuser decelerates the compressor discharge flow to a Mach number of about 0.2–0.3. The low-speed flow will provide an efficient burning environment in the combustor. Mixing improvement with the fuel in the combustor primary zone is achieved via the air swirler. A recirculation zone is created that provides the necessary stability in the primary combustion zone (i.e. by increasing residence time). To create a fuel-rich environment in the primary zone to sustain combustion, a large percentage of air is diverted around a dome-like structure. The airflow that has bypassed the burner primary zone will enter the combustor mainly as the cooling flow through a series of cooling and dilution holes (as shown). The fuel–air mixture is ignited in the combustor primary zone via an igniter properly positioned in the dome area.

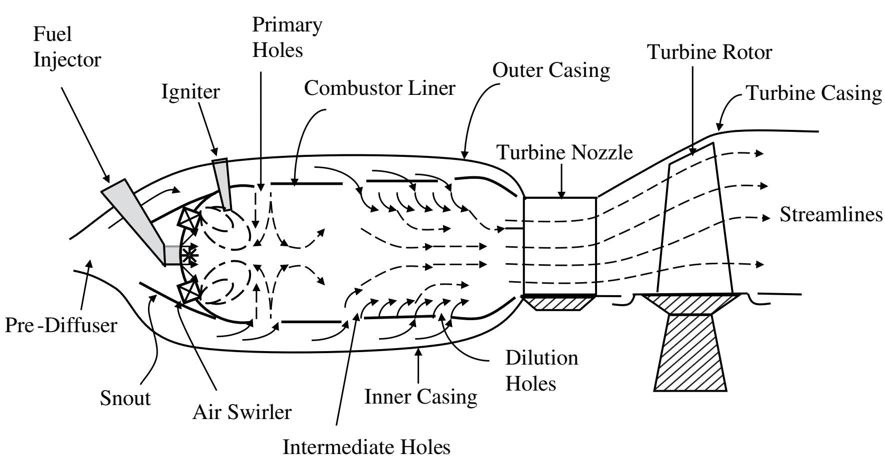

Figure 1.22 Components of a conventional combustion chamber and the first turbine stage.

For the purposes of *cycle analysis*, a combustor flow is only analyzed at its inlet and outlet. Thus, we will not consider the details of combustion processes such as atomization, vaporization, mixing, chemical reaction, and dilution in the cycle analysis phase. Nor do we consider pollutant formation and the means of reducing them in this chapter. A block diagram representation of a combustor, useful in cycle analysis, is shown in Figure 1.23.

Figures 1.23a,b are the steady-state mass and the energy balance applied to the combustion chamber, i.e.

$$\dot{m}_4 = \dot{m}_0 + \dot{m}_f = \dot{m}_0\left(1+f\right) \tag{1.147}$$

where f is the fuel-to-air ratio, $f \equiv \dfrac{\dot{m}_f}{\dot{m}_0}$, and energy balance in Figure 1.23b gives:

$$\dot{m}_0 h_{t3} + \dot{m}_f Q_R \eta_b = \left(\dot{m}_0 + \dot{m}_f\right)\mathrm{h}_{t4} = \dot{m}_0\left(1+f\right)h_{t4} \tag{1.148}$$

The fuel is characterized by its *energy content per unit mass*, i.e. the amount of thermal energy inherent in the fuel, capable of being released in a chemical reaction. This parameter is heat of reaction and is given the symbol, Q_R. The unit for this parameter is energy/mass, which in the metric system is $\mathrm{kJ\,kg^{-1}}$ and in the British system of units is $\mathrm{BTU\,lbm^{-1}}$. In an actual combustion chamber, primarily due to volume limitations, the entirety of the Q_R cannot be realized. The fraction that can be realized is called *burner efficiency* η_b. Therefore,

$$\eta_b \equiv \frac{Q_{R,\mathrm{Actual}}}{Q_{R,\mathrm{Ideal}}} \tag{1.149}$$

The ideal heat of reaction or lower heating value of typical hydrocarbon fuels (e.g. Jet-A), to be used in our cycle analysis, are:

$$Q_R \simeq 43000\,\mathrm{kJ\,kg^{-1}} \quad \text{or} \quad Q_R \simeq 18600\,\mathrm{BTU\,lbm^{-1}} \tag{1.150a}$$

However, the most energetic fuel (on mass basis) is the hydrogen, which is capable of releasing roughly three times the energy of typical hydrocarbon fuels per unit mass, i.e.

$$Q_R \simeq 127500\,\mathrm{kJ\,kg^{-1}} \quad \text{or} \quad Q_R \simeq 55400\,\mathrm{BTU\,lbm^{-1}} \tag{1.150b}$$

However, there are major drawbacks in fuels such as hydrogen. The low molecular weight of hydrogen makes it the lightest fuel, even in liquid form (LH_2), with a density

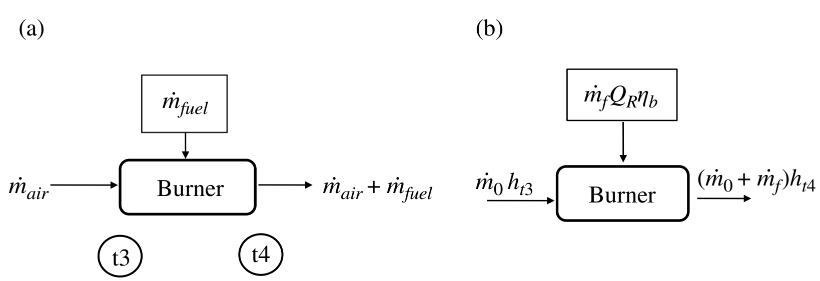

Figure 1.23 Block diagram of a burner with mass and energy balance: (a) mass balance; (b) energy balance.

ratio of about 1/10 of typical hydrocarbon fuels, such as Jet-A. This implies a comparatively very large volume requirement for LH_2. Consequently, *volumetric efficiency* (energy/volume) of the hydrogen is the lowest of all fuels. Second, hydrogen in liquid form is cryogenic, which means a very low boiling point temperature, i.e. −423 °F or 20 K at ambient pressure. The cryogenic aspect of hydrogen requires thermally insulated fuel tanks, fuel lines, valves, and the associated weight penalty. Therefore, due to space/volume limitations and fuel system requirement, current commercial aviation uses fossil fuel (e.g. Jet-A) instead of hydrogen. In hypersonic air-breathing propulsion as well as in rockets, LH_2 has been a fuel of choice since its cryogenic property can be used in regenerative cooling of the vehicle.

Typically in modern gas turbine engines, the burner efficiency can be as high as 98–99%. In a cycle analysis, we need to make assumptions about the loss parameters in every component, which in a combustion chamber are: $\pi_b < 1$ and $\eta_b < 1$. The real and ideal combustion process can be depicted on a T-s diagram, which later will be used to perform cycle analysis. Figure 1.24 shows the burner thermodynamic process on a T-s diagram.

The isobars, p_{t3} and p_{t4}, drawn at the entrance and exit of the combustor in Figure 1.24, clearly show a total pressure drop in the burner, $\Delta p_{t,\,\text{burner}}$. The maximum temperature limit, T_{t4} is governed by the level of cooling technology, material selection and the thermal protective coating used in the turbine. Typical current values for the maximum T_{t4} is about 3200–3600 °R or 1775–2000 K.

Another burner parameter is the temperature rise, ΔT_t, across the combustion chamber, as shown in Figure 1.24. The thermal power invested in the engine (by the fuel) is proportional to the temperature rise across the combustor, i.e. it is nearly equal to: $\dot{m}_0 c_p \left(\Delta T_t\right)_{burner}$.

The application of energy balance across the burner will yield the fuel-to-air ratio, f, as the only unknown parameter. To derive an expression for the fuel-to-air ratio, we will divide Eq. (1.148) by $\dot{m}_0$, the air mass flow rate, to get:

$$h_{t3} + fQ_R\eta_b = (1+f)h_{t4} \tag{1.151}$$

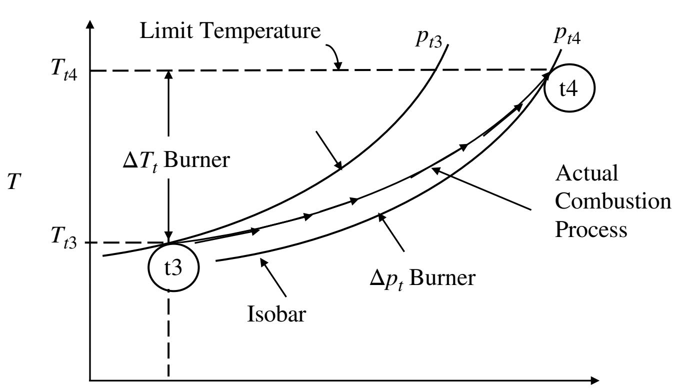

Figure 1.24 Actual flow process in a burner (note total pressure loss, Δp_t, across the burner).

The unknown parameter, f, can be isolated and expressed as:

$$f = \frac{h_{t4} - h_{t3}}{Q_R \eta_b - h_{t4}} \tag{1.152}$$

Knowing the fuel property, Q_R, assuming burner efficiency, η_b, and having specified a turbine inlet temperature, T_{t4}, the denominator of Eq. (1.152) is fully known. The compressor discharge temperature, T_{t3}, is established via compressor pressure ratio, efficiency, and inlet condition, as described in the compressor section, which renders the numerator of Eq. (1.152) fully known as well. Therefore, application of energy balance to a burner, usually results in the establishment of fuel-to-air ratio parameter, f. It is customary to express Eq. (1.152) in terms of nondimensional parameters, by dividing each term in the numerator and denominator by the flight static enthalpy, h_0, to get:

$$f = \frac{\dfrac{h_{t4}}{h_0} - \dfrac{h_{t3}}{h_0}}{\dfrac{Q_R \eta_b}{h_0} - \dfrac{h_{t4}}{h_0}} = \frac{\tau_\lambda - \tau_r \tau_c}{\dfrac{Q_R \eta_b}{h_0} - \tau_\lambda} \tag{1.153}$$

where we recognize the product $\tau_r \tau_c$ as h_{t3}/h_0 and τ_λ as the cycle thermal limit parameter, h_{t4}/h_0.

In summary, we learned that:

- The fuel is characterized by its lower heating value, Q_R (maximum releasable thermal energy per unit mass).
- The burner is characterized by its efficiency, η_b, and its total pressure ratio, π_b.
- Burning at finite Mach number, frictional losses on the walls, and turbulent mixing are identified as the sources of irreversibility, i.e. losses, in a burner.
- The fuel-to-air ratio, f, and the burner exit temperature, T_{t4}, are the thrust control/engine design parameters.
- The application of the energy balance across the burner yields either f or T_{t4}.

1.6.5 The Turbine

The high pressure and temperature gas that leaves the combustor is directed into a turbine. The turbine may be thought of as a *valve,* because on one side, it has a high-pressure gas and on the other side, it has a low-pressure gas of the exhaust nozzle or the tailpipe. Therefore the first *valve*, i.e. the throttle station, in a gas turbine engine is at the turbine. The throat of an exhaust nozzle in a supersonic aircraft is the second and final throttle station in an engine. Thus, the flow process in a turbine (and exhaust nozzle) involves significant (static) pressure drop, and in harmony with it, the (static) temperature drop, which is called *flow expansion*. The flow expansion produces the necessary power for the compressor and the propulsive power for the aircraft. The turbine is connected to the compressor via a common shaft (see Figure 1.25), which provides the shaft power to the compressor. In drawing an analogy, we can think of the expansion process in a gas turbine engine as the counterpart of *power stroke* in an intermittent combustion engine. However in a turbine, the power transmittal is continuous.

Due to high temperatures of the combustor exit flow, e.g. 1600–2000 K, the first few stages of the turbine, i.e. the HPT, need to be cooled. The coolant is the air bleed from

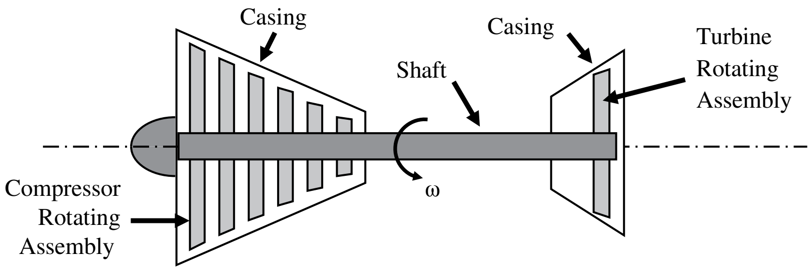

Figure 1.25 Common shaft in a gas generator connects the compressor and turbine (ω is the shaft angular speed in rad s^{-1} or rpm).

the compressor, which may be bled from different compression stages, e.g. between the LPC and HPC and/or at the compressor exit. It has been customary however to analyze an *uncooled* turbine in the preliminary cycle analysis, then followed by an analysis of the cycle with cooling effects in the turbine and the exhaust nozzle. Other cooling media, such as water, have been used in stationary gas turbine power plants. However, in a design-to-weight environment of aircraft, carrying extra water to cool the turbine blades is not feasible. A cooling solution, which uses the engine cryogenic fuel, such as hydrogen or methane, as the coolant to cool the engine and aircraft components is called *regenerative cooling* and has proven its effectiveness in liquid propellant chemical rocket engines for decades.

A real flow process in an uncooled turbine involves irreversibility such as frictional losses in the boundary layer, tip clearance flows, and shock losses in transonic turbine stages. The viscous dominated losses, i.e. boundary layer separation, reattachment, and tip vortex flows, are concentrated near the end walls; thus, a special attention in turbine flow optimization is made on the *end-wall* regions. Another source of irreversibility in a real turbine flow is related to the cooling losses. Coolant is typically injected from the blade attachment (to the hub or casing) into the blade, which provides internal convective cooling and usually external film cooling on the blades. The turbulent mixing associated with the coolant stream and the hot gases is the primary mechanism for (the turbine stage) cooling losses.

The thermodynamic process for an uncooled turbine flow may be shown in an h-s diagram (see Figure 1.26). The actual expansion process in the turbine is depicted by the solid line connecting the total (or stagnation) states $t4$ and $t5$ (see Figure 1.26). The isentropically reached exit state, $t5s$, represents the ideal, loss-free flow expansion in the turbine to the same backpressure, p_{t5}. The relative height, on the enthalpy scale in Figure 1.26, between the inlet total and outlet total condition of the turbine represents the power production potential (i.e. ideal) and the actual power produced in a turbine. The ratio of these two heights is called the turbine adiabatic efficiency, η_t, i.e.

$$\wp_{\text{t,actual}} = \dot{m}_t \left(h_{t4} - h_{t5}\right) = \dot{m}_t \Delta h_{t,\text{actual}} \tag{1.154}$$

$$\wp_{\text{t,ideal}} = \dot{m}_t \left(h_{t4} - h_{t5s}\right) = \dot{m}_t \Delta h_{t,\text{isentropic}} \tag{1.155}$$

$$\eta_t \equiv \frac{h_{t4} - h_{t5}}{h_{t4} - h_{t5s}} = \frac{\Delta h_{t,\text{actual}}}{\Delta h_{t,\text{isentropic}}} \tag{1.156}$$

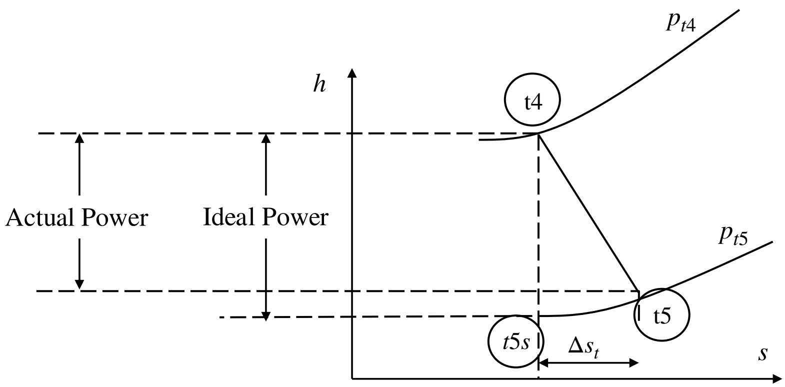

Figure 1.26 Expansion process in an uncooled turbine (note the entropy rise across the turbine, Δs_t).

In Eqs. (1.154) and (1.155), the turbine mass flow rate is identified as $\dot{m}_t$, which accounts for the air and fuel mass flow rate that emerge from the combustor and expand through the turbine, i.e.

$$\dot{m}_t = \dot{m}_0 + \dot{m}_f = (1 + f)\dot{m}_0 \tag{1.157}$$

The numerator in Eq. (1.156) is the actual power produced in a *real uncooled turbine* and the denominator is the *ideal* power that in a reversible and adiabatic turbine could be produced. If we divide the numerator and denominator of Eq. (1.156) by h_{t4}, we get:

$$\eta_t = \frac{1 - T_{t5}/T_{t4}}{1 - T_{t5s}/T_{t4}} \tag{1.158}$$

Since the thermodynamic states $t5s$ and t4 are on the same isentrope, the temperature and pressure ratios are then related via the isentropic formula, i.e.

$$\frac{T_{t5s}}{T_{t4}} = \left(\frac{p_{t5s}}{p_{t4}}\right)^{\frac{\gamma-1}{\gamma}} = \left(\frac{p_{t5}}{p_{t4}}\right)^{\frac{\gamma-1}{\gamma}} = \pi_t^{\frac{\gamma-1}{\gamma}} \tag{1.159}$$

Therefore, turbine adiabatic efficiency may be expressed in terms of the turbine total pressure and temperature ratios as:

$$\eta_t = \frac{1 - \tau_t}{1 - \pi_t^{\frac{\gamma-1}{\gamma}}} \tag{1.160}$$

We may also define a *small-stage* efficiency for a turbine, as we did in a compressor, and call it the turbine polytropic efficiency, e_t. For a small expansion, representing a small stage, we can replace the finite jumps, i.e. Δs, with incremental step, *d*, in Eq. (1.156) and write:

$$e_t \equiv \frac{dh_t}{dh_{ts}} = \frac{dh_t}{\frac{dp_t}{\rho_t}} \tag{1.161}$$

Expressing enthalpy in terms of temperature and specific heat at constant pressure as $dh_t = C_p dT_t$, which is suitable for a perfect gas, and simplify Eq. (1.161) similar to the compressor section, we get:

$$\tau_t = \pi_t^{\frac{(\gamma-1)e_t}{\gamma}} \quad \text{or} \quad \pi_t = \tau_t^{\frac{\gamma}{(\gamma-1)e_t}} \tag{1.162}$$

$$\tau_t \equiv T_{t5} / T_{t4} \tag{1.163}$$

$$\pi_t \equiv p_{t5} / p_{t4} \tag{1.164}$$

We note that in Eq. (1.162), in the limit of e_t approaching 1, i.e. isentropic expansion, we will recover the isentropic relationship between the temperature and pressure ratio, as expected. Replacing π_t in Eq. (1.159) by its equivalent expression (from Eq. (1.162)), we derive a relation between the two types of turbine efficiencies, η_t and e_t, as

$$\eta_t = \frac{1-\tau_t}{1-\tau_t^{1/e_t}} \tag{1.165}$$

Equation (1.165) is plotted in Figure 1.27. For a small-stage efficiency of 90%, i.e. $e_t = 0.90$, the turbine adiabatic efficiency, η_t, grows with the inverse of turbine expansion parameter, $1/\tau_t$.

The temperature ratio parameter, τ_t, across the turbine is established via a power balance between the turbine, compressor, and other shaft power extraction (e.g. electric generator) on the gas generator. Let us first consider the power balance between the turbine and compressor in its simplest form and then try to build on the added parameters. Ideally, the compressor absorbs all the turbine shaft power, i.e.

$$\wp_t = \wp_c \tag{1.166a}$$

$$\dot{m}_0(1+f)(h_{t4}-h_{t5}) = \dot{m}_0(h_{t3}-h_{t2}) \tag{1.166b}$$

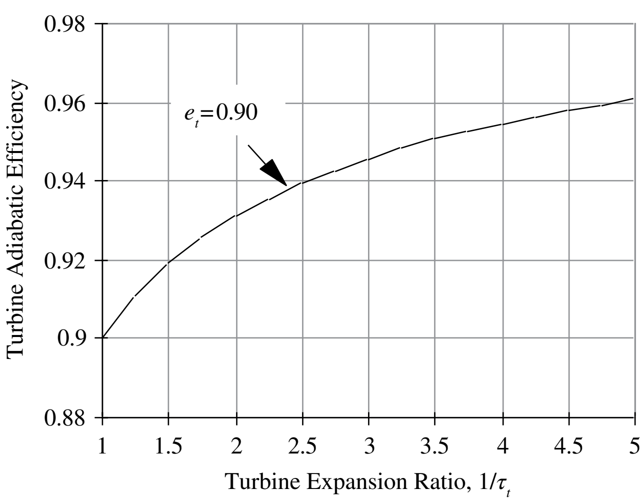

Figure 1.27 Variation of turbine adiabatic efficiency, η_t, with the inverse of turbine expansion ratio, $1/\tau_t$.

which simplifies to the following nondimensional form:

$$(1+f)\tau_\lambda(1-\tau_t)=\tau_r(\tau_c-1) \tag{1.166c}$$

The only unknown in the above equation is τ_t, as all other parameters either flow from upstream components, e.g. combustor will provide f, the compressor produces τ_c, etc. or are design parameters such as τ_λ or τ_r. Hence, the turbine expansion parameter, τ_t, is:

$$\tau_t=1-\frac{\tau_r(\tau_c-1)}{(1+f)\tau_\lambda} \tag{1.166d}$$

Next, we consider the practical issue of hydrodynamic (frictional) losses in bearings holding the shaft in place and provide dynamic stability under operating conditions to the rotating assemblies of turbine and compressor. Therefore, a small fraction of the turbine power output is dissipated through viscous losses in the bearings, i.e.

$$\wp_{\mathrm{t}}=\wp_{\mathrm{c}}+\Delta\wp_{\mathrm{bearings}} \tag{1.167}$$

Where, $\Delta\wp_{\mathrm{bearings}}$ is the power loss due to bearings. In addition, an aircraft has electrical power needs for its flight control system and other aircraft subsystems, which requires tapping into the turbine shaft power. Consequently, the power balance between the compressor and turbine should account for the electrical power extraction, which usually accompanies the gas generator, i.e.

$$\wp_{\mathrm{t}}=\wp_{\mathrm{c}}+\Delta\wp_{\mathrm{bearing}}+\Delta\wp_{\mathrm{electric\ generator}} \tag{1.168a}$$

$$\wp_{\mathrm{c}}=\wp_{\mathrm{t}}-\Delta\wp_{\mathrm{bearing}}-\Delta\wp_{\mathrm{electric\ generator}} \tag{1.168b}$$

In a simple cycle analysis, it is customary to lump all power dissipation and power extraction terms into a single *mechanical efficiency* parameter, η_m, that is multiplied by the turbine shaft power, to derive the compressor shaft power, i.e.

$$\wp_{\mathrm{c}}=\eta_{\mathrm{m}}\wp_{\mathrm{t}} \tag{1.169}$$

where η_{m} is the mechanical efficiency parameter, which is assumed, e.g. $\eta_{\mathrm{m}}=0.995$.

An uncooled turbine is assumed to be adiabatic:

$$\wp_t=\dot{m}_0(1+f)(h_{t4}-h_{t5})$$

$$\pi_t\equiv\frac{p_{t5}}{p_{t4}}$$

$$\tau_t\equiv\frac{T_{t5}}{T_{t4}}$$

$$\wp_c=\eta_{\mathrm{m}}\wp_t$$

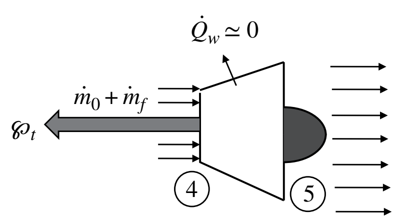

To cool the high-pressure turbine stages, a small fraction of compressor air can be diverted from various stages of the compression. Engine cooling is essentially a *pressure-driven* process, which calls for a pressure scheduling of the coolant to achieve the highest cooling efficiency. For example, to cool the first nozzle and the first rotor in a turbine, we need to tap the compressor exit air, as it has the *right* pressure. Earlier stages of the compressor have not yet developed the necessary pressure to overcome downstream pressure in the high-pressure end of a turbine. To cool the medium-pressure turbine stages, we need to divert compressor air from the medium-pressure compressor. Therefore, the problem of *pressure matching* between the coolant stream and the hot gas in a turbine is real and significant. The consequence of a mismatch is either inadequate cooling flow in a turbine blade with a possibility of even a *reverse flow* of hot gases into the cooling channels or the need for excessive throttling of the coolant stream and associated cycle losses. Figure 1.28 shows the schematic drawing of turbine blade-casing cooling.

We can simplify the investigation of the thermodynamics of cooled turbine stages significantly by assuming that each blade row coolant is discharged at the blade row exit, i.e. trailing edge ejection. This simplifies the thermodynamics as we consider *dumping* the entire coolant used in a given blade row at the trailing edge of the blades and then apply conservation laws to the coolant-hot gas mixing process. This approach avoids the discrete coolant-hot gas mixing that may be distributed over the suction and pressure surfaces of the blade row, as in film-cooled blades. Application of the energy equation to the coolant-hot gas mixing process will result in a lower mixed-out temperature for the hot gas. Consequently, the hot-gas stream will experience a reduced entropy state after mixing with the coolant. In return, the coolant stream, which is heated by the hot gas, will experience an entropy rise. The expansion process in a turbine with two cooled stages followed by an uncooled low-pressure turbine is depicted in an h-s diagram in Figure 1.29. The mixing process at the exit of each blade row is identified with negative entropy production and the cooling path is roughly drawn in as a nearly constant pressure process. In contrast, the coolant stream will undergo a heating process from the blade and then through mixing with the hot gases in the turbine. The thermodynamic state of the coolant is shown in Figure 1.29.

The h-s diagram for the hot gas (shown in Figure 1.29) shows a constant h_t process for the first and second turbine nozzle. Constant total enthalpy indicates an adiabatic process with no mechanical energy exchange. These two criteria are met in an uncooled turbine nozzle, which is stationary and consequently exchanges no mechanical energy with the fluid. Across the nozzle, due to frictional and shock losses, a total pressure

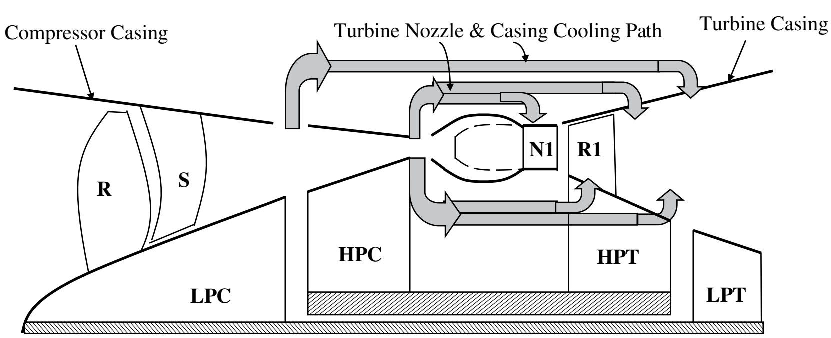

Figure 1.28 Two-spool GT engine with two stations of compressor bleed for cooling purposes (LPC: low-pressure compressor, HPC: high-pressure compressor, HPT: high-pressure turbine, LPT: low-pressure turbine, R: rotor, S: stator, N: nozzle).

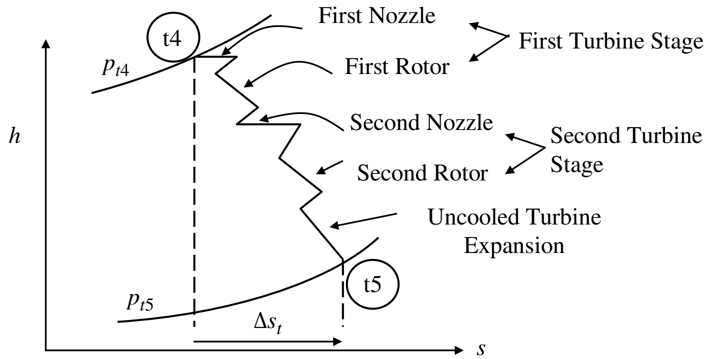

Figure 1.29 Enthalpy-entropy (h-s) diagram for a turbine with two cooled stages followed by an uncooled LPT (A negative Δ*s* and a temperature drop indicate blade row exit mixing with the coolant).

drop is indicated in Figure 1.29. The cooling process results in a lower total temperature of the mixture of hot and cold gas, as well as a total pressure drop due to turbulent mixing of the two streams. This process can be seen in Figure 1.30. The drop of total enthalpy across the rotor is proportional to the shaft power production by the rotor blade row. This shaft power may be written as:

$$\wp_{\text{rotor}} = \tau_{\text{rotor}}\,\omega = \dot{m}_{\text{rotor}}\,\Delta h_t \tag{1.170}$$

The product of rotor torque τ, and the angular speed, ω, of the rotor is the shaft power. The irreversibility in the flow through the rotor is shown via a process involving entropy rise across the rotor in Figure 1.30. Again, the flow expansion after the rotor is cooled by the blade row coolant. To establish the mixed-out state of the coolant and the hot gas, we will apply the conservation principles, as noted earlier. The law of conservation of energy applied to a coolant stream of $\dot{m}_c$ mass flow rate carrying a total enthalpy of $h_{t,c}$ mixing with a hot gas stream of $\dot{m}_g$ with a total enthalpy of $h_{t,g}$ is written as:

$$\dot{m}_c h_{t,c} + \dot{m}_g h_{t,g} = \left(\dot{m}_c + \dot{m}_g\right) h_{t,\text{mixed-out}} \tag{1.171}$$

where the only unknown is the mixed-out enthalpy state of the coolant-hot gas mixture, $h_{t,\text{mixed-out}}$. In nondimensional form, Eq. (1.171) is:

$$\frac{h_{t,\text{mixed out}}}{h_{t,g}} = \frac{1+\dfrac{\dot{m}_c}{\dot{m}_g}\dfrac{h_{t,c}}{h_{t,g}}}{1+\dfrac{\dot{m}_c}{\dot{m}_g}} \approx \left(1-\frac{\dot{m}_c}{\dot{m}_g}\right)\left(1+\frac{\dot{m}_c}{\dot{m}_g}\frac{h_{t,c}}{h_{t,g}}\right) \tag{1.172}$$

In Eq. (1.172), two nondimensional parameters emerge that basically govern the energetics of a hot and a cold mixture:

- $\dfrac{\dot{m}_c}{\dot{m}_g}$ The coolant mass fraction (typically ~10%), and
- $\dfrac{h_{t,c}}{h_{t,g}}$ Cold-to-hot total enthalpy ratio (typically, ~0.5)

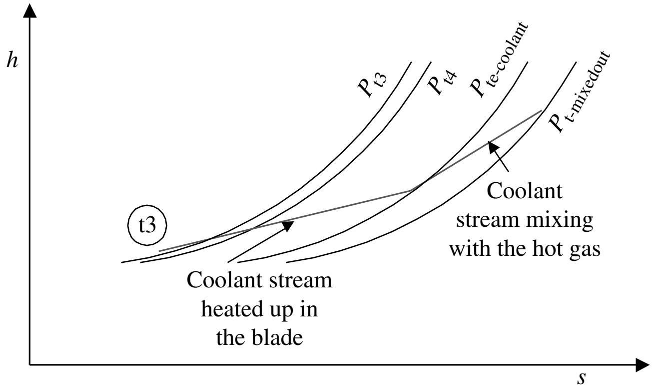

Figure 1.30 h-s diagram of the coolant stream, first inside the blade, then mixing with the hot turbine gas.

We have also used a mathematical approximation in Eq. (1.172), in the form of binomial expansion:

$$\frac{1}{1+\varepsilon} \approx 1-\varepsilon \tag{1.173}$$

where $\varepsilon << 1$ and the largest neglected term in the series is $O(\varepsilon^2)$.

The coolant stream experiences a total pressure drop in the cooling channels of the blade as a result of frictional losses and a total pressure drop as a result of turbulent mixing with the hot gas. The enthalpy-entropy diagram for the coolant stream is depicted in Figure 1.30.

In summary we learned that:

- The flow expansion in the turbine produces the needed shaft power for the compressor and other propulsion system needs, e.g. an electric generator.
- There are two figures of merit in a turbine, which measure the extent of irreversibility in a turbine, η_t and e_t, and they are related.
- The gas expansion in an uncooled turbine is treated as adiabatic.
- The frictional losses on the blades and the casing as well as any shock losses, in relative supersonic passages, are the sources of irreversibility in an uncooled turbine.
- Turbulent mixing losses between the coolant and the hot gas is an added source of irreversibility in a cooled turbine.
- The TET, T_{t4}, is a design parameter that sets the stage for the turbine material and cooling requirements.
- The power balance between the turbine, the compressor, and other known power drainage, establishes the turbine expansion ratio, τ_t.
- Cooling of the high-pressure turbine is achieved through compressor air bleed that is injected through the blade root in the rotor and the casing for the turbine nozzle.
- The turbine nozzle is choked (i.e. the throat Mach number is one), over a wide operating range of the engine, and as such is the first *throttle station* of the engine.

1.7 Performance Evaluation of a Turbojet Engine

The TJ performance parameters are:

- Specific thrust, $F / \dot{m}$
- Thrust-specific fuel consumption, TSFC, or specific impulse, I_s
- Thermal, propulsive, and overall efficiencies

Our approach to calculating the performance parameters of an aircraft engine is to *march through* an engine, component by component, until we calculate the target parameters, which are:

- Fuel-to-air ratio, f
- Exhaust velocity, V_9

Once we establish these unknowns, i.e. V_0, f, and V_9, the specific thrust, as a figure of merit for an aircraft engine, may be written as:

$$\frac{F_n}{\dot{m}_0} = (1+f)V_9 - V_0 + \frac{(p_9 - p_0)A_9}{\dot{m}_0} \tag{1.174}$$

This can be expressed in terms of the calculated parameters by recognizing that the air mass flow rate is only a factor $(1 + f)$ away from the exhaust mass flow rate, i.e.

$$\dot{m}_0 = \frac{\dot{m}_9}{1+f} = \frac{\rho_9 A_9 V_9}{1+f} = \frac{p_9 A_9 V_9}{RT_9(1+f)} \tag{1.175}$$

Now, substituting Eq. (1.175) in (1.174), we get:

$$\frac{F_n}{\dot{m}_0} = (1+f)V_9 - V_0 + \frac{(p_9 - p_0)A_9}{\dfrac{p_9 A_9 V_9}{RT_9(1+f)}} = (1+f)V_9 - V_0 + \frac{RT_9(1+f)}{V_9}\left(1 - \frac{p_0}{p_9}\right) \tag{1.176a}$$

Note that we have calculated all the terms on the RHS of the Eq. (1.176a), namely, f, V_9, V_0, and T_9. Therefore,

$$\frac{F_n}{\dot{m}_0} = (1+f)V_9 - V_0 + \frac{RT_9(1+f)}{V_9}\left(1 - \frac{p_0}{p_9}\right) \tag{1.176b}$$

The primary contribution to the specific thrust in an air-breathing engine comes from the first two terms in Eq. (1.176b), i.e. the momentum contribution. The last term would identically vanish if the nozzle is perfectly expanded, i.e. $p_9 = p_0$. Otherwise, its contribution is small compared to the momentum thrust.

It is very tempting to insert γ in the numerator and denominator of the last term in Eq. (1.176b), and identify the γRT_9 as the a_9^2 to recast the above equation in a more elegant form:

$$\frac{F_n}{\dot{m}_0} = (1+f)V_9\left(1 + \frac{1}{\gamma M_9^2}\left(1 - \frac{p_0}{p_9}\right)\right) - V_0 \tag{1.176c}$$

Thrust-specific fuel consumption was defined in a turbojet engine as:

$$TSFC \equiv \frac{\dot{m}_f}{F_n} = \frac{f}{F_n / \dot{m}_0} \tag{1.177}$$

and we have calculated the fuel-to-air ratio and the specific thrust, which are combined as in Eq. (1.177) to create the fuel efficiency parameter, or figure of merit, of the engine.

The engine overall efficiency can be recast in terms of the TSFC:

$$\eta_o = \frac{(F_n / \dot{m}_0)V_0}{fQ_R} = \frac{V_0 / Q_R}{TSFC} \tag{1.178a}$$

The inverse proportionality between the engine overall efficiency and the thrust-specific fuel consumption, i.e. the lower the specific fuel consumption, the higher the engine overall efficiency, is noted in Eq. (1.178a), i.e.

$$\eta_0 \propto \frac{1}{TSFC} \tag{1.178b}$$

In concluding the section on turbojet engines, it is appropriate to show a *real cycle* depicted on an T-s diagram. This is shown in Figure 1.31a,b.

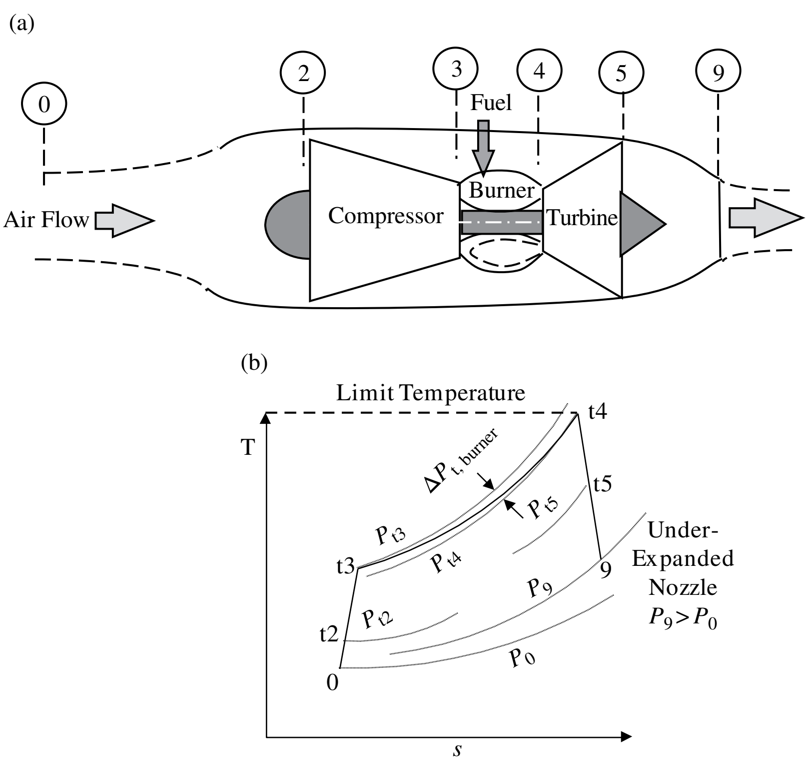

Figure 1.31 T-s diagram of a turbojet engine with component losses and Imperfect expansion in the nozzle: (a) a turbojet engine; (b) thermodynamic cycle of a turbojet engine.

1.8 Turbojet Engine with an Afterburner

1.8.1 Introduction

To augment the thrust of an aircraft gas turbine engine, an afterburner can be used. This solution is often sought in military aircraft, primarily due to its simplicity and effectiveness. It is interesting to note that an afterburner has the potential of nearly doubling the thrust produced in an aircraft gas turbine engine while in the process more than quadruple the engine fuel consumption rate. Figure 1.32 shows the schematics of an afterburning turbojet (AB-TJ) engine. The new station numbers 7 and 8 refer to the exit of the afterburner and the nozzle throat, respectively. Suitable nozzle geometry for an afterburning turbojet (or turbofan) engine is a *supersonic nozzle* with a convergent-divergent (C-D) geometry, i.e. a nozzle with a well-defined throat before a divergent cone or ramp. The throat Mach number is one, over a wide range of operating conditions, which is referred to as the *choked* throat. As the afterburner operation causes the gas temperature to rise, the gas density shall decrease in harmony with the temperature rise. Consequently, to accommodate the lower density gas at the sonic condition prevailing at the nozzle throat and satisfy continuity equation, the throat area needs to be opened. This is referred to as a *variable-geometry* nozzle requirement of the exhaust system. The continuity equation for a steady flow of a perfect gas is rewritten here to demonstrate the extent of the nozzle throat-opening requirement in a variable-geometry, convergent-divergent nozzle:

$$\dot{m} = \sqrt{\frac{\gamma}{R}} \cdot \frac{p_t}{\sqrt{T_t}} A.M. \left(\frac{1}{1 + \frac{\gamma - 1}{2} M^2} \right)^{\frac{\gamma+1}{2(\gamma-1)}} \tag{1.179}$$

Let us examine the various terms in Eq. (1.179), as a result of the afterburner operation. First, the mass flow rate increases slightly by the amount of $\dot{m}_{f,AB}$, which is but a small percentage of the gas flow with the afterburner-off condition, say 3–4%. The total pressure, p_t, drops with the afterburner operation, but this too is a small percentage, say 5–8%. The nozzle throat Mach number will remain as one; therefore, except for the gas

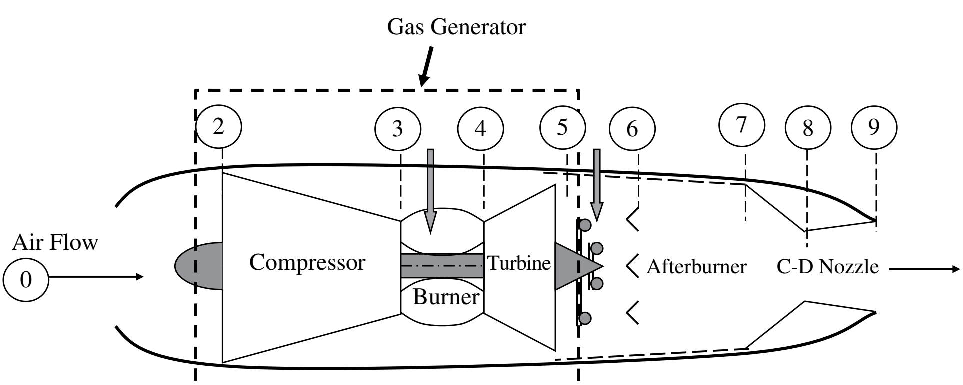

Figure 1.32 Schematic drawing of an afterburning turbojet engine.

property variation, the last parentheses in Eq. (1.179), will remain unchanged as a result of afterburner operation. Now, again neglecting small variations in the gas properties, γ and R, which are in reality a function of the gas temperature, the first term under the square root in Eq. (1.179) shall be unchanged. This brings us to the main driver for the nozzle throat area increase requirement when the afterburner is in operation, namely the gas total temperature, T_t. The effect of increasing T_t with afterburner operation is in creating lower density gas, which requires a larger area at the nozzle throat at sonic speed to accommodate the mass flow rate at lower density. Therefore, the nozzle throat area is opened directly proportional to the square root of the gas total temperature in the nozzle throat, i.e.

$$\frac{A_{8,AB-ON}}{A_{8,AB-OFF}} \approx \sqrt{\frac{T_{t8,AB-ON}}{T_{t8,AB-OFF}}} \tag{1.180}$$

The afterburner is composed of an inlet diffuser, a fuel spray bar, a flameholder to stabilize the combustion, some cooling provisions, and a screech damper, as shown in Figures 1.32 and 1.33. The inlet diffuser decelerates the gas to allow for higher efficiency combustion in the afterburner. A similar prediffuser is found at the entrance to the primary burner. The fuel spray bar is typically composed of one or more rings with distinct fuel injection heads circumferentially distributed around the ring. The V-shaped flame holder ring(s) create a fuel–air mixture recirculation region in its turbulent wake, which allows for a stable flame front to be established. There is also a perforated liner, which serves two functions. One, it serves as a cooling conduit which blankets, i.e. protects, the outer casing from the hot combustion gases. Two, it serves as an acoustic liner, which dampens the high-frequency noise, i.e. screech, which is generated as a result of combustion instability.

An afterburner is considered to be an adiabatic duct with insulated walls, which essentially neglects the small heat transfer through the casing, as compared to energy release in the AB, due to combustion, i.e.

$$_5\left(\dot{Q}_{wall}\right)_7 \cong 0 \tag{1.181}$$

Figure 1.32 shows the basic building block of an afterburning turbojet is gas generator.

Additional parameters (beyond the simple turbojet engine) are needed to analyze the performance of an afterburning turbojet engine. These are related to the physical

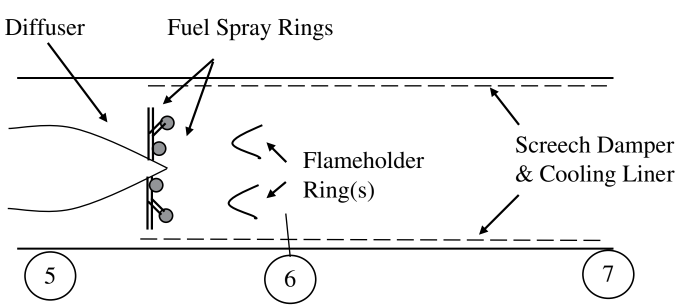

Figure 1.33 Schematic drawing of an afterburner with its station numbers.

Table 1.2 New parameters in afterburner.

1.	$Q_{R,\text{AB}}$	(Ideal) heating value of the fuel in the afterburner
2.	$\dot{m}_{f,\text{AB}}$ *or* T_{t7} *or* $\tau_{\lambda\text{-AB}} \equiv \dfrac{c_{p\text{AB}}T_{t7}}{c_{\text{pc}}T_0}$	Fuel flow rate or the exit temperature or $\tau_{\lambda\text{-AB}}$
3.	$\eta_{\text{AB}} \equiv \dfrac{(Q_{R,\text{AB}})_{\text{actual}}}{(Q_{R,\text{AB}})_{\text{ideal}}}$	Afterburner efficiency (<1)
4.	$\pi_{\text{AB}} \equiv \dfrac{p_{t7}}{p_{t5}}$	Total pressure ratio across the afterburner (<1)

characteristics of the afterburning system, e.g. the type of fuel used in the afterburner (which is typically the same as the fuel in the primary burner), either the fuel-flow setting of the afterburner fuel pump or the exit total temperature of the afterburner, the afterburner efficiency, and the afterburner total pressure loss.

Symbolically, we represent the new parameters in Table 1.2.

1.8.2 Analysis

A nondimensional T-s diagram for an ideal afterburning turbojet engine is shown in Figure 1.34. It is interesting to note the appearance of τ parameters on the nondimensional temperature axis. Also, we note that the thermodynamic process from the flight static, 0, to the turbine exit, i.e. $t5$, is unaffected by the afterburner. Although the T-s diagram depicts an ideal afterburning turbojet engine in Figure 1.34, the real engine afterburner is to operate with no *back influence* on the upstream components as well. We will continue using the *marching technique* in establishing the stagnation flow properties throughout the engine as we used in the turbojet section. The above stipulation, that the operation of an afterburner does not affect the upstream components, will bring our analysis, unchanged, to station $t5$. We will take up the analysis from station $t5$ and establish exit conditions at $t7$.

To allow marching through the afterburner, we need to know or estimate its losses in total pressure and its inefficiency in heat release in the confines of the finite volume of the afterburner. These are π_{AB} and η_{AB}, respectively. So far, the afterburner loss depiction through the total pressure and heat release capability is the same as the primary or main burner. However, unlike the primary burner, an afterburner may or may not be in operation, and this has a large influence on the total pressure loss characteristics of the afterburner. It is only obvious to expect the operating total pressure loss in the afterburner to be larger than the afterburner-off total pressure loss. One may think of it as the *compounding* of the burning losses as well as the frictional losses on the walls and the flame holder, which add up to the total pressure loss in an operating afterburner. Thus, we distinguish between $\pi_{\text{AB-Off}}$ and $\pi_{\text{AB-On}}$ by:

$$\pi_{\text{AB-Off}} \succ \pi_{\text{AB-On}} \tag{1.182}$$

We perform energy balance across the afterburner to establish the afterburner fuel-to-air ratio, f_{AB}:

$$\left(\dot{m}_0 + \dot{m}_f + \dot{m}_{f,\text{AB}}\right)h_{t7} - \left(\dot{m}_0 + \dot{m}_f\right)h_{t5} = \dot{m}_{f,\text{AB}}Q_{R,\text{AB}}\eta_{\text{AB}} \tag{1.183}$$

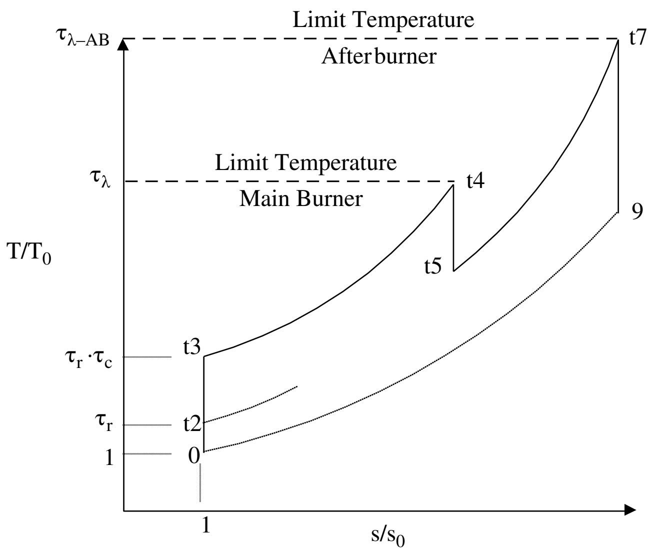

Figure 1.34 Nondimensional T-s diagram for an *ideal* afterburning turbojet engine.

Divide both sides by the air mass flow rate, $\dot{m}_0$, to get:

$$\left(1+f+f_{\mathrm{AB}}\right)h_{t7}-\left(1+f\right)h_{t5}=f_{\mathrm{AB}}Q_{R,\mathrm{AB}}\eta_{\mathrm{AB}} \tag{1.184}$$

Now, we can isolate f_{AB}, as:

$$f_{\mathrm{AB}}=\frac{\left(1+f\right)\left(h_{t7}-h_{t5}\right)}{Q_{R,\mathrm{AB}}\eta_{\mathrm{AB}}-h_{t7}}\approx\frac{\left(1+f\right)\left(T_{t7}-T_{t5}\right)}{\dfrac{Q_{R,\mathrm{AB}}\eta_{\mathrm{AB}}}{c_{p,\mathrm{AB}}}-T_{t7}} \tag{1.185}$$

where $c_{p\mathrm{AB}}$ represents an average specific heat at constant pressure in the afterburner, i.e. between the temperatures T_{t5} and T_{t7}.

The only unknown in Eq. (1.185) is the fuel-to-air ratio in the afterburner, as we had calculated all the upstream parameters, e.g. f, T_{t5}, values, and the afterburner fuel-heating value and the efficiency as well as the exit temperature are all specified. The total pressure at the afterburner exit, p_{t7}, is

$$p_{t7}=\pi_{\mathrm{AB}}\cdot p_{t5} \tag{1.186}$$

The operation of the afterburner changes the inlet conditions to the nozzle due to a change in mass flow rate, total pressure, and temperature. The mass flow rate due to the fuel in the afterburner is calculated via Eq. (1.185), the total pressure is calculated via Eq. (1.186), and the total temperature at the exit of the afterburner constitutes another thermal limit, which is often specified. The analysis of the nozzle, therefore, remains unchanged, except the nozzle inlet values are different as a result of the afterburner operation.

The fundamental definitions of the cycle thermal and propulsive efficiency as given earlier in the turbojet section remain the same for an afterburning turbojet engine as well:

$$\eta_{th} \equiv \frac{\Delta K\dot{E}}{\wp_{\text{thermal}}} = \frac{\Delta K\dot{E}}{\dot{m}_f .Q_R + \dot{m}_{f,\text{AB}}.Q_{R,\text{AB}}} \tag{1.187a}$$

$$\eta_{th} = \frac{\left(\dot{m}_0 + \dot{m}_f + \dot{m}_{f,\text{AB}}\right)\dfrac{V_9{}^2}{2} - \dot{m}_0\dfrac{V_0{}^2}{2}}{\dot{m}_f .Q_R + \dot{m}_{f,\text{AB}}.Q_{R,AB}} \tag{1.187b}$$

$$\eta_p \equiv \frac{F.V_0}{\Delta K\dot{E}} \tag{1.188a}$$

$$\eta_p = \frac{\left(F_n / \dot{m}_0\right)V_0}{\left(1 + f + f_{AB}\right)\dfrac{V_9{}^2}{2} - \dfrac{V_0{}^2}{2}} \tag{1.188b}$$

We may use chain rule on the nozzle total pressure ratio for a turbojet, according to:

$$\pi_n = \left\{\left(\pi_t\pi_b\pi_c\pi_d\pi_r\frac{p_0}{p_9}\right)^{\frac{\gamma-1}{\gamma}} - \eta_n\left[\left(\pi_t\pi_b\pi_c\pi_d\pi_r\frac{p_0}{p_9}\right)^{\frac{\gamma-1}{\gamma}} - 1\right]\right\}^{\frac{-\gamma}{\gamma-1}} \quad (\text{Turbojet}) \tag{1.189}$$

By inserting the π_{AB} in the total pressure chain, we get:

$$\pi_n = \left\{\left(\pi_{AB}\pi_t\pi_b\pi_c\pi_d\pi_r\frac{p_0}{p_9}\right)^{\frac{\gamma-1}{\gamma}} - \eta_n\left[\left(\pi_{AB}\pi_t\pi_b\pi_c\pi_d\pi_r\frac{p_0}{p_9}\right)^{\frac{\gamma-1}{\gamma}} - 1\right]\right\}^{\frac{-\gamma}{\gamma-1}} \quad (\text{AB TJ}) \tag{1.190}$$

The nozzle exit Mach number then becomes

$$M_9 = \sqrt{\frac{2}{\gamma-1}\left[\left(\pi_n\pi_{AB}\pi_t\pi_b\pi_c\pi_d\pi_r\frac{p_0}{p_9}\right)^{\frac{\gamma-1}{\gamma}} - 1\right]} \quad (\text{AB TJ}) \tag{1.191}$$

The nozzle exit velocity is

$$V_9 = a_0 M_9\sqrt{\frac{\tau_{\lambda,AB}}{1 + \dfrac{\gamma-1}{2}M_9^2}} \quad (\text{AB TJ}) \tag{1.192}$$

The specific thrust for an afterburning turbojet engine is:

$$\frac{F_n}{\dot{m}_o} = \left(1 + f + f_{AB}\right)V_9\left[1 + \frac{1 - \dfrac{p_0}{p_9}}{\gamma M_9^2}\right] - V_0 \quad (\text{AB TJ}) \tag{1.193}$$

TSFC for an afterburning turbojet engine is defined as:

$$TSFC \equiv \frac{\dot{m}_f + \dot{m}_{f,AB}}{F_n} = \frac{f + f_{AB}}{F_n / \dot{m}_0} \left(\text{AB TJ}\right) \tag{1.194}$$

1.9 Turbofan Engine

1.9.1 Introduction

To create a turbofan engine, a basic gas generator is followed by an additional turbine stage(s), which will tap into the exhaust stream thermal energy to provide shaft power to a fan. This arrangement of multiple loading demands on the turbine stages leads to a multiple shaft arrangement, referred to as *spools*. The fan stages and potentially several (low-pressure) compressor stages may be driven by a shaft, which is connected to the low-pressure turbine. The HPC stages are driven by the high-pressure turbine stage(s). The rotational speeds of the two shafts are called N_1 and N_2, respectively for the low-and high-pressure spools. An additional two new parameters enter our gas turbine vocabulary when we consider turbofan engines. The first is the *bypass ratio* and the second is the *fan pressure ratio*. The ratio of the flow rate in the fan *bypass duct* to that of the gas generator (i.e. the *core*) is called *the bypass ratio* α. The fan pressure ratio is the ratio of total pressure at the fan exit to that of the fan inlet. It is given the symbol, π_f.

$$\alpha \equiv \dot{m}_{\text{fan bypass}} / \dot{m}_{\text{core}} \tag{1.195}$$

$$\pi_f \equiv p_{t13} / p_{t2} \tag{1.196}$$

The principle behind the turbofan concept comes from sharing the power with a larger mass flow rate of air at a smaller velocity increment pays dividend at low speed flight. As we have seen earlier, the smaller the velocity increment across the engine, the higher the propulsive efficiency will be. This principle is Mach number independent; however, for supersonic flight the *installation drag* of large bypass ratio turbofan engines become excessive, and consequently, *small-frontal-area engines* are more suitable to high-speed flight. The fan exhaust stream may be separate from the *core* stream, which is then referred to as *separate exhaust turbofan engine*. Figure 1.35 shows the schematic drawing of a two-spool, separate-exhaust turbofan engine. Note that the gas generator is still the heart of this engine.

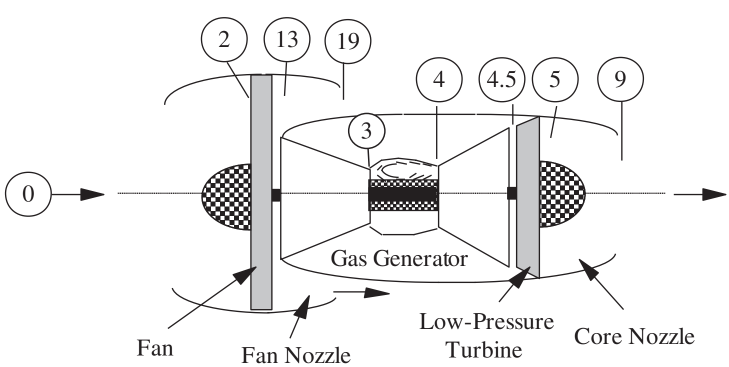

Figure 1.35 Schematic drawing of a separate-exhaust turbofan engine with two spools.

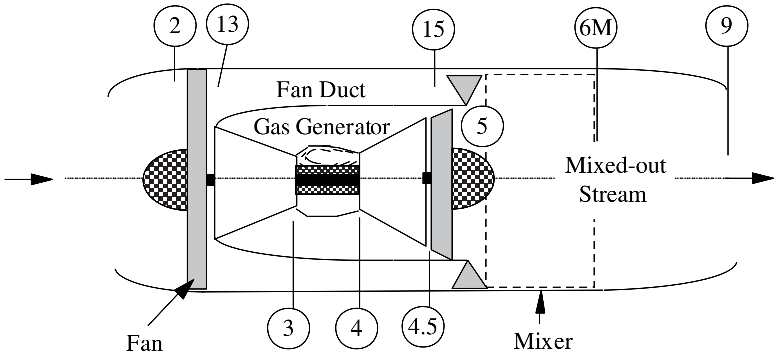

Figure 1.36 Schematic of a long-duct turbofan engine with a mixer.

It is possible to extend the fan duct and provide mixing of the fan and the core stream before entering a common exhaust nozzle. The weight penalty of the long-duct turbofan engine needs to be assessed against the thrust enhancement potential of mixing a cold and hot stream in a mixer before the exhaust nozzle. The schematic drawing of this configuration is shown in Figure 1.36.

1.9.2 Analysis of a Separate-Exhaust Turbofan Engine

In applying our marching technique developed in the analysis of a turbojet engine to a turbofan engine, we are confronted with the fan. As in a compressor, a fan is characterized by its pressure ratio and efficiency. Figure 1.37 shows the thermodynamics of fan compression on an h-s diagram.

The fan adiabatic efficiency is defined as:

$$\eta_f \equiv \frac{h_{t13s} - h_{t2}}{h_{t13} - h_{t2}} = \frac{\Delta h_{t,\text{isentropic}}}{\Delta h_{t,\text{actual}}} = \frac{\text{ideal power}}{\text{actual power}} \tag{1.197}$$

Upon dividing the numerator and denominator of Eq. (1.197) by h_{t2}, we get

$$\eta_f = \frac{T_{t13s}/T_{t2} - 1}{T_{t13}/T_{t2} - 1} = \frac{\pi_f^{\frac{\gamma-1}{\gamma}} - 1}{\tau_f - 1} \tag{1.198}$$

which relates the fan pressure and temperature ratio through adiabatic fan efficiency:

$$\tau_f = 1 + \frac{1}{\eta_f}\left(\pi_f^{\frac{\gamma-1}{\gamma}} - 1\right) \tag{1.199}$$

$$\pi_f = \left\{1 + \eta_f\left(\tau_f - 1\right)\right\}^{\frac{\gamma}{\gamma-1}} \tag{1.200}$$

The power balance between the turbine and compressor now includes the fan:

$$\eta_m \dot{m}_0 (1+f)(h_{t4} - h_{t5}) = \dot{m}_0 (h_{t3} - h_{t2}) + \alpha \dot{m}_0 (h_{t13} - h_{t2}) \tag{1.201}$$

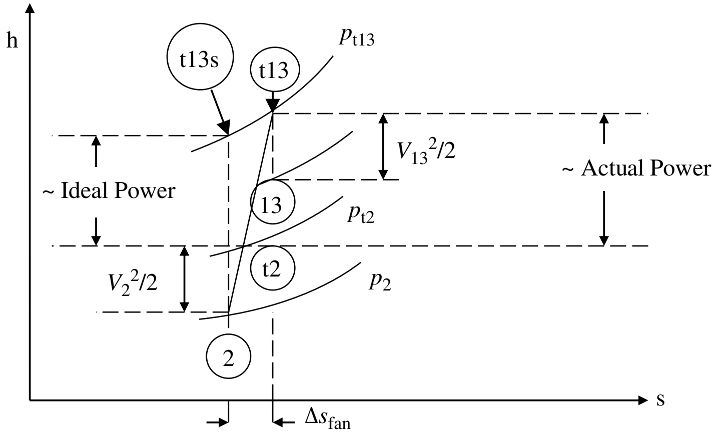

Figure 1.37 Enthalpy-entropy (h-s) diagram representing the flow process in an (adiabatic) fan.

Note that the mass flow rates in a turbofan engine are:

$\dot{m}_0$: Air mass flow rate through the engine core
$\alpha\dot{m}_0$: Air mass flow rate through the fan duct
$(1+\alpha)\dot{m}_0$: Air mass flow rate through the inlet (which later splits into core and the fan duct flow rates)
$\dot{m}_f$: The fuel flow rate in the main burner and the fuel-to-air ratio, f, is defined as $\frac{\dot{m}_f}{\dot{m}_0}$, as logically expected

This is depicted graphically in Figure 1.38.

From the power balance Eq. (1.201), the core mass flow rate $\dot{m}_0$ cancels out, and if we divide both sides by flight static enthalpy, h_0, to nondimensionalize the equation, we get:

$$\eta_m(1+f)\frac{h_{t4}}{h_0}(1-\tau_t)=\frac{h_{t2}}{h_0}\left[(\tau_c-1)+\alpha(\tau_f-1)\right] \tag{1.202}$$

We recognize the ratio of total enthalpy at the turbine inlet to the flight static enthalpy as $\tau_\lambda$and the ratio h_{t2}/h_0 as τ_r, and we proceed to isolate τ_t in terms of known quantities, namely

$$\tau_t=1-\frac{\tau_r\left[(\tau_c-1)+\alpha(\tau_f-1)\right]}{\eta_m(1+f)\tau_\lambda} \tag{1.203}$$

In Eq. (1.203), all the terms on the RHS are either directly specified, e.g. α,η_m, or τ_λ, or easily calculated from the given engine design parameters. The fuel-to-air ratio in a turbofan engine is expressed the same way as the fuel-to-air ratio in a turbojet engine, i.e.

$$f=\frac{\tau_\lambda-\tau_r\tau_c}{\frac{Q_R\eta_b}{h_0}-\tau_\lambda} \tag{1.204}$$

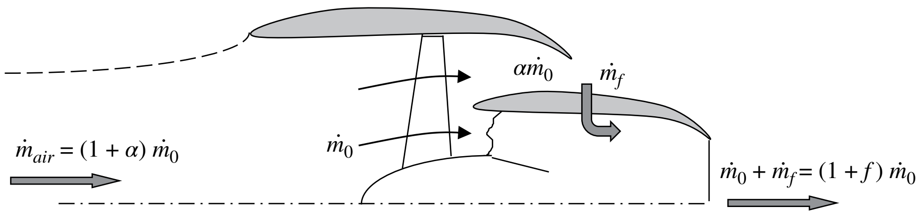

Figure 1.38 Definition sketch for various mass flow rates in a separate-exhaust turbofan engine.

The only point of caution in using Eq. (1.204) is to note that the fuel-flow rate is referenced to the airflow rate *in the core* of a turbofan engine and not the entire airflow rate through the inlet, which partially goes through the fan.

Note that the turbine expansion parameter, τ_t is a strong function of fan bypass ratio and the compressor pressure ratio, as fully expected. However, we note that under certain conditions of, say, large fan pressure ratio or the engine bypass ratio, we may end up in a negative turbine expansion! To see this, we split Eq. (1.203) into its rational constituents, namely:

$$\tau_t = 1 - \frac{\tau_r(\tau_c - 1)}{\eta_m(1+f)\tau_\lambda} - \frac{\tau_r\alpha(\tau_f - 1)}{\eta_m(1+f)\tau_\lambda} = 1 - A - B \tag{1.205}$$

where A and B are the second and third terms on the RHS of Eq. (1.205). Let us further rearrange Eq. (1.205) as follows:

$$1 - \tau_t = A + B \tag{1.206}$$

We note that $(1 - \tau_t)$ term that appears on the LHS of Eq. (1.206) is a nondimensional expression for the turbine power output:

$$1 - \tau_t = \frac{T_{t4} - T_{t5}}{T_{t4}} = \frac{\wp_t}{\dot{m}_t C_{pt} T_{t4}} \tag{1.207}$$

The quantity "A" represents the turbine expansion needed to power the compressor, as in the turbojet analysis. The magnitude of A is therefore independent of the fan bypass and pressure ratio. The last term in Eq. (1.205), namely, the B-term, represents the additional turbine expansion of gases needed to run the fan. Now, this is the term that could render Eq. (1.206) physically meaningless, i.e. lead to a negativeτ_t! We further note that the maximum expansion in an aircraft gas turbine engine is produced when the turbine exit pressure is equal to the ambient pressure, i.e. $p_{t5} = p_0$. This assumes that there is no *exhaust diffuser* downstream of the turbine (in place of the exhaust nozzle) as is customary in stationary gas turbine power plants. Therefore, not only a negative τ_t is impossible but also $1 - \tau_t \succ \frac{\wp_{t,\max}}{\dot{m}_t C_{pt} T_{t4}}$, based on the expansion beyond the ambient pressure, is impossible. All of these arguments are presented graphically in Figure 1.39.

In terms of fan pressure ratio, we show the α_{max} that a TF engine can support in Figure 1.40.

The question of thrust developed in a turbofan engine is best answered if we apply the momentum principles that we learned in the turbojet section to *two separate streams*

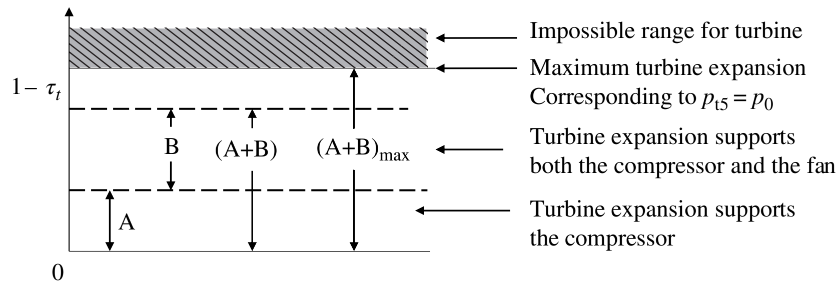

Figure 1.39 Turbine expansion possibilities, including the impossible range.

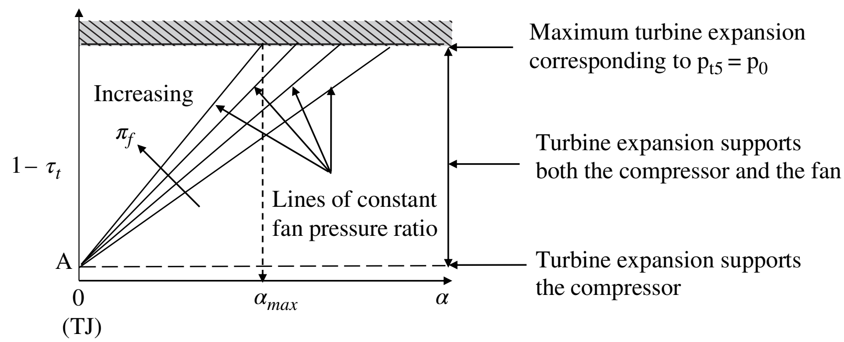

Figure 1.40 Variation of turbine power parameter $(1-\tau_t)$ with the fan bypass and pressure ratios.

and write the gross thrust for two nozzles and account for the entire ram drag through the inlet, namely:

$$F_n = \dot{m}_0(1+f)V_9 + \alpha\dot{m}_0V_{19} - (1+\alpha)\dot{m}_0V_0 + (p_9 - p_0)A_9 + (p_{19} - p_0)A_{19} \qquad (1.208)$$

We recognize the terms on the RHS of Eq. (1.208) as the two-nozzle momentum thrusts followed by the ram drag and then the pressure thrust of the primary and the fan nozzles. The specific thrust for a turbofan engine is the ratio of the net (uninstalled) thrust divided by the entire airflow rate through the inlet, i.e. specific thrust is:

$$\frac{F_n}{(1+\alpha)\dot{m}_0} = \frac{1+f}{1+\alpha}V_9 + \frac{\alpha}{1+\alpha}V_{19} - V_0 + \frac{(p_9 - p_0)A_9}{(1+\alpha)\dot{m}_0} + \frac{(p_{19} - p_0)A_{19}}{(1+\alpha)\dot{m}_0} \qquad (1.209)$$

We immediately note that the specific thrust drops for a turbofan engine (see $1+\alpha$ in the denominator of the LHS of Eq. (1.209)), in comparison to a turbojet engine that has zero bypass ratio, as more air is handled to produce the thrust in a bypass configuration. Therefore, this observation of lower specific thrust for a turbofan engine leads to the conclusion that bypass engines have by necessity larger frontal areas, again in comparison to a turbojet engine producing the same thrust. Now, we know that the larger frontal areas will result in a higher level of nacelle and installation drag. Therefore, the benefit of higher propulsive efficiency promised in a bypass engine should be carefully weighed against the penalties of higher installation drag for such configurations. The general conclusions are that for subsonic-transonic applications, the external drag penalty of a turbofan engine installation is significantly smaller than the benefits gained by higher engine propulsive efficiency. As a result, in a subsonic-transonic cruise civil transport, for example, the trend has been and continues to be in developing higher bypass ratio engines to reduce fuel burn and possibly use a gearbox on the low-pressure spool to better match the turbine efficiency. Ground clearance for an underwing installation poses the main constraint on the bypass ratio/engine envelope (especially on low-wing commercial aircraft). As the flight Mach number increases into supersonic regime, the optimum bypass ratio is then reduced. For a perfectly expanded primary and fan nozzles, the Eq. (1.209) simplifies to:

$$\frac{F_n}{(1+\alpha)\dot{m}_0} = \frac{1+f}{1+\alpha}V_9 + \frac{\alpha}{1+\alpha}V_{19} - V_0 \tag{1.210}$$

Applying the definition of specific fuel consumption to a turbofan engine, we get:

$$TSFC = \frac{\dot{m}_f}{F_n} = \frac{f}{F_n/\dot{m}_0} = \frac{f/(1+\alpha)}{F_n/(1+\alpha)\dot{m}_0} \tag{1.211}$$

1.9.3 Thermal Efficiency of a Turbofan Engine

The ideal cycle thermal efficiency η_{th} is unaffected by the placement of a fan stage in a gas generator where the fan discharge is then expanded in a nozzle. The reason is that the power utilized to compress the gas in the fan is balanced by the power turbine and therefore the net energy exchange in the bypass duct comes from the balance of the fan inlet and the fan nozzle. A perfectly expanded nozzle will recover the kinetic energy exchange of the inlet diffuser and thus the ideal thermal efficiency of a turbofan engine is unaffected. We can see this, for an ideal fan inlet and a nozzle, in the following T-s diagram shown in Figure 1.41.

Therefore, the thermal efficiency of an ideal turbofan engine is identical to a turbojet engine with the same overall cycle, pressure ratio:

$$\eta_{th} = 1 - \frac{1}{\tau_r \tau_c} = 1 - \frac{1}{\left(1+\frac{\gamma-1}{2}M_0^2\right)\pi_c^{\frac{\gamma-1}{\gamma}}} \tag{1.212}$$

For the real, i.e. nonideal, turbofan engine, we start from the definition of thermal efficiency:

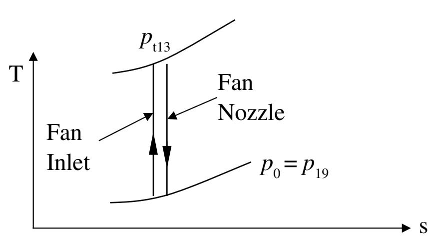

Figure 1.41 T-s diagram of a compression (fan) inlet stream followed by the expansion in a nozzle.

$$\eta_{th} \equiv \frac{\Delta K\dot{E}}{\dot{m}_f Q_R} = \frac{\alpha \dot{m}_0 \frac{V_{19}^2}{2} + (1+f)\dot{m}_0 \frac{V_9^2}{2} - (1+\alpha)\dot{m}_0 \frac{V_0^2}{2}}{\dot{m}_f Q_R} = \tag{1.213a}$$
$$\frac{\alpha V_{19}^2 + (1+f)V_9^2 - (1+\alpha)V_0^2}{2fQ_R} = \frac{(1+f)V_9^2 - V_0^2}{2fQ_R} + \alpha \frac{V_{19}^2 - V_0^2}{2fQ_R}$$

The RHS of Eq. (1.213a) identifies the bypass ratio, the two exhaust velocities, the fuel-to-air ratio, the fuel-heating value and the burner efficiency as the parameters in a turbofan engine that affect the thermal efficiency of the engine. The typical unknowns however, for the design point analysis of a turbofan engine with a given bypass ratio and a fuel type, are the two nozzle exhaust velocities and the combustor fuel-to-air ratio. We note from the last equality in Eq. (1.213a) that all the bypass contribution to engine cycle thermal efficiency is lumped in the last term and the core contribution is in the first term. Ideally, the lower kinetic energy of the core due to power drainage of the fan, i.e. the first term, appears as the kinetic energy rise in the bypass stream, i.e. the second term. Therefore, the thermal efficiency of a turbofan engine is ideally unaffected by the magnitude of the bypass stream.

The Eq. (1.213a) is correct for a turbofan engine with perfectly expanded nozzles. In case the exhaust nozzles are not perfectly expanded, we have to use *effective exhaust speeds* $V_{19\text{eff}}$ and $V_{9\text{eff}}$ in place of actual exit velocities V_{19} and V_9. We define the nozzle effective exhaust speed as:

$$V_{19\,\text{eff}} \equiv \frac{F_{g-\text{fan}}}{\dot{m}_{19}} \tag{1.213b}$$

$$V_{9\,\text{eff}} \equiv \frac{F_{g-\text{core}}}{\dot{m}_9} \tag{1.213c}$$

Example 1.1 shows the nearly constant thermal efficiency even for a TF engine with losses and underexpanded nozzles. Figure 1.42b shows the TF efficiencies.

1.9.4 Propulsive Efficiency of a Turbofan Engine

The propulsive efficiency of a turbofan engine, in contrast to the thermal efficiency of such engines, is a strong function of the engine bypass ratio. Start from the definition of propulsive efficiency:

$$\eta_p \equiv \frac{F_n V_0}{\Delta K\dot{E}} = \frac{\left[(1+f)V_9 + \alpha V_{19} - (1+\alpha)V_0 + (p_9 - p_0)A_9 + (p_{19} - p_0)A_{19}\right]V_0}{(1+f)\frac{V_{9eff}^2}{2} + \alpha \frac{V_{19eff}^2}{2} - (1+\alpha)\frac{V_0^2}{2}} \tag{1.214}$$

Assuming the nozzles are perfectly expanded and $f \ll 1$, Eq. (1.214) simplifies to:

$$\eta_p \approx \frac{2V_0\left[V_9 + \alpha V_{19} - (1+\alpha)V_0\right]}{V_9^2 + \alpha V_{19}^2 - (1+\alpha)V_0^2} \tag{1.215}$$

By dividing the numerator and denominator of Eq. (1.215) by V_0^2, we get

$$\eta_p \approx \frac{2\left[\left(\frac{V_9}{V_0}\right)+\alpha\left(\frac{V_{19}}{V_0}\right)-(1+\alpha)\right]}{\left(\frac{V_9}{V_0}\right)^2+\alpha\left(\frac{V_{19}}{V_0}\right)^2-(1+\alpha)} \tag{1.216}$$

In a turbofan engine, the propulsive efficiency seems to be influenced by three parameters, as shown in Eq. (1.216), the bypass ratio, α, the primary jet-to-flight velocity ratio, V_9/V_0, and the fan jet-to-flight velocity ratio, V_{19}/V_0. In case the fan nozzle and the primary nozzle velocities are equal, Eq. (1.216) reduces to

$$\eta_p \approx 2/(1+V_9/V_0) \tag{1.217}$$

Interestingly, this does not explicitly depend on the bypass ratio, α! The effect of bypass ratio is implicit however in the exhaust velocity reduction that appears in the denominator of Eq. (1.217). Again as noted earlier, if the nozzles are not perfectly expanded, we have to use the *effective exhaust speeds* instead of the "actual" velocities.

Example 1.1

For a parametric study of the effect of bypass ratio on the thermal, propulsive, and overall efficiencies of a separate-flow turbofan engine with convergent nozzles, we performed design-point cycle analysis using the following parameters:

Cycle overall pressure ratio, OPR, p_{t3}/p_0 ~61

Cruise altitude: 12 km ($p_0 = 19.19$ kPa, $T_0 = 216$ K)
Cruise Mach number of 0.80
Fan pressure ratio, p_{t13}/p_{t2}, of 1.6
Compressor pressure ratio (including inner fan), p_{t3}/p_{t2}, of 40
Turbine entry temperature (TET): 2000 K, which is high for cruise in current practice
Fuel LHV: 43.3 MJ kg^{-1}

Component efficiencies were assumed to be: $\pi_d = 0.995$, $e_f = 0.90$, $e_c = 0.90$, $\pi_{fn} = 0.98$, $\pi_b = 0.95$, $\eta_b = 0.99$, $e_t = 0.85$, $\eta_m = 0.99$, $\pi_n = 0.98$

Gas thermal properties: $\gamma_c = 1.4$, $c_{pc} = 1004$ J kgK^{-1}, $\gamma_t = 1.33$, $c_{pt} = 1156$ J kgK^{-1}

The range of bypass ratio (BPR) was: 5–17.

First, we look at the effect of bypass ratio on core and fan nozzle (effective) jet speeds in Figure 1.42a. The fan jet speed remains constant, as it is independent of bypass ratio. However, core effective jet speed is reduced with increasing bypass ratio. On energy basis, we are draining the energy from the core stream, as we supply more shaft power to a larger fan. The thermal, propulsive, and overall efficiencies of the turbofan engine are shown in Figure 1.42b. The propulsive efficiency continuously improves with BPR (with $\eta_{p,\max}$~76%), whereas thermal efficiency remains nearly constant (at ~45%), as the overall cycle pressure ratio is kept constant in this example. The overall engine efficiency improves with bypass ratio in harmony with propulsive efficiency.

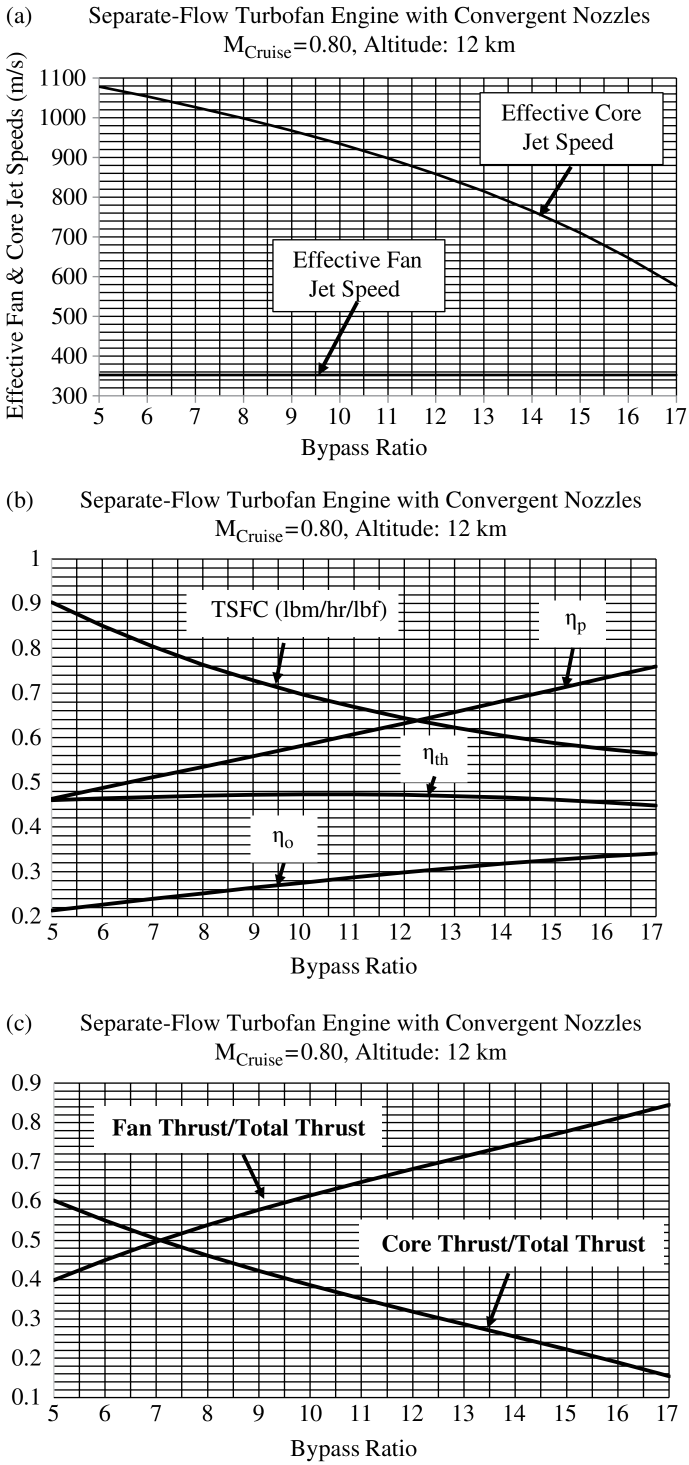

Figure 1.42 The effect of bypass ratio on TF-efficiency and fuel burn.

The fuel burn (TSFC) drops by nearly 40% as we increase the BPR. Finally, in Figure 1.42 (c) we have plotted the fraction of total thrust provided by fan and core as a function of BPR. The fan's share of thrust production steadily increases from nearly 40% to 84% as BPR increases from 5 to 17. The core loses thrust, as we drain the power from core stream and provide it to the fan; consequently, the core share of thrust drops from nearly 60% to about 15%.

Based on this simple example, we can deduce the direction that industry is pursuing in achieving fuel burn improvements; namely, push toward higher BPR, i.e. ultra-high BPR or UHB. By performing similar parametric studies for OPR or TET, we note the direction that industry must follow in those parameters, namely push toward higher OPR and higher TET. There are other parameters that we did not examine, e.g. the use of renewable fuel instead of fossil fuel, hybrid gas-electric propulsion, and finally, electric propulsion.

Comments

We note that the peak overall efficiency is still (dismal) 34%. The implication for this example of GT-propulsor, with $\eta_{o,\max}$~0.34, is that ~66% of the thermal power invested in the combustor by the fuel $\left(\dot{m}_f Q_R\right)$ was not converted to thrust power ($F_n V_0$). This wasted energy appears as the heat in the (hot) exhaust jet from the core! For the best case, i.e. BPR = 17, we calculated the disparity between the core and the fan nozzle exit temperatures:

Core (primary nozzle) exit temperature: $T_8 \sim 840\,\mathrm{K}$ $\quad T_{t8} \sim 978\,\mathrm{K}$
Fan nozzle exit temperature: $T_{18} \sim 236\,\mathrm{K}$ $\quad T_{t18} \sim 283\,\mathrm{K}$

The jet velocities (for BPR = 17) are comparable and are listed here for reference.

Core exhaust jet speed: $V_8 \sim 566\,\mathrm{m\,s^{-1}}$ $\quad V_{8,\mathrm{eff}} \sim 577\,\mathrm{m\,s^{-1}}$
Fan nozzle exhaust jet speed: $V_{18} \sim 308\,\mathrm{m\,s^{-1}}$ $\quad V_{18,\mathrm{eff}} \sim 353\,\mathrm{m\,s^{-1}}$

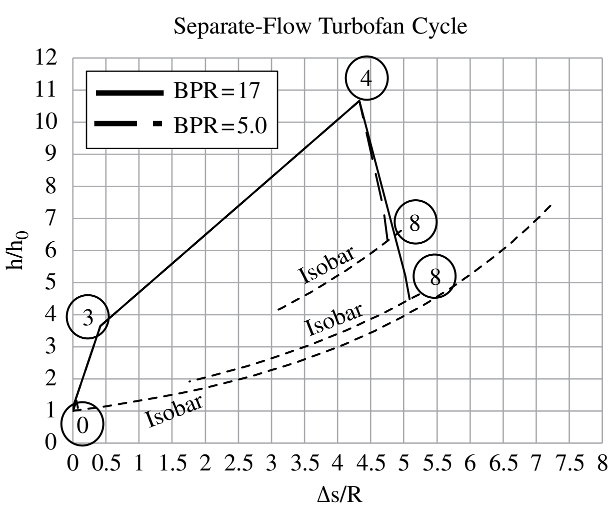

Figure 1.43 The effect of bypass ratio on thermodynamics of a turbofan cycle.

Finally, we note that the low overall efficiency in this turbofan engine is not caused by its low component efficiencies; rather, it is due to the thermal efficiency limitations of Brayton cycle. We ran the same engine at max-BPR (in this example, it was 17), and assumed ideal components throughout the engine and we produced the whopping $\eta_{o,\ max}$~38%. It is instructive to plot the h-s diagram of the TF cycle. Figure 1.43 shows Brayton cycle for two BPRs of 5 and 17. Note the core nozzle in both cycles ($\alpha = 5$ and 17) is underexpanded. Turbine in $\alpha = 17$ produces more power; thus, its exit temperature is lower than BPR 5.0 case. Propulsive efficiency improved by ~64% and the overall efficiency by ~60% with BPR.

1.9.5 Ultra-High Bypass (UHB) Geared Turbofan Engines

There is a new class of turbofan engines, called ultra-high bypass, or UHB, that promises to reduce fuel consumption (by nearly −16% as compared to International Aero Engines V2500 as baseline), cut noise (by −20 dB margin to FAA Stage 4 Aircraft Noise Standards), and produce less pollutants/emissions. Typical bypass ratio in this class starts around 12. To make a comparison to the advanced turboprops (ATPs) that were developed in 1980s and 1990s (also known as Propfan or Unducted Fan); they had bypass ratios of 35–70 (GE-UDF had a bypass ratio of 35 and the P&W/AGT had a bypass ratio of 70). Therefore, the UHB turbofan engines of 2010 fall between the current conventional turbofans with bypass ratio in 6–8 range and the ATP of 35–70. We had learned that propulsive efficiency improved with bypass ratio in a turbofan engine in subsonic aircraft. We derived an expression for the thrust-specific fuel consumption in a jet engine (see Farokhi 2014) that was inversely proportional to propulsive efficiency, η_p, namely:

$$TSFC = \frac{V_0 / Q_R}{\eta_p \eta_{th}} \tag{1.218}$$

Therefore, UHB development mainly targets propulsive efficiency improvements to reduce fuel consumption as well as offering other attractive features (e.g. reduced noise and pollution). Airline industry and commercial cargo business/transporters are most affected by the fuel consumption performance as it represents the lion's share of their direct operating cost (DOC). So, it stands to reason to increase the bypass ratio as long as we can innovate our way through the technology challenges associated with the UHB engines. The practical problems of developing/implementing a high-efficiency large bypass ratio turbofan engine are inherent in operational disparity between a large-diameter fan and a very small engine core diameter, i.e. LPT and intermediate pressure compressor (IPC) have much smaller diameters than the fan, yet driven by the same shaft (i.e. the low-pressure spool).

To improve the efficiency of the fan, IPC, and LPT, we need a suitable (i.e. lightweight, reliable) fan drive gear system.

The UHB turbofan installation concerns on aircraft are mainly (i) wing/fuselage integration, clearance/envelope, limits on fan diameter; (ii) transonic nacelle drag calling for a "slim line" nacelle design with natural laminar flow or hybrid laminar flow (i.e. with boundary layer suction); (iii) nacelle weight concerns demanding the use of advanced composite materials; and (iv) innovative fan reverser design and integration into nacelle. Pratt & Whitney and NASA have worked closely to develop the geared turbofan (GTF)

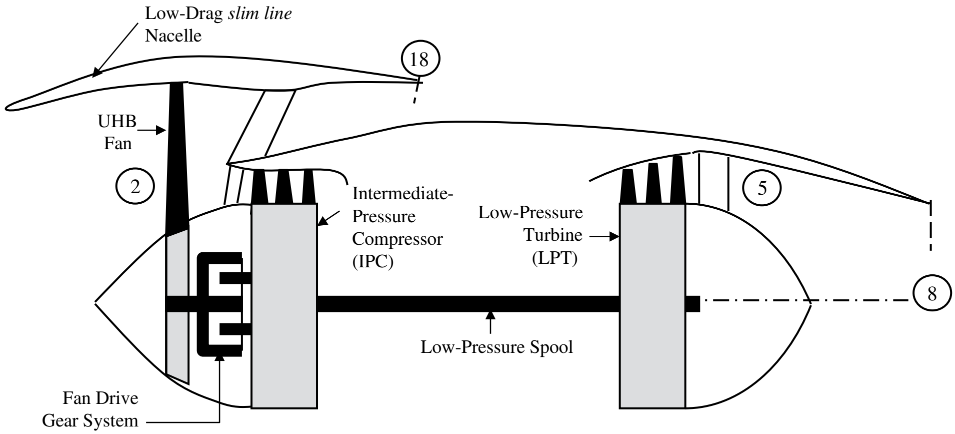

Figure 1.44 Schematic drawing of the low-pressure spool in a UHB with fan drive gear system.

engine technology in connection with the UHB requirements. The first GTF entry into service, PW1000G family, was in 2013. The engine uses a patented lightweight "floating gearbox" system that separates the fan from the IPC and LPT. The gear ratio is 3 : 1 (for more details, see Duong, McCune, Dobek, 2009).

The weight reduction in the nacelle is accomplished through a composite fan nacelle design. The schematic drawing of the low-pressure spool in a GTF engine is shown in Figure 1.44.

To appreciate the cycle parameters of typical UHB engines, for example its fan low-pressure ratio, and their thrust-specific fuel consumption performance, we solve an example problem.

Example 1.2

A GTF is used in a UHB engine with a single-stage, low-pressure ratio, fan. The engine design point is at the standard sea level static condition, according to:

$M_0 = 0$, $p_0 = 101\,\text{kPa}$, $T_0 = 288\,\text{K}$, $\gamma_c = 1.4$, and $c_{pc} = 1004\,\text{J kgK}^{-1}$ and the engine at the design point is sized for the air mass flow rate (into the inlet) of $600\,\text{kg s}^{-1}$.

The inlet at the design point is assumed to have $\pi_d = 0.995$ total pressure recovery.

The fan bypass ratio at the design point is $\alpha = 12$, its design pressure ratio is $\pi_f = 1.36$ (which is considered low as compared to 1.6 fan pressure ratio), and its polytropic efficiency, $e_f = 0.90$. The reduction gearbox is characterized by its efficiency, which is the ratio of power transmission across the gearbox, namely:

$$\eta_{gb} \equiv \frac{\left(\wp_{\text{gearbox}}\right)_{\text{out}}}{\left(\wp_{\text{gearbox}}\right)_{\text{in}}} \tag{1.219}$$

We assume $\eta_{gb} = 0.998$. The core compressor pressure ratio (i.e. excluding the inner fan section) is $p_{t3}/p_{t13} = 22$ with polytropic efficiency, $e_c = 0.90$. Note that the overall compressor (total) pressure ratio that includes the inner fan section is then $p_{t3}/p_{t2} = (1.36)(22) = 29.92$.

The combustor at takeoff is characterized by:

$T_{t4} = 1600\,\text{K}$, $Q_R = 42\,800\,\text{kJ kg}^{-1}$ (lower heating value of fuel), $\eta_b = 0.99$, $\pi_b = 0.96$

The turbine has a polytropic efficiency of $e_t = 0.85$ and power transmission (or mechanical) efficiency, $\eta_m = 0.975$. The gas in the hot section may be modeled as $\gamma_t = 1.33$ and $c_{pt} = 1156\,\text{J kgK}^{-1}$.

Both the fan and the core nozzles are of convergent design with $\pi_{fn} = 0.985$ and $\pi_{cn} = 0.990$.

We simplify our analysis in this example by treating the gas properties as specified in two "cold" and "hot" zones as described.

Calculate:

a) Total pressures and temperatures at every station inside the engine
b) Combustor fuel flow rate in kg s^{-1} and lbm s^{-1}
c) Shaft power delivered to the gearbox in MW and hp.
d) Shaft power delivered to the fan in MW and hp.
e) Fan nozzle exit Mach number, M_{18}
f) Core nozzle exit Mach number, M_8
g) Fan nozzle gross thrust, F_{gf} in kN and lbf
h) Core nozzle gross thrust, F_{gc} in kN and lbf
i) Thrust-specific fuel consumption, TSFC in mg/s/N and lbm/h/lbf

Estimate the gearbox mass if its mass is proportional to the shaft horsepower according to the following gearbox mass density rule: gearbox mass density = 0.008 lbm hp^{-1}.

Solution

Since $M_0 = 0$, $p_{t0} = p_0 = 101\,\text{kPa}$ and $T_{t0} = T_0 = 288\,\text{K}$. The total temperature is the inlet remains constant (adiabatic flow), which gives, $T_{t2} = 288\,\text{K}$. The total pressure in the inlet suffers some loss due to friction, which results in $p_{t2} = \pi_d.p_{t0} = 100.5\,\text{kPa}$

Based on fan total pressure ratio, we get the total pressure in station 13 as $p_{t13} = \pi_f.p_{t2} = 136.7\,\text{kPa}$. We use $\tau_c = \pi_c^{\frac{\gamma-1}{\gamma e_c}}$ to get $T_{t13} = 317.5\,\text{K}$. To march toward the fan nozzle exit, we use the fan nozzle total pressure ratio to get $p_{t18} = p_{t13}.\ \pi_{fn} = 134.6\,\text{kPa}$. Since the fan nozzle flow is adiabatic, the total temperature remains constant, therefore, $T_{t18} = T_{t13} = 317.5\,\text{K}$.

We calculate the fan NPR p_{t13}/p_0 to check it against the "critical" NPR where the nozzle chokes. In this problem, $\text{NPR}_{fn} = 1.353$ which is far less than the critical value (of ~2). Therefore, we conclude that the exit of our convergent fan nozzle is unchoked and thus subsonic. We also conclude that the static pressure at the nozzle exit is the same as the ambient pressure; therefore, $p_{18} = p_0 = 101\,\text{kPa}$. From p_{18} and p_{t18} we calculate M_{18}, which produces $M_{18} = 0.654$. From T_{t18} and M_{18}, we calculate $T_{18} = 292.5\,\text{K}$, with the corresponding speed of sound, $a_{18} = 342.7\,\text{m s}^{-1}$, and fan nozzle exit velocity is $V_{18} = M_{18}.a_{18} = 224.2\,\text{m s}^{-1}$. Since the nozzle is perfectly expanded, $V_{18,\text{eff}} = V_{18} = 224.2\,\text{m s}^{-1}$. Therefore, the fan nozzle gross thrust is:

$$F_{gf} = \alpha \dot{m}_0 V_{18} = 124.16\,\text{kN}\left(\text{or}\,27{,}913\,\text{lbf}\right)$$

Now, we do the core calculations. The compressor OPR, including the fan inner section is the product of the fan and the core pressure ratio, i.e. $\pi_c = \pi_f.\ \pi_{core} = 29.92$ (this is the cycle pressure ratio). Based on π_c and p_{t2}, we get $p_{t3} = 3006.8\,\text{kPa}$. From the polytropic efficiency of the compressor, we calculate the compressor total temperature ratio, $\tau_c = 2.9414$. Therefore the compressor exit total temperature is $T_{t3} = 847\,\text{K}$. The combustor exit total temperature is a given design value at takeoff of $T_{t4} = 1600\,\text{K}$; therefore, through energy balance across the combustor, we calculate the fuel-to-air ratio to be $f = 0.0247$. From total pressure ratio across the burner, π_b, we get the exit total pressure, $p_{t4} = 2886.5\,\text{kPa}$. The turbine shaft power is delivered to the core compressor and the fan gearbox. The gearbox delivers its input power times the efficiency of gearbox to the fan. We calculate fan power through energy balance across the fan, namely,

$$\begin{aligned}\wp_f &= (1+\alpha)\dot{m}_0 c_{pc}(T_{t13} - T_{t2}) = 600\frac{\text{kg}}{\text{s}}\left(1004\frac{\text{J}}{\text{kgK}}\right)(317.5 - 288)\text{K}\\ &= 17.789\,\text{MW}\left(\text{or}\,23859\,\text{hp}\right)\end{aligned}$$

The power delivered to the gearbox is $\wp_{gb-in} = \dfrac{\wp_f}{\eta_{gb}} = 17.825\,\text{MW}$ (or 23 907 hp).

The core compressor shaft power is calculated from the power balance across the core compressor:

$$\wp_{core} = \dot{m}_0 c_{pc}(T_{t3} - T_{t13}) = 46.15\frac{\text{kg}}{\text{s}}\left(1004\frac{\text{J}}{\text{kgK}}\right)(847 - 317.5)\text{K} = 24.54\,\text{MW}$$

The turbine shaft power produced is

$$\wp_t = \frac{\wp_f + \wp_{core}}{\eta_m} = 43.452\,\text{MW}$$

Therefore, the turbine exit total temperature is calculated from the power balance across the turbine to be: $T_{t5} = 805.2\,\text{K}$. From the polytropic efficiency of the turbine and its τ_t, we calculate $\pi_t = 0.0385$ and thus $p_{t5} = 111.2\,\text{kPa}$. The core nozzle exit total pressure is the product of π_{cn} and p_{t5}; therefore, $p_{t8} = 110.14\,\text{kPa}$. The total temperature in the adiabatic nozzle remains constant; therefore $T_{t8} = T_{t5} = 805.2\,\text{K}$.

The core nozzle pressure ratio, $NPR_{\text{core-nozzle}} = 1.10$, which is far below the critical NPR of ~2. Therefore, the core nozzle exit is subsonic and it is perfectly expanded, i.e. $p_8 = p_0 = 101\,\text{kPa}$, and we calculate M_8 from p_{t8} and p_8 to be $M_8 = 0.363$. In the core nozzle calculations we use the hot gas properties. From the T_{t8} and M_8, we calculate $T_8 = 788\,\text{K}$ and thus $a_8 = 548.3\,\text{m}\,\text{s}^{-1}$ and $V_8 = 199\,\text{m}\,\text{s}^{-1}$. The core nozzle gross thrust is:

$$F_{gc} = (1+f)\dot{m}_0 V_8 = 9.411\,\text{kN}\left(\text{or}\ 2116\,\text{lbf}\right)$$

The ratio of fan-to-core thrust is thus 27 913/2116 = 13.2

The engine thrust is the sum of the two gross thrusts (since there is no ram drag at takeoff),

$F_{total} = 133.6$ kN (or 30 000 lbf).

The thrust-specific fuel consumption is TSFC = 8.519 mg/s/N, which is equal to 0.301 lbm/h/lbf, which is about 20% below a conventional turbofan engine (of bypass ratio 6) that delivers a TSFC of about 0.367 lbm/h/lbf.

When we calculate the specific impulse, I_s, for this engine, we get $I_s \approx 12\,000$ sec, which is again another indicator for a tremendous takeoff performance, more in line with turboprops.

The mass of the gearbox is directly proportional to the power delivered to the gearbox through this correlation: 0.008 lbm hp^{-1} (as suggested by Ian Halliwell 2013). Consequently, since the power into the gearbox was calculated to be 23 907 hp, the mass of the gearbox is estimated at 191 lbm or 86.6 kg, which is insignificant as a key component in a 30 000-pound thrust class engine.

Comments

In this example, we performed a one-dimensional cycle analysis with a simple gas model (i.e., as either cold or hot). Our turbine was uncooled, but we specified a lower turbine efficiency to partially offset or account for the effect of cooling. Also, we did not extract any auxiliary shaft power, as it is always done in aircraft gas turbine engines. However, more accurate engine simulators are available (e.g. see GasTurb by Joachim Kurzke 2017) that will properly model the gas and perform cooling bleed and power extraction, which must be used for higher accuracy. In our simple analysis, we demonstrated a 20% reduction in TSFC whereas in real engine testing a 16% reduction in TSFC is measured compared to the baseline International Aero Engines V2500. Additional information on GTF can be found on the P&W website, Asbury and Yetter (2000), which may be consulted for thrust reversers, and Guynn et al. (2013) have treated advanced cycles for single-aisle transport aircraft. CFM website provides performance parameters of other modern turbofan engines.

A new book on gas turbine performance modeling, by Kurzke and Halliwell (2018), is highly recommended for students and practicing engineers in propulsion and power industry.

1.9.6 Analysis of Mixed-Exhaust Turbofan Engines with Afterburners

The schematic diagram in Figure 1.45 of a mixed-exhaust turbofan engine shows the station numbers for this engine and identifies a new component, namely the mixer. The engine core discharges a hot gas into the mixer whereas the fan duct injects a "cold" gas into the mixer. Upon mixing of the two streams, the gas will attain a "mixed-out" state at station 6 M. Now, what about the pressure of the two incoming streams? On the question of static pressure between the two streams, as they enter the mixer, we rely on our understanding of *Kutta trailing-edge condition* applied to airfoils with sharp trailing edge. We learned this

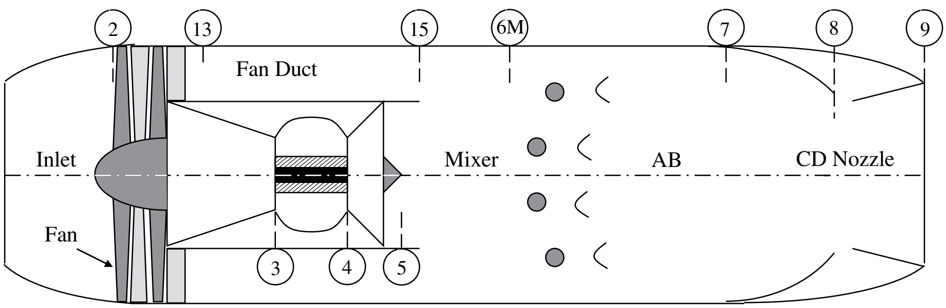

Figure 1.45 Long-duct turbofan engine with a mixer and an afterburner.

principle in aerodynamics. In simple terms, Kutta condition demands the continuity of static pressure at the (sharp) trailing edge, i.e. $p_{\text{upper}} = p_{\text{lower}}$ on an airfoil at its trailing edge. It physically suggests that the two merging streams at the trailing edge of an airfoil, or fan duct and engine core streams, cannot support a *static pressure jump*. Therefore, we demand:

$$p_{15} = p_5 \tag{1.220}$$

We can think of Eq. (1.220) as that the static pressure is *communicated* between the core and the fan duct, which is a physical principle. Therefore, the fan pressure ratio and hence the fan mass flow rate are basically set by the *engine backpressure*. Here, we note that the two parameters of a fan, namely, its pressure ratio and the bypass ratio, cannot be independently set in this configuration. Here, we can only stipulate one parameter, and the second parameter *falls out* of the common back-pressure requirement.

1.9.6.1 Mixer

To analyze a constant-area mixer, we employ the conservation principles of mass, momentum, and energy. Also, the mixture gas laws establish the mixed-out gas properties at the mixer exit. Figure 1.46 shows a constant-area mixer where mixed-out gas properties c_{p6M} and c_{v6M} are mass averaged and γ_{6M} is the ratio of the two.

The thermodynamic state of gas before and after the mixing process is shown on a T-s diagram in Figure 1.47. The physical mixing process takes place in the shear layer, where large-scale vortical structures are formed, which entrain cold flow into the central hot jet and cause mixing (on the macro-scale).

The application of the law of conservation of energy to an insulated mixer gives:

$$\dot{m}_5 h_{t5} + \dot{m}_{15} h_{t15} = \dot{m}_{6M} h_{t6M} \tag{1.221}$$

Assuming the inlet conditions are known for the mixer, the only unknown in the above equation is the mixed-out total enthalpy, h_{t6M}, namely

$$h_{t6M} = \frac{(1+f)h_{t5} + \alpha h_{t15}}{1+\alpha+f} \tag{1.222}$$

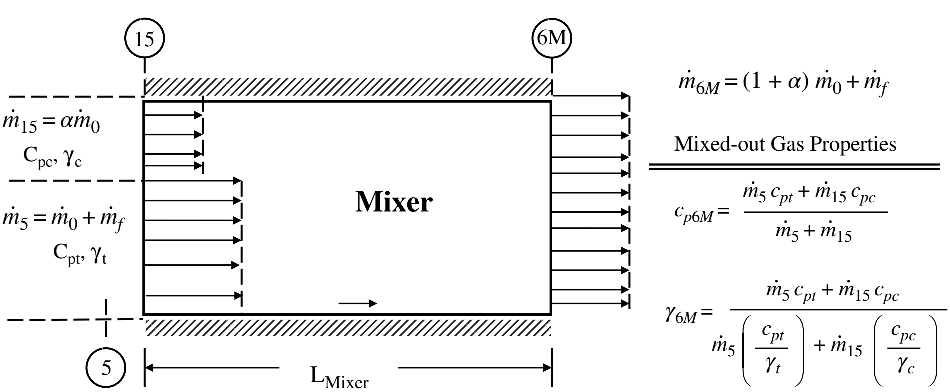

Figure 1.46 Mixer control volume showing nonuniform inlet and *mixed-out* exit velocity.

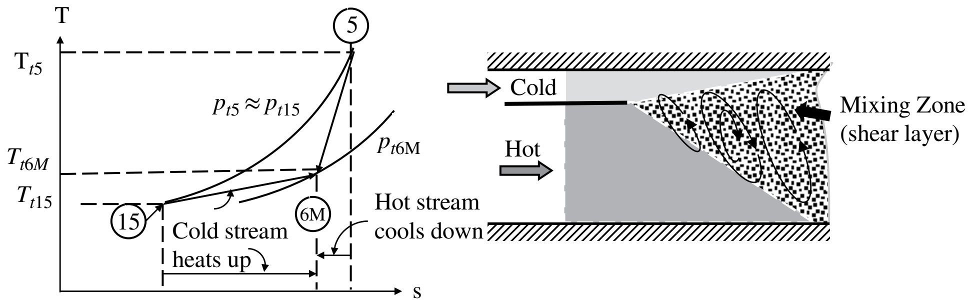

Figure 1.47 Mixing of two streams at different temperatures on a T-s diagram and in physical domain.

Here, we introduce the nondimensional parameters in the above equation as follows:

$$h_{t6M} = h_0 . \frac{(1+f)\tau_t . \tau_\lambda + \alpha \tau_r . \tau_f}{1+\alpha+f} \tag{1.223}$$

In order to establish the mixed-out pressure, p_{6M}, at the exit of the mixer, we apply the conservation of momentum in the streamwise direction, i.e. x as shown in Figure 1.46. A simple expression for the x-momentum is just $\dot{m}V_x$, which holds for a steady uniform flow and may be applied to the mixer control volume as follows:

$$\dot{m}_{6M}V_{6M} - \left[\dot{m}_5 V_5 + \dot{m}_{15} V_{15}\right] = \sum F_x \tag{1.224}$$

In Eq. (1.224), the right-hand side is the sum of all external forces acting on the control volume in the x-direction. The external forces are:

$$\sum F_x = p_5 A_5 + p_{15} A_{15} - p_{6M} A_{6M} - \int \tau_w dA_{\text{wetted}} \tag{1.225}$$

where the last term is the wall friction drag force acting on the mixer wall, $D_{f\text{mixer}}$, associated with the mixer. We also note that the static pressures at the entrance to the mixer from the core and the fan duct side are equal according to the Kutta condition:

$$p_5 = p_{15} \tag{1.226}$$

For a constant-area mixer

$$A_{6M} = A_5 + A_{15} \tag{1.227}$$

Substitution of Eqs. (1.226) and (1.227) in Eq. (1.224) gives:

$$\left(\dot{m}_{6M}V_{6M} + p_{6M}A_{6M}\right) - \left(\dot{m}_5 V_5 + p_5 A_5\right) - \left(\dot{m}_{15} V_{15} + p_{15} A_{15}\right) = -D_f \tag{1.228}$$

The grouped terms in the above equation are the *impulse*, given a symbol I, corresponding stations, namely 6 M, 5 and 15, respectively. We note that the fluid impulse out of the mixer is somewhat less than the (sum of the) fluid impulse entering the mixer and this difference or loss is caused by the friction drag on the mixer wall. Therefore, had we assumed frictionless flow in the mixer, we would have concluded that the impulse is conserved, i.e.

$$I_{6M} = I_5 + I_{15} \tag{1.229}$$

We proceed with our analysis using the assumption of zero boundary layer frictional losses on the walls of the mixer in order to derive a closed form solution for the unknown mixer exit conditions. We then incorporate a correction factor due to friction to account for the viscous flow losses on the total pressure.

The impulse function I attains a very simple form when we express it in terms of flow Mach number:

$$I \equiv \dot{m}V + pA = A\left(\rho V^2 + p\right) = Ap\left(\frac{\rho V^2}{p} + 1\right) = Ap\left(1 + \gamma M^2\right) \tag{1.230}$$

We had used the equation for the speed of sound, $a^2 = \gamma p/\rho$, in the above derivation. Now, in light of this expression for impulse, let us recast Eq. (1.228) in terms of flow Mach number and pressure area terms:

$$p_{6M}A_{6M}\left(1+\gamma_{6M}M_{6M}{}^2\right) - p_5A_5\left(1+\gamma_5 M_5{}^2\right) - p_{15}A_{15}\left(1+\gamma_c M_{15}{}^2\right) = 0 \tag{1.231}$$

By dividing Eq. (1.231) by A_5, we get:

$$p_{6M}1+\gamma_{6M}M_{6M}{}^2\left(1+A_{15}/A_5\right) - p_5\left(1+\gamma_5 M_5{}^2\right) + \left(A_{15}/A_5\right)\left(1+\gamma_c M_{15}{}^2\right) = 0 \tag{1.232}$$

Eq. (1.232) has two unknowns, namely p_{6M} and M_{6M}. The continuity equation is expressed in terms of pressure and Mach number according to:

$$\dot{m} \equiv \rho AV = AVp/RT = \frac{\gamma pAM}{\sqrt{\gamma RT}} = \frac{\gamma pAM}{\sqrt{\gamma RT_t}}\sqrt{1+\frac{\gamma-1}{2}M^2} \tag{1.233}$$

Therefore, applying the continuity equation to the mixer, we get:

$$\begin{aligned}&\frac{p_{6M}M_{6M}\sqrt{1+\left(\gamma_{6M}-1\right)M_{6M}{}^2/2}}{\sqrt{\gamma_{6M}R_{6M}T_{t6M}}}\left(1+A_{15}/A_5\right) = \\ &\frac{p_5M_5\sqrt{1+\left(\gamma_t-1\right)M_5{}^2/2}}{\sqrt{\gamma_t R_t T_{t5}}} + \frac{p_{15}M_{15}\sqrt{1+\left(\gamma_c-1\right)M_{15}{}^2/2}}{\sqrt{\gamma_c R_c T_{t15}}}\left(A_{15}/A_5\right)\end{aligned} \tag{1.234}$$

Equation (1.234) and the impulse equation, (1.232), form two equations, two unknown system in terms of the unknowns, p_{6M} and M_{6M}. We may solve the equations in closed form as they reduce to a quadratic equation in $M_{6M}{}^2$.

1.9.6.2 Mixed-Turbofan Cycle Analysis

To reinforce the powerful *marching technique* that we have learned so far in cycle analysis, let us apply it to a mixed-flow turbofan engine at this time.

First, we will identify a *mix of parameters* that we need to specify in order to start the cycle analysis in a mixed-flow turbofan engine.

Flight Condition:

We need the flight Mach number (or speed), static temperature, and pressure at the flight altitude, i.e. M_0 (or V_0), T_0, and p_0, as well as air properties (γ, c_p, humidity level), in this case we treat air as *dry*.

Inlet:
We need the inlet adiabatic efficiency or its total pressure recovery parameter, i.e. η_d or π_d, only one figure-of-merit is needed.

Fan:
We need the fan's pressure ratio, $\pi_f \equiv (p_{t13}/p_{t2})$, *or* the fan bypass ratio, α, and its polytropic efficiency, e_f or its adiabatic efficiency, η_f.

Compressor:
We need compressor's total pressure ratio, $\pi_c \equiv p_{t3}/p_{t2}$, which is the cycle OPR and its polytropic efficiency e_c or its adiabatic efficiency, η_c.

Combustor:
We need combustor's total pressure ratio, π_b, combustion efficiency, η_b, and fuel heating value, Q_R and either turbine inlet temperature, T_{t4} or the fuel-to-air ratio, f.

Turbine:
We need turbine's polytropic efficiency, e_t, or adiabatic efficiency, η_t, mechanical efficiency, η_m, exit Mach number, M_5, and an extra assumption about the pressure matching condition between the core and fan ducts at their merging boundary, typically $p_{t5} = p_{t15}$ or $p_5 = p_{15}$.

Mixer:
We need a viscous loss parameter that accounts for the mixer wall friction on the total pressure loss across the mixer, namely, $\pi_{M,f}$

Afterburner
We need the afterburner efficiency, η_{AB}, the maximum temperature T_{t7} (or f_{AB}), afterburner total pressure ratio, π_{AB}, and the heating value of the fuel, $Q_{R,AB}$ in the afterburner.

Nozzle:
We need adiabatic efficiency of the nozzle, η_n or its total pressure loss parameter, π_n, and the nozzle exit pressure, p_9, or instead of exit pressure, we may specify nozzle's (exit-to-throat) area ratio, A_9/A_8.

1.9.6.3 Solution Procedure

We first calculate the total temperature and pressure distribution throughout the engine. We follow a streamline that passes through the core and a streamline that passes through the fan. Once we establish the total fluid properties after each interaction along the streamline path, we have the 1-D information for the core and the fan streams. Then we allow the Kutta condition to establish the communication between the two streams before the mixer takes over and achieves a mixed-out state of the gas prior to discharge into the nozzle or afterburner. These steps are summarized as follows.

Station 0

$$p_{t0} = p_0\left(1+\frac{\gamma_c-1}{2}M_0^{\,2}\right)^{\frac{\gamma_c}{\gamma_c-1}}$$

$$\pi_r = \left(1+\frac{\gamma_c-1}{2}M_0^{\,2}\right)^{\frac{\gamma_c}{\gamma_c-1}} \tag{1.235}$$

$$T_{t0} = T_0\left(1+\frac{\gamma_c - 1}{2}{M_0}^2\right)$$

$$\tau_r = \left(1+\frac{\gamma_c - 1}{2}{M_0}^2\right) \tag{1.236}$$

$$a_0 = \sqrt{\gamma_c R_c T_0}$$

$$V_0 = a_0 M_0$$

Station 2

$$p_{t2} = \pi_d \,.\, p_{t0} \text{ or in terms of adiabatic efficiency, } p_{t2} = p_0\left(1+\eta_d\frac{\gamma_c - 1}{2}{M_0}^2\right)^{\frac{\gamma_c}{\gamma_c - 1}} \tag{1.237}$$

$$T_{t2} = T_{t0}$$

Now, following a streamline that enters the core, we proceed to station 3.

Station 3

$$p_{t3} = p_{t2} . \pi_c$$

$$T_{t3} = T_{t2} . {\pi_c}^{\frac{\gamma - 1}{\gamma . e_c}}$$

$$\tau_c = {\pi_c}^{\frac{\gamma_c - 1}{\gamma_c e_c}} \tag{1.238}$$

Station 4

$$p_{t4} = p_{t3} . \pi_b$$

T_{t4} is either explicitly given as the engine maximum temperature or can be calculated from the fuel-to-air ratio, *f*, according to:

$$h_{t4} = C_{pt} T_{t4} = \frac{1}{1+f}\left(h_{t3} + f Q_R \eta_b\right)$$

We also calculate the fuel-to-air ratio in the burner, if only T_{t4} is specified, i.e.

$$f = \frac{h_{t4} - h_{t3}}{Q_R \eta_b - h_{t4}} = \frac{\tau_\lambda - \tau_r\left(\tau_c - 1\right)}{\frac{Q_R \eta_b}{h_0} - \tau_\lambda} \tag{1.239}$$

where $\tau_\lambda \equiv \dfrac{h_{t4}}{h_0}$

Before marching to station 5, let us follow a streamline that passes through the fan.

Station 13

$$p_{t13} = p_{t2}.\pi_f$$

$$T_{t13} = T_{t2}.\pi_f^{\frac{\gamma_c - 1}{\gamma_c . e_f}}$$

$$or\, \tau_f = \pi_f^{\frac{\gamma_c - 1}{\gamma_c e_f}} \tag{1.240}$$

Station 15

Here, we assume the fan duct to be frictional but *adiabatic* and we characterize the frictional aspect of it by a total pressure ratio π_{fd} parameter,

$$p_{t15} = p_{t13}.\pi_{fd} \tag{1.241}$$

where π_{fd} is given/assumed. Also, our adiabatic flow assumption in the fan duct gives:

$$T_{t15} = T_{t13} \quad \left[\text{for a calorically perfect gas, otherwise, } h_{t15} = h_{t13}\right]$$

or

$$\tau_{fd} = 1$$

Now, let us proceed through the turbine by a representative core streamline.

Station 5

Power balance between the turbine and the compression system (fan and compressor) gives:

$$\eta_m (1 + f)(h_{t4} - h_{t5}) = (h_{t3} - h_{t2}) + \alpha (h_{t13} - h_{t2}) \tag{1.242}$$

We note that in the above equation; there are two unknowns, namely the bypass ratio, α and the turbine exit (total) enthalpy, h_{t5}. Let us divide the above equation by the flight static enthalpy, h_0, to get the nondimensional power balance equation:

$$\eta_m (1 + f)\tau_\lambda (1 - \tau_t) = \tau_r (\tau_c - 1) + \alpha \tau_r (\tau_f - 1) \tag{1.243}$$

Here, we still have the two unknowns in terms of the bypass ratio and the turbine expansion ratio, τ_t. We can make a reasonable assumption that the total pressure in the fan duct and turbine exit are nearly equal, since static pressures were equal by Kutta condition and we may choose the Mach number (i.e. sizing parameter) in the two streams to yield:

$$p_{t5} \approx p_{t15} \tag{1.244}$$

This immediately ties the turbine pressure ratio to the fan pressure ratio:

$$\frac{p_{t5}}{p_{t2}} = \pi_t.\pi_b.\pi_c = \frac{p_{t15}}{p_{t2}} = \pi_{fd}.\pi_f \tag{1.245}$$

Consequently, turbine total pressure ratio may be expressed in terms of all known parameters of the cycle as:

$$\pi_t = \frac{\pi_{fd}.\pi_f}{\pi_b.\pi_c} \tag{1.246}$$

The turbine temperature expansion ratio, τ_t may be linked to $\pi_t$via the polytropic efficiency, namely

$$\tau_t = \pi_t^{\frac{\gamma_t-1}{\gamma_t}e_t} = \left(\frac{\pi_{fd}.\pi_f}{\pi_b.\pi_c}\right)^{\frac{\gamma_t-1}{\gamma_t}e_t} \tag{1.247}$$

Now, we see that the power balance equation written in Eq. (1.243), fan and compressor contains only one unknown, and that is the bypass ratio, α, which is expressed as:

$$\alpha = \frac{\eta_m(1+f)\tau_\lambda(1-\tau_t)-\tau_r(\tau_c-1)}{\tau_r(\tau_f-1)} \tag{1.248}$$

The assumption of constant total pressure at the exit of the turbine and the fan duct is a reasonable assumption for our design-point analysis. This has enabled us to calculate the turbine pressure ratio and hence the temperature ratio. The power balance then produced the bypass ratio.

Station 6M

From the energy balance across an adiabatic mixer, we obtain:

$$h_{t6M} = h_0.\frac{(1+f)\tau_t.\tau_\lambda + \alpha\tau_f.\tau_r}{1+\alpha+f} \tag{1.249}$$

All parameters in the above equation are either given as design/limit parameters or have been calculated in the previous steps, thus enabling us to march through the gas turbine. Now, we are ready to calculate the flow Mach number at the fan duct exit, M_{15}, in terms of turbine exit Mach number, M_5, according to:

$$p_{t15} = p_{15}.\left(1+\frac{\gamma_c-1}{2}M_{15}^2\right)^{\frac{\gamma_c}{\gamma_c-1}} = p_5.\left(1+\frac{\gamma_t-1}{2}M_5^2\right)^{\frac{\gamma_t}{\gamma_t-1}} \tag{1.250}$$

Equation (1.250) reduces to the trivial solution, $M_{15} = M_5$, except for different γ_c and γ_t:

$$M_{15}^2 = \frac{2}{\gamma_c-1}\left\{\left[\left(1+\frac{\gamma_t-1}{2}M_5^2\right)^{\frac{\gamma_t}{\gamma_t-1}}\right]^{\frac{\gamma_c-1}{\gamma_c}} -1\right\} \tag{1.251}$$

We use the mass flow rate expressions:

$$\dot{m}_{15} = \frac{\gamma_c p_{15} A_{15} M_{15}}{a_{15}} = \alpha\dot{m}_0 \tag{1.252}$$

$$\dot{m}_5 = \frac{\gamma_t p_5 A_5 M_5}{a_5} = (1+f)\dot{m}_0 \tag{1.253}$$

Now, if we take the ratio of the above two expressions and note that static pressures are identical (a' la Kutta condition), we get an expression for the unknown area ratio, i.e.

$$\frac{A_{15}}{A_5}=\frac{\alpha}{1+f}.\left(\frac{\gamma_t}{\gamma_c}\right)\frac{a_{15}}{a_5}\frac{M_5}{M_{15}} \tag{1.254}$$

So far, we have established the mixed-out total enthalpy, h_{t6M} and all the upstream parameters to the mixer, such as M_{15} and the area ratio A_{15}/A_5. In the mixer analysis, we had derived two equations and two unknowns in Eqs. (1.232) and (1.234):

$$p_{6M}1+\gamma_{6M}M_{6M}{}^2\left(1+A_{15}/A_5\right)-p_5\left(1+\gamma_t M_5{}^2\right)+\left(A_{15}/A_5\right)\left(1+\gamma_c M_{15}{}^2\right)=0 \tag{1.255}$$

$$\frac{\gamma_{6M}p_{6M}M_{6M}\sqrt{1+\left(\gamma_{6M}-1\right)M_{6M}{}^2/2}}{\sqrt{\left(\gamma_{6M}-1\right)c_{p6M}T_{t6M}}}\left(1+A_{15}/A_5\right)=\frac{\gamma_t p_5 M_5}{a_5}+\frac{\gamma_c p_{15}M_{15}}{a_{15}}\left(A_{15}/A_5\right) \tag{1.256}$$

Let us nondimensionalize Eq. (1.255) by dividing through by p_5 and rewriting it in the following form:

$$\frac{p_{6M}}{p_5}\left[1+\gamma_{6M}M_{6M}{}^2\right]=\left[\left(1+\gamma_t M_5{}^2\right)+\left(A_{15}/A_5\right)\left(1+\gamma_c M_{15}{}^2\right)\right]/\left(1+A_{15}/A_5\right)=C_1 \tag{1.257}$$

The right-hand side of the above equation is known and we have given it a shorthand notation of C_1. Now, we can isolate the same unknowns in Eq. (1.256) to get:

$$\frac{p_{6M}}{P_5}\left(M_{6M}\sqrt{1+\left(\gamma_{6M}-1\right)M_{6M}{}^2/2}\right)=\left[\left(\frac{\gamma_t}{\gamma_{6M}}\right)\frac{M_5}{a_5}+\left(\frac{\gamma_c}{\gamma_{6M}}\right)\frac{M_{15}\left(A_{15}/A_5\right)}{a_{15}}\right]\frac{\sqrt{\left(\gamma_{6M}-1\right)c_{p6M}T_{t6M}}}{\left(1+A_{15}/A_5\right)}=C_2 \tag{1.258}$$

Again, the RHS of the above equation is known and it is labeled C_2. By dividing Eq. (1.257) by (1.258), we eliminate the mixer static pressure ratio and get M_{6M} via:

$$\frac{1+\gamma_{6M}M_{6M}{}^2}{M_{6M}\sqrt{1+\left(\gamma_{6M}-1\right)M_{6M}{}^2/2}}=\frac{C_1}{C_2}=\sqrt{C} \tag{1.259}$$

Let us cross multiply and square both sides of the Eq. (1.259) to arrive at a quadratic equation in $M_{6M}{}^2$, as follows:

$$\left(1+\gamma_{6M}M_{6M}{}^2\right)^2=C.M_{6M}{}^2\left(1+\left(\gamma_{6M}-1\right)M_{6M}{}^2/2\right) \tag{1.260}$$

$$\gamma_{6M}{}^2-C\left(\gamma_{6M}-1\right)/2M_{6M}{}^4+\left(2\gamma_{6M}-C\right)M_{6M}{}^2+1=0 \tag{1.261}$$

$$M_{6M}^2 = \frac{C - 2\gamma_{6M} - \sqrt{\left(C - 2\gamma_{6M}\right)^2 - 4\left[\gamma_{6M}^2 - C\left(\gamma_{6M} - 1\right)/2\right]}}{2\gamma_{6M}^2 - C\left(\gamma_{6M} - 1\right)} \tag{1.262}$$

where C is defined in Eq. (1.259) and is expressible in terms of earlier established parameters C_1 and C_2. Now, the mixer static pressure ratio can be determined from:

$$\frac{p_{6M}}{p_5} = \frac{C_1}{1 + \gamma_{6M} M_{6M}^2} \tag{1.263}$$

The *ideal* (i.e. inviscid) total pressure ratio across the mixer is p_{t6M}/p_{t5}, which is expressible in terms of the static pressure ratio of Eq. (1.263) and Mach number according to:

$$\pi_{M_i} \equiv \frac{p_{t6M}}{p_{t5}} = \frac{p_{6M}}{p_5} \frac{\left[1 + \left(\gamma_{6M} - 1\right) M_{6M}^2 / 2\right]^{\frac{\gamma_{6M}}{\gamma_{6M-1}}}}{\left[1 + \left(\gamma_t - 1\right) M_5^2 / 2\right]^{\frac{\gamma_t}{\gamma_t - 1}}} \tag{1.264}$$

The *actual* total pressure ratio across the mixer should also account for the mixer wall frictional losses, which may be expressed as a multiplicative factor of the ideal parameter:

$$\pi_M \equiv \pi_{M_i} . \pi_{M_f} \tag{1.265}$$

where the frictional loss parameter, π_{M_f}, needs to be specified or assumed.

Station 7

Application of the energy equation to the afterburner yields an expression for the fuel-to-air ratio in the afterburner in terms of known parameters as follows:

$$\left(\dot{m}_{6M} + \dot{m}_{fAB}\right) h_{t7} - \dot{m}_{6M} h_{t6M} = \dot{m}_{fAB} Q_{R,AB} \eta_{AB} \tag{1.266}$$

$$f_{AB} \equiv \frac{\dot{m}_{fAB}}{\dot{m}_{6M}} = \frac{h_{t7} - h_{t6M}}{Q_{R,AB}\eta_{AB} - h_{t7}} = \frac{\tau_{\lambda AB} - h_{t6M} / h_0}{\frac{Q_{R,AB}\eta_{AB}}{h_0} - \tau_{\lambda AB}} \tag{1.267}$$

The total pressure at the afterburner exit is known via the loss parameter according to:

$$p_{t7} = p_{t6M} . \pi_{AB} \tag{1.268}$$

Note that we need two afterburner total pressure loss parameters, one for the *afterburner on* and the second for the *afterburner off*, i.e. $\pi_{\text{AB-On}}$ and $\pi_{\text{AB-Off}}$. We expect $\pi_{\text{AB-On}} < \pi_{\text{AB-Off}}$.

Station 9

For adiabatic flow and constant gas properties in the (CD) nozzle, we have

$$T_{t9} = T_{t7} \tag{1.269}$$

The total pressure at the nozzle exit, p_{t9} is expressible in terms of the nozzle total pressure ratio parameter, according to:

$$p_{t9} = p_{t7} . \pi_n \tag{1.270}$$

or in case of an adiabatic nozzle efficiency, η_n, we have:

$$\eta_n = \left[\left(\frac{p_{t7}}{p_9} \right)^{\frac{\gamma_{AB}-1}{\gamma_{AB}}} - \pi_n^{\frac{\gamma_{AB}-1}{-\gamma_{AB}}} \right] / \left[\left(\frac{p_{t7}}{p_9} \right)^{\frac{\gamma_{AB}-1}{\gamma_{AB}}} - 1 \right] \tag{1.271}$$

Now, with the total pressure calculated at the nozzle exit and the static pressure, p_9, as a given in the cycle analysis, we establish the nozzle exit Mach number, according to:

$$M_9^2 = \frac{2}{\gamma_{AB} - 1} \left[\left(\frac{p_{t9}}{p_9} \right)^{\frac{\gamma_{AB}-1}{\gamma_{AB}}} - 1 \right] \tag{1.272}$$

The exit speed of sound from the exit Mach number and total temperature is:

$$a_9^2 = \frac{\gamma_{AB} R_{AB} T_{t9}}{1 + (\gamma_{AB} - 1) M_9^2 / 2} \tag{1.273}$$

The nozzle exit velocity, as the product of $M_9.a_9$, is:

$$V_9 = M_9.a_9 \tag{1.274}$$

Example 1.3

We calculate the performance of a mixed-flow TF engine cruising at Mach 2.0 at an altitude where $p_0 = 10\,\text{kPa}$, $T_0 = 223\,\text{K}$, and dry air is characterized by $\gamma_c = 1.4$, $c_{pc} = 1004\,\text{J kgK}^{-1}$. The fan pressure ratio was chosen as $\pi_f = 2.0$ and the compressor pressure ratio (including the inner fan) varies between 6 and 16 (for a parametric study). The main burner is set at $T_{t4} = 1600\,\text{K}$ and the afterburner was on with $T_{t7} = 2000\,\text{K}$. The turbine exit (axial) Mach number, M_5 is set at 0.50. The fuel LHV in both primary and the afterburner is $43\,\text{MJ kg}^{-1}$ and the nozzle exit pressure is assumed to be $p_9/p_0 = 3.8$. The component efficiencies and losses are assumed to be: $\pi_d = 0.90$, $\pi_{fd} = 0.99$, $\pi_b = 0.95$, $\pi_{AB} = 0.92$, $\pi_n = 0.95$, $e_f = e_c = 0.90$, $e_t = 0.80$, $\eta_b = 0.99$, $\eta_m = 0.98$, $\Pi_{Mf} = 0.98$. The gas properties in the turbine and afterburner are assumed to be: $\gamma_t = 1.33$, $c_{pt} = 1156\,\text{J kgK}^{-1}$, and $\gamma_{AB} = 1.30$ and $c_{pAB} = 1243\,\text{J kgK}^{-1}$, respectively.

Figure 1.48a shows the variation of mixed-turbofan engine efficiency with compressor pressure ratio. Propulsive efficiency remains constant (at nearly 62%) whereas thermal efficiency shows a peak (with η_{th}~49.4%, at an *optimal* OPR $\simeq$ 11.0. Note that the peak overall engine efficiency is still dismal, i.e. $\eta_{o,max}$~31%.

In part (b) of Figure 1.48, we note that the engine bypass ratio varies between 0.44 and 0.63. The engine fuel burn parameter (TSFC in lbm/h/lbf) and specific thrust is shown in Figure 1.48c. The specific fuel consumption is at its minimum, $TSFC_{min}$~1.61 lbm/h/lbf, where the compressor pressure ratio is ~11, i.e. the optimal π_c for this engine at this Mach number and altitude. The specific thrust is shown in the nondimensional form as $F_n / (1+\alpha)\dot{m}_0 a_0$

And shows a nearly constant behavior (~2.77) with compressor pressure ratio.

Comment

The low overall efficiency of the mixed-exhaust TF engine is due to the thermal efficiency limitations in heat engines, such as the Brayton cycle. The slightly higher thermal

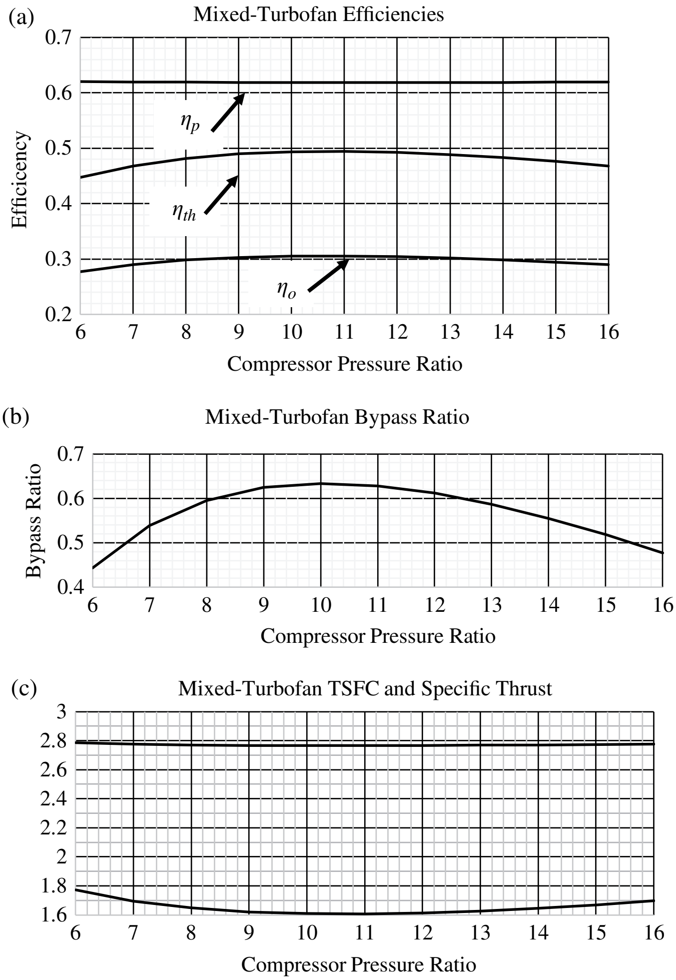

Figure 1.48 Performance characteristics of a mixed TF engine with AB in cruise.

efficiency in this engine as compared to the separate-flow TF engine (Example 1.1), i.e. ~50% vs. 45%, is due to the higher ram compression, π_r, in this engine at Mach 2 flight that produces the cycle OPR of ~86 versus ~61 in Example 1.1.

1.10 Turboprop Engine

1.10.1 Introduction

To construct a turboprop engine, we start with a gas generator.

The turbine in the gas generator provides the shaft power to the compressor. However, we recognize that the gas at the turbine exit is still highly energetic (i.e. high p_t and T_t) and capable of producing shaft power, similar to a turbofan engine.

Once this shaft power is produced in a follow-on turbine stage that we is called "power" or "free" turbine, we can supply the shaft power to a propeller. A schematic drawing of this arrangement is shown in Figure 1.49.

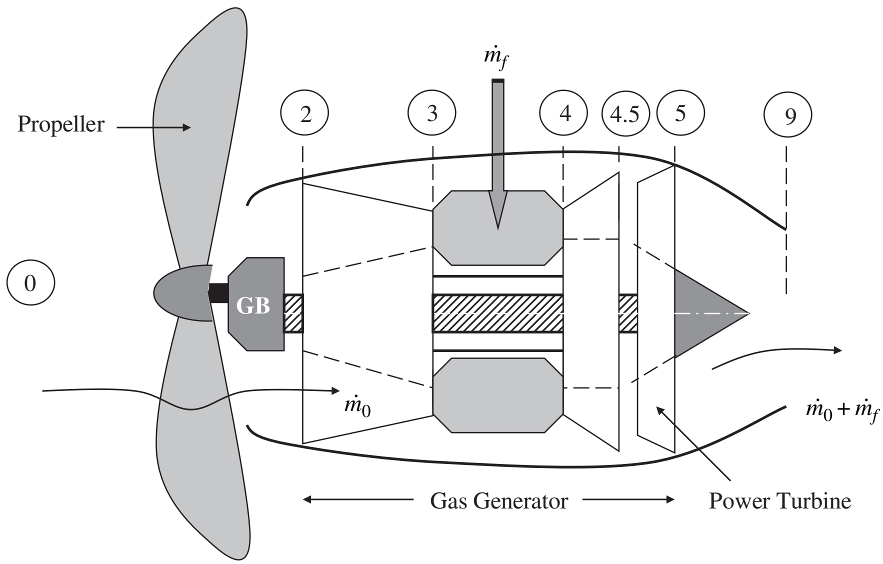

Figure 1.49 Schematic drawing of a turboprop engine with station numbers identified.

The attractiveness of a turbo-propeller engine as compared to a turbo-fan engine lies in its ability to offer a very large bypass ratio, which may be between 30 and 100. The large bypass ratio, by necessity, will then cut back on the exhaust velocities of the propulsor, thereby attaining higher propulsive efficiencies for the engine. The high propulsive efficiency, however, comes at a price. The limitation on the tip Mach number of a rotating propeller, say to less than 1.3, leads to a cruise Mach number in the 0.7 to ~0.8 range for advanced turboprops and to 0.4–0.6 for conventional propellers. We do not have *this limitation* on cruise Mach number in a turbofan engine. Also, the large diameter of the propeller often requires a reduction gearbox.

1.10.2 Turboprop Cycle Analysis

1.10.2.1 The New Parameters

Let us identify the new parameters that we have introduced by inserting a propeller in the gas turbine engine. We will examine the turboprop from the power distribution point of view as well as its thrust producing capabilities namely the propeller thrust contribution to the overall thrust, which includes the core thrust.

From the standpoint of power, the low-pressure turbine power is supplied to a gearbox, which somewhat diminishes it in its frictional loss mechanism in the gearing and then delivers the remaining power to the propeller. We will call the fractional delivery of shaft power through the gearbox, the *gearbox efficiency*, η_{gb}, which symbolically is defined as:

$$\eta_{gb} \equiv \wp_{\text{prop}} / \wp_{\text{LPT}} \tag{1.275}$$

where the numerator is the power supplied to the propeller and the denominator is the shaft power provided by the power turbine to the gearbox. Also, we define the fraction of *propeller shaft power* that is converted in the *propeller thrust power* as the *propeller efficiency*, η_{prop}, as

$$\eta_{\text{prop}} \equiv F_{\text{prop}}.V_0 / \wp_{\text{prop}} \tag{1.276}$$

We recognize that the propeller and the engine core both contribute to thrust production:

$$F_{\text{total}} = F_{\text{prop}} + F_{\text{core}} \tag{1.277}$$

The contribution of the engine core to the overall thrust, which we have called as the *core thrust*, takes on the familiar form of the gross thrust of the nozzle minus the ram drag, i.e.

$$F_{\text{core}} = \left(\dot{m}_0 + \dot{m}_f\right)V_9 - \dot{m}_0 V_0 + \left(p_9 - p_0\right)A_9 \tag{1.278}$$

The pressure thrust contribution of the nozzle, i.e. the last term in Eq. (1.278), for a turboprop engine is often zero due to perfectly expended exhaust, i.e. $p_9 = p_0$. So, for all practical purposes, the engine core of a turboprop produces a thrust based solely on the momentum balance between the exhaust and the intake of the engine, namely,

$$F_{\text{core}} \cong \left(\dot{m}_0 + \dot{m}_f\right)V_9 - \dot{m}_0 V_0 \tag{1.279}$$

1.10.2.2 Design-Point Analysis

We require the following set of input parameters in order to estimate the performance of a turboprop engine. The following list, which sequentially proceeds from the flight condition to the nozzle exit, summarizes the input parameters per component. In this section, we will practice the powerful marching technique that we have learned so far in this book.

Station 0

The flight Mach number, M_0, the ambient pressure and temperature, p_0 and T_0, and air properties γ and R, are needed to characterize the flight environment. We can calculate the flight total pressure and temperature, p_{t0} and T_{t0}, the speed of sound at the flight altitude, a_0 and the flight speed V_0, based on the input.

Station 2

At the engine face, we need to establish the total pressure and temperature, p_{t2} and T_{t2}. From adiabatic flow assumption in the inlet, we conclude that:

$$T_{t2} = T_{t0}$$

We need to define an inlet total pressure ratio parameter, π_d, or adiabatic diffuser efficiency, η_d. This results in establishing p_{t2}, similar to our earlier cycle analysis; for example,

$$p_{t2} = \pi_d . p_{t0}$$

Station 3

To continue our march through the engine, we need to know the compressor pressure ratio, π_c, which again is treated as a design choice, and the compressor polytropic efficiency, e_c. This allows us to calculate the compressor total temperature ratio in terms of compressor total pressure ratio using the polytropic exponent, i.e.

$$\tau_c = \pi_c^{\frac{\gamma_c - 1}{\gamma_c e_c}}$$

Now, the compressor discharge total pressure and temperature, p_{t3} and T_{t3} are determined.

Station 4

To establish the burner exit conditions, we need to know the loss parameters, π_b and η_b, as well as the limiting temperature T_{t4}. The fuel type with its energy content, that we had called the *heating value* of the fuel, Q_R, needs to be specified. Again, we establish the fuel-to-air ratio, f, by energy balance across the burner and the total pressure at the exit, p_{t4}, by loss parameter π_b.

Station 4.5

For the upstream turbine, or the so-called *high-pressure turbine*, HPT, we need to know the mechanical efficiency, η_{mHPT}, which is a power transmission efficiency, and the turbine polytropic efficiency, e_{tHPT}, which measures the internal efficiency of the turbine. The power balance between the compressor and high-pressure turbine is

$$\eta_{mHPT}(1+f)(h_{t5} - h_{t4.5}) = h_{t3} - h_{t2} \tag{1.280a}$$

$$h_{t4.5} = h_{t4} - \frac{h_{t3} - h_{t2}}{\eta_{mHPT}(1+f)} \tag{1.280b}$$

leads to the only unknown in the above equation, which is $h_{t4.5}$. The total pressure at station 4.5 may be linked to the turbine total temperature ratio according to:

$$\frac{p_{t4.5}}{p_{t4}} = \left(\frac{T_{t4.5}}{T_{t4}}\right)^{\frac{\gamma_t}{(\gamma_t - 1)e_{tHPT}}} \tag{1.281}$$

$$\pi_{HPT} = \tau_{HPT}^{\frac{\gamma_t}{(\gamma_t - 1)e_{tHPT}}} \tag{1.282}$$

Stations 5 and 9

Since the power turbine drives the *load*, i.e. the propeller, we need to specify the turbine expansion ratio that supports this *load*. In this sense, we consider the propeller as an external load to the cycle and hence as an input parameter to the turboprop analysis. It serves a purpose to put this and the following station, i.e. 9, together, as both are responsible for the thrust production. Another view of stations 5 and 9 downstream of 4.5 points to the *power split*, decision made by the designer, between the propeller and the exhaust jet. The following T-s diagram best demonstrates this principle.

In the T-s diagram (Figure 1.50), both the actual and the ideal expansion processes are shown. We will use this diagram to define the component efficiencies as well as the

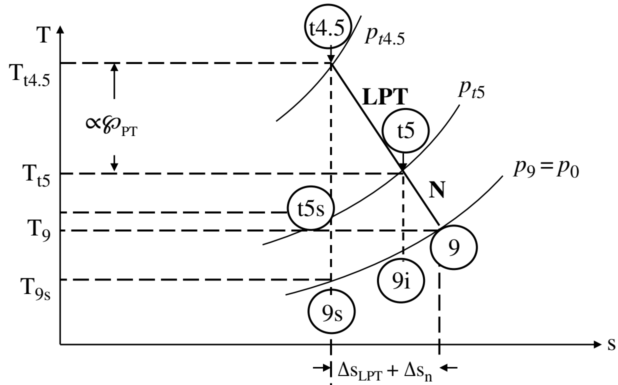

Figure 1.50 Thermodynamic states of an expansion process in free turbine and nozzle of a turboprop engine.

power split choice. For example, we define the power turbine (i.e. LPT) adiabatic efficiency as:

$$\eta_{\mathrm{LPT}} \equiv \frac{h_{t4.5} - h_{t5}}{h_{t4.5} - h_{t5s}} = \frac{h_{t4.5}\left(1-\tau_{\mathrm{LPT}}\right)}{h_{t4.5}\left[1-\pi_{\mathrm{LPT}}^{\frac{\gamma_t-1}{\gamma_t}}\right]} = \frac{1-\tau_{\mathrm{LPT}}}{1-\pi_{\mathrm{LPT}}^{\frac{\gamma_t-1}{\gamma_t}}} \tag{1.283}$$

Also, we may define the nozzle adiabatic efficiency, η_n, as:

$$\eta_n \equiv \frac{h_{t5} - h_9}{h_{t5s} - h_{9s}} \tag{1.284}$$

We note that the above definition for the nozzle adiabatic efficiency deviates slightly from our earlier definition in that we have assumed

$$h_{t5} - h_{9i} \approx h_{t5s} - h_{9s} \tag{1.285}$$

which, in light of small expansions in the nozzle and hence near parallel isobars, is considered reasonable.

The total ideal power available at station 4.5, per unit mass flow rate, may be written as:

$$\frac{\wp}{\dot{m}_0\left(1+f\right)} = h_{t4.5} - h_{9s} = h_{t4.5}\left[1-\left(\frac{p_9}{p_{t4.5}}\right)^{\frac{\gamma_t-1}{\gamma_t}}\right] = \wp_{i,\mathrm{total}} / \dot{m}_9 \tag{1.286}$$

If we examine the RHS of Eq. (1.286), we note that all terms on the RHS are known. Therefore, the total ideal power is known to us *a priori*. Now, let us assume that the power split between the free turbine and the nozzle is, say α and 1 − α, respectively (see Figure 1.51).

We can define the power split as:

$$\alpha \equiv \frac{h_{t4.5} - h_{t5s}}{h_{t4.5} - h_{9s}} = \frac{\dfrac{\wp_{\mathrm{LPT}} / \dot{m}_9}{\eta_{\mathrm{LPT}}}}{\wp_{i,\mathrm{total}} / \dot{m}_9} \tag{1.287}$$

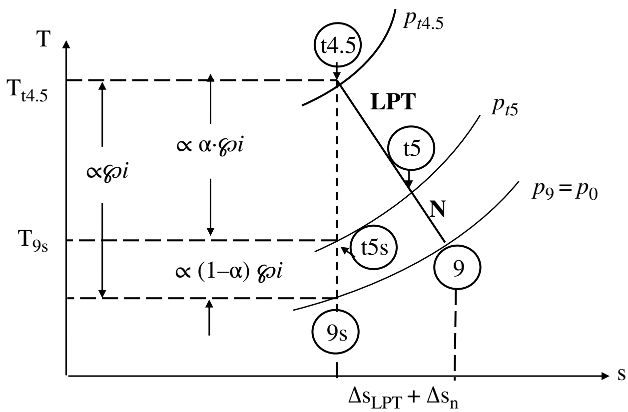

Figure 1.51 Definition of power split, α, in a turboprop engine.

which renders the following equation for the free turbine (LPT) power in terms of a given α,

$$\wp_{\mathrm{LPT}} = \dot{m}_9 \eta_{\mathrm{LPT}} .\alpha .h_{t4.5} \left[1 - \left(\frac{p_9}{p_{t4.5}} \right)^{\frac{\gamma_t - 1}{\gamma_t}} \right] = \dot{m}_9 \left(h_{t4.5} - h_{t5} \right) \tag{1.288}$$

This expression for the power turbine (LPT) can be applied to the propeller through gearbox and propeller efficiency in order to arrive at the thrust power produced by the propeller, namely

$$F_{\mathrm{prop}} .V_0 = \eta_{\mathrm{prop}} .\eta_{\mathrm{gb}} .\eta_{m\mathrm{LPT}} .\wp_{\mathrm{LPT}} = \dot{m}_0 \left(1 + f \right) \left[\alpha \eta_{\ \mathrm{LPT}} \eta_{m\mathrm{LPT}} \eta_{\mathrm{gb}} \eta_{prop} \right] h_{t4.5} \left[1 - \left(\frac{p_9}{p_{t4.5}} \right)^{\frac{\gamma_t - 1}{\gamma_t}} \right] \tag{1.289}$$

We note that the R.H.S. of the above equation, per unit mass flow rate, is known. Now, let us examine the nozzle thrust. The kinetic energy per unit mass at the nozzle exit is linked to:

$$V_9^2 / 2 \cong \eta_n \left(h_{t5s} - h_{9s} \right) = \eta_n \left(1 - \alpha \right) \wp_{\mathrm{i,total}} / \dot{m}_9 = \left(1 - \alpha \right) \eta_n h_{t4.5} \left[1 - \left(\frac{p_9}{p_{t4.5}} \right)^{\frac{\gamma_t - 1}{\gamma_t}} \right] \tag{1.290}$$

Therefore, the exhaust velocity is now approximated by the power split parameter, α, and the total ideal power available after the gas generator, i.e. station 4.5, according to:

$$V_9 \approx \sqrt{2\left(1 - \alpha \right) \eta_n h_{t4.5} \left[1 - \left(\frac{p_9}{p_{t4.5}} \right)^{\frac{\gamma_t - 1}{\gamma_t}} \right]} \tag{1.291}$$

Now, the turboprop thrust per unit air mass flow rate (through the core) can be expressed in terms of the propeller thrust, the core thrust using Eq. (1.291) incorporated for the exhaust velocity.

$$\frac{F_{\text{total}}}{\dot{m}_0} = (1+f)V_9 - V_0 + \frac{(1+f)\left[\alpha\eta_{\text{PT}}\eta_{m\text{LPT}}\eta_{\text{gb}}\eta_{\text{prop}}\right]h_{t4.5}\left[1-\left(\frac{p_9}{p_{t4.5}}\right)^{\frac{\gamma_t-1}{\gamma_t}}\right]}{V_0} \tag{1.292}$$

The fuel efficiency of a turboprop engine is often expressed in terms of the fraction of the fuel consumption in the engine to produce a unit shaft/mechanical power, according to:

$$PSFC \equiv \frac{\dot{m}_f}{\wp_{\text{prop}} + \wp_{\text{core}}} = \frac{f}{\left(\frac{\wp_{\text{prop}}}{\dot{m}_0} + \frac{\wp_{\text{core}}}{\dot{m}_0}\right)} \tag{1.293}$$

$$\wp_{\text{prop}} = \eta_{\text{gb}}\eta_{mLPT}\wp_{\text{LPT}} = \dot{m}_0(1+f)\eta_{\text{gb}}\eta_{mLPT}\eta_{\text{LPT}}.\alpha.h_{t4.5}\left[1-\left(\frac{p_9}{p_{t4.5}}\right)^{\frac{\gamma_t-1}{\gamma_t}}\right] \tag{1.294}$$

$$\wp_{\text{core}} = \frac{\dot{m}_0}{2}\left[(1+f)V_9^2 - V_0^2\right] \quad \text{for a perfectly expanded nozzle,otherwise use } V_{9\text{eff}} \tag{1.295}$$

We can define the thermal efficiency of a turboprop engine as:

$$\eta_{th} \equiv \frac{\wp_{\text{prop}} + \wp_{\text{core}}}{\dot{m}_f Q_R} = \frac{\left(\frac{\wp_{\text{prop}}}{\dot{m}_0} + \frac{\wp_{\text{core}}}{\dot{m}_0}\right)}{fQ_R} \tag{1.296}$$

The propulsive efficiency, η_p, may be defined as:

$$\eta_p \equiv \frac{F_{\text{total}}.V_0}{\wp_{\text{prop}} + \wp_{\text{core}}} = \frac{\frac{F_{\text{total}}}{\dot{m}_0}.V_0}{\left(\frac{\wp_{\text{prop}}}{\dot{m}_0} + \frac{\wp_{\text{core}}}{\dot{m}_0}\right)} \tag{1.297}$$

where all the terms in the above efficiency definitions have been calculated in earlier steps and the overall efficiency is again the product of the thermal and propulsive efficiencies

1.10.2.3 Optimum Power Split between the Propeller and the Jet

For a given fuel flow rate, flight speed, compressor pressure ratio, and all internal component efficiencies, we may ask a very important question, which is, "At what power split, α, would the total thrust be maximized?" This is a simple mathematics question. What we need first is to express the total thrust in terms of all independent parameters, i.e. f, V_0, π_c etc., and then differentiate it with respect to α and set the derivative equal to zero. From that equation, obtain the solution(s) for α that satisfies the equation. We use Eq. (1.292)

$$\frac{F_{\text{total}}}{\dot{m}_0} = (1+f)V_9 - V_0 + \frac{(1+f)\left[\alpha\eta_{\text{LPT}}\eta_{mLPT}\eta_{\text{gb}}\eta_{\text{prop}}\right]h_{t4.5}\left[1-\left(\frac{p_9}{p_{t4.5}}\right)^{\frac{\gamma_t-1}{\gamma_t}}\right]}{V_0}$$

We express the exhaust velocity, V_9, as Eq. (1.291):

$$V_9 \approx \sqrt{2(1-\alpha)\eta_n h_{t4.5}\left[1-\left(\frac{p_9}{p_{t4.5}}\right)^{\frac{\gamma_t-1}{\gamma_t}}\right]}$$

We note that the bracketed term in the above equations, i.e.

$$1-\left(\frac{p_9}{p_{t4.5}}\right)^{\frac{\gamma_t-1}{\gamma_t}} = 1-\left(\frac{p_9}{p_0}\frac{p_0}{p_{t0}}\frac{p_{t0}}{p_{t2}}\frac{p_{t2}}{p_{t3}}\frac{p_{t3}}{p_{t4}}\frac{p_{t4}}{p_{t4.5}}\right)^{\frac{\gamma_t-1}{\gamma_t}} = 1-\left(\frac{p_9}{p_0}\left(\pi_r\pi_d\pi_c\pi_b\pi_{\text{HPT}}\right)^{-1}\right)^{\frac{\gamma_t-1}{\gamma_t}} \tag{1.298}$$

which is a constant. Also let us examine the total enthalpy at station 4.5, $h_{t4.5}$,

$$h_{t4.5} = \frac{h_{t4.5}}{h_{t4}}\frac{h_{t4}}{h_0}h_0 = \tau_{\text{HPT}}.\tau_\lambda.h_0 \tag{1.299}$$

which is a constant, as well. Therefore, the expression for the total thrust of the engine (per unit mass flow rate in the engine nozzle) is essentially composed of a series of constants and the dependence on power split parameter, α takes on the following simplified form:

$$\frac{F_{\text{total}}}{(1+f)\dot{m}_0} = C_1\sqrt{1-\alpha} + C_2\alpha + C_3 \tag{1.300}$$

where C_1, C_2, and C_3 are all constants. Now, let us differentiate the above function with respect to α and set the derivative equal to zero, i.e.

$$\frac{d}{d\alpha}\left[\frac{F_{\text{total}}}{(1+f)\dot{m}_0}\right] = \frac{-C_1}{2\sqrt{1-\alpha}} + C_2 = 0 \tag{1.301}$$

which produces a solution for the power split parameter, α, that maximizes the total thrust of a turboprop engine. Hence, we may call this special value of α, the "optimum" α, namely

$$\alpha_{\text{opt}} = 1-\left(\frac{C_1}{2C_2}\right)^2 \tag{1.302}$$

Now, upon substitution for the constants C_1 and C_2 and some simplification, we get:

$$\alpha_{\text{opt}} = 1 - \frac{\eta_n}{\left(\eta_{\text{PT}}\eta_{\text{mLPT}}\eta_{\text{gb}}\eta_{\text{prop}}\right)^2} \cdot \frac{\gamma_c - 1}{2} \frac{M_0^{\,2}}{\tau_{\text{HPT}}\tau_\lambda\left[1 - \left(\dfrac{p_9/p_0}{\pi_r\pi_d\pi_c\pi_b\pi_{\text{HPT}}}\right)^{\frac{\gamma_t - 1}{\gamma_t}}\right]} \tag{1.303}$$

This expression for the optimum power split between the propeller and the jet involves all component and transmission (of power) efficiencies, as expected. However, let us assume that all efficiencies were 100% and further assume that the exhaust nozzle was perfectly expanded, i.e. $p_9 = p_0$. What does the above expression tell us about the optimum power split in a perfect turboprop engine? Let us proceed with the simplifications.

$$\alpha_{\text{opt}_{\text{ideal}}} = 1 - \frac{\dfrac{\gamma_c - 1}{1} M_0^{\,2}}{\tau_{\text{HPT}}\tau_\lambda - \dfrac{\tau_\lambda}{\tau_r\tau_c}} \tag{1.304}$$

From power balance between the compressor and the high-pressure turbine, we can express the following:

$$\tau_r\left(\tau_c - 1\right) = \left(1 + f\right)\tau_\lambda\left(1 - \tau_{\text{HPT}}\right) \approx \tau_\lambda\left(1 - \tau_{\text{HPT}}\right) \tag{1.305}$$

This simplifies to

$$\tau_\lambda\tau_{\text{HPT}} \cong \tau_\lambda - \tau_r\left(\tau_c - 1\right) \tag{1.306}$$

Substitute the above equation in the optimum power split in an ideal turboprop engine, Eq. (1.304), to get:

$$\alpha_{\text{opt}_{\text{ideal}}} = 1 - \frac{\dfrac{\gamma_c - 1}{2} M_0^{\,2}}{\tau_\lambda - \tau_r\left(\tau_c - 1\right) - \dfrac{\tau_\lambda}{\tau_r\tau_c}} = 1 - \frac{\tau_r - 1}{\tau_\lambda - \tau_r\left(\tau_c - 1\right) - \dfrac{\tau_\lambda}{\tau_r\tau_c}} \tag{1.307}$$

At takeoff condition and low-speed climb/descent ($\tau_r \to 1$), the optimum power split approaches 1, as expected. The propeller is the most efficient propulsor at low speeds, as it attains the highest propulsive efficiency. As flight Mach number increases, the power split term α becomes less than one.

Example 1.4

For the turboprop, we chose Mach 0.6 cruise at 12 km (standard) altitude. Compressor pressure ratio is $\pi_c = 30$, turbine entry temperature TET = 1600 K. To examine the effect of power drainage in the exhaust stream, we vary the power split parameter, α, between 0.78 and 0.98. We choose propeller efficiency at cruise $\eta_{\text{prop}} = 0.80$, fuel LHV is 43 MJ kg^{-1}, and component efficiency and loss parameters: $\pi_d = 0.98$, $\pi_b = 0.96$, $e_c = 0.92$, $e_{t\text{HPT}} = 0.82$, $\eta_{t\text{LPT}} = 0.88$, $\eta_n = 0.96$, $\eta_{m,H} = 0.99$, $\eta_{m,L} = 0.99$, $\eta_b = 0.99$ and the nozzle was perfectly expanded, with $p_9/p_0 = 1.0$. Gas properties were assumed to be: $\gamma_c = 1.4$, $c_{pc} = 1004$ J kgK^{-1} and $\gamma_t = 1.33$, $c_{pt} = 1156$ J kgK^{-1}.

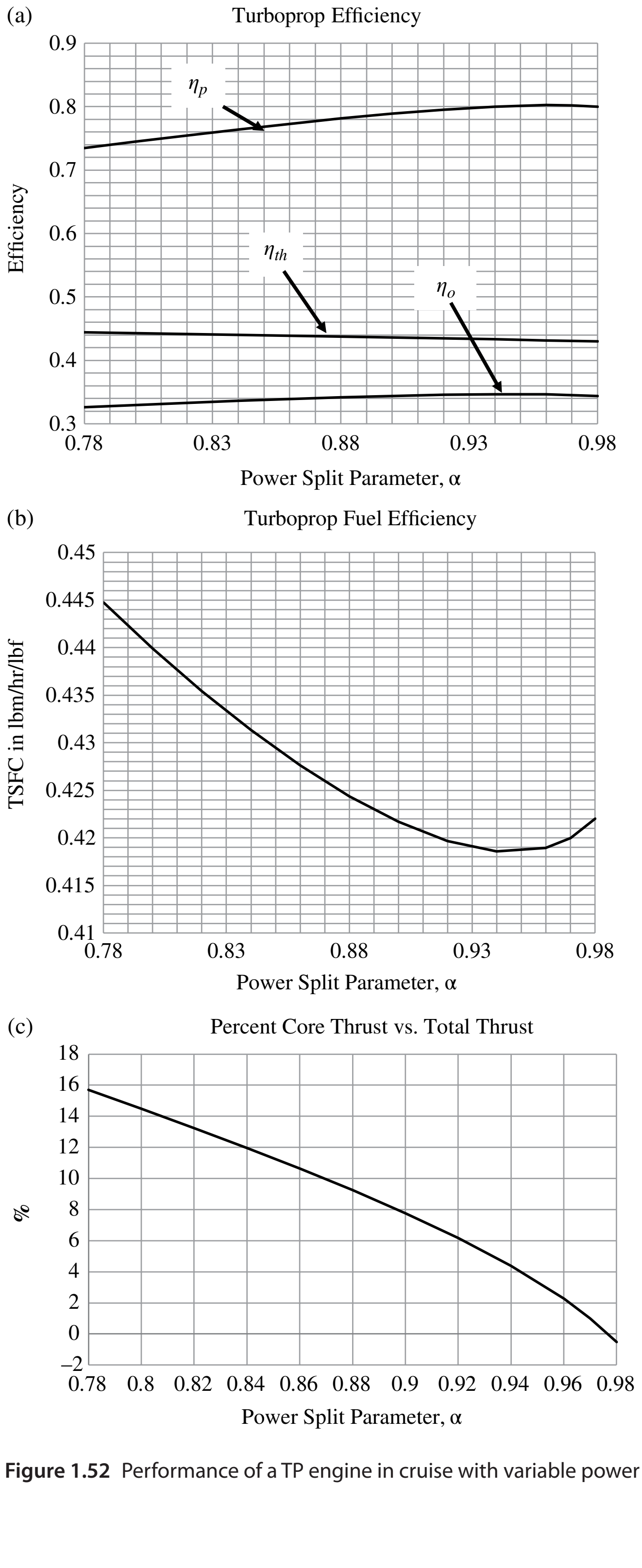

Figure 1.52 Performance of a TP engine in cruise with variable power split, α.

Figure 1.52a shows that the propulsive efficiency increases with power split in favor of the propeller, until it plateaus at ~0.94, whereas thermal efficiency remains nearly constant at ~43%. The peak overall efficiency is slightly better than TF, but it is dismal at ~ 35%.

Figure 1.52b shows that the TP fuel burn continually improves until it reaches a plateau at α~0.94 power split. The core starts to produce a net drag, instead of thrust as the nozzle jet speed falls below flight speed when we drain the exhaust stream at levels of $\alpha \gtrsim 0.97$.

The behavior of core thrust as percent total shows energy drainage with α. Core ceases to produce thrust at $\alpha \gtrsim 0.97$, as shown in Figure 1.52c.

1.10.2.4 Advanced Propeller: Prop-Fan

Conventional propellers lose their thrust production capability when their tip operates in supersonic flow and stall, also known as compressibility losses. In the United States, Pratt & Whitney/Allison Gas Turbine, GE Aviation, and NASA collaborated in developing the technology of advanced turboprop engines in the 1970s and 1980s (Hager and Vrabel 1988). These engines represent open-rotor architecture, which are at times called Propfan, while GE's gearless, direct-drive ATP is called the unducted fan (UDF). The advanced propellers operate with relative (or helical) supersonic tip Mach number (M_T~1.1–1.15) without stalling! With increasing capability in relative tip Mach number of the advanced propeller, the cruise flight Mach number is increased to M_0~0.8–0.85. Several configurations in co- and counter-rotating propeller sets and pusher versus tractor configurations were developed and flight-tested. The advanced propellers are thin (with 3–5% thickness-to-chord ratio) and highly swept at the tip (between 30–40°) to improve tip efficiency at high relative Mach numbers. This is akin to reducing effective Mach number on a transonic aircraft wing based on sweep angle and thickness. Maximum tip sweep, within the aeroelastic stability constraints of the fan, has resulted in 30°–40° angle in advanced propellers. The subjects of sweep and aeroelasticity are detailed in a modern transonic aerodynamic textbook by Vos and Farokhi (2015) that may be consulted for review.

Figure 1.53 shows the first generation of ATP tested at NASA (from NASA SP-495 1988).

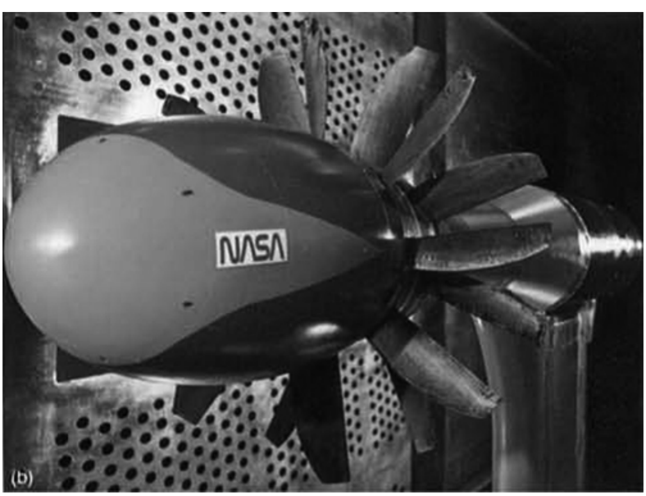

Figure 1.53 Unducted-Fan (UDF) counter-rotating model at NASA-Lewis (now Glenn) wind tunnel. *Source:* Courtesy of NASA.

The critical design areas in an ATP powered aircraft are:

- ATP integration issues, e.g. tractor vs. pusher, wing vs. aft-fuselage
- Fan blade aero-structural design for max aero-efficiency and dynamic stability
- Fan actuation/pitch control
- Blade retention system
- Blade-out condition
- Nacelle cowl system design
- Spinner area-ruling to prevent blade root choking (in tractor configuration)

1.11 High-Speed Air-Breathing Engines

Ramjets offer the highest (fuel) specific impulse at flight Mach numbers above ~4, as depicted in Figure 1.54. However, they produce no static thrust. The analysis of conventional, i.e. subsonic combustion, ramjets is the same as other air-breathing engines such as turbojets (see Kerrebrock (1992) or Hill and Peterson (1992)). A typical flow path in a conventional ramjet engine is shown in Figure 1.55.

The T-s diagram of the ramjet cycle is shown in Figure 1.56. The ram compression in supersonic-hypersonic flow includes shock compression that causes an increase in gas temperature and a reduction in the Mach number. In the conventional ramjet, there is a normal shock in the inlet that transitions the flow into subsonic regime. The typical combustor Mach numbers in a conventional ramjet is ~0.2–0.3. The combustor exit temperature, T_{t4}, may reach stoichiometric levels of ~2000–2500 K.

The equations that are used in the calculation of conventional ramjet performance are listed in Tables 1.3 and 1.4. The equations in these tables are listed sequentially;

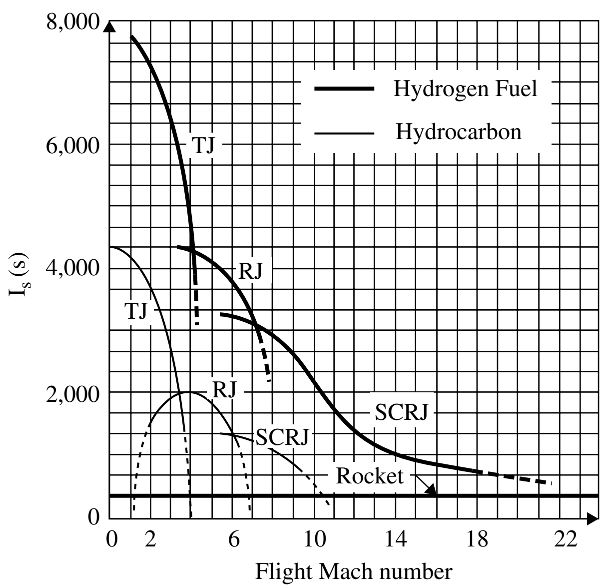

Figure 1.54 Approximate variation of specific impulse with flight Mach number for different air-breathing engines (TJ: turbojet, RJ: ramjet and SCRJ: scramjet) and a typical chemical rocket. *Source:* Adapted from Kerrebrock 1992.

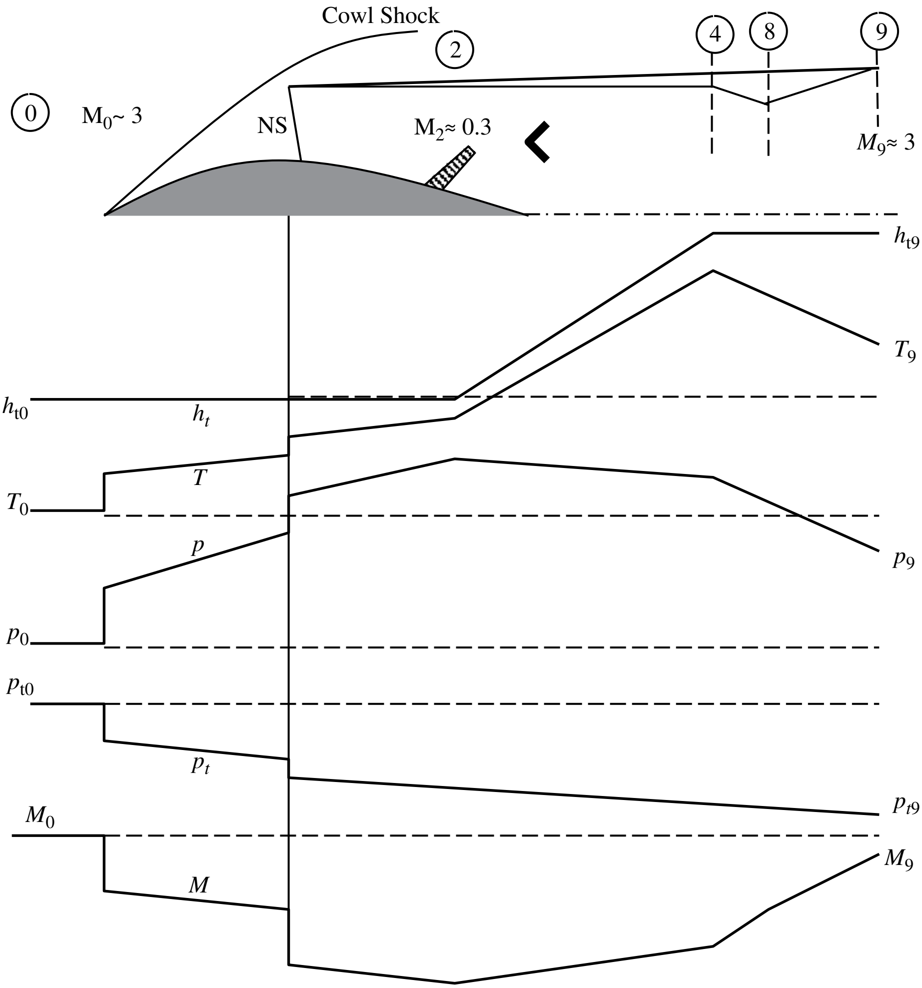

Figure 1.55 Flow parameter trends in a typical subsonic-combustion ramjet.

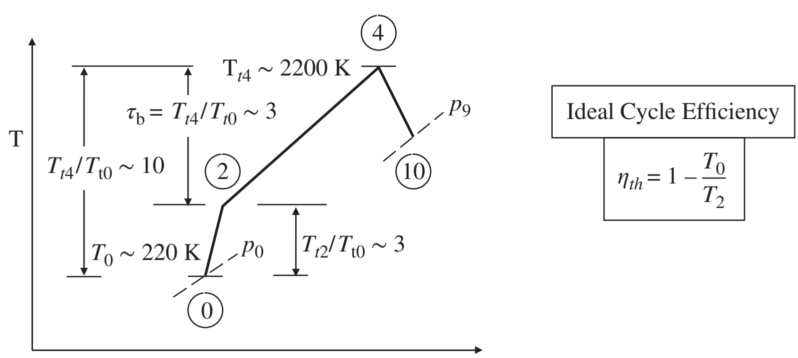

Figure 1.56 Conventional (subsonic-combustion) ramjet cycle and its ideal thermal efficiency.

Table 1.3 Summary of ramjet equations in terms of dimensional parameters (for calorically perfect gas).

Given:
M_0, p_0, T_0 (or altitude), γ and R
η_d or π_d
π_b, η_b, Q_R and T_{t4} or τ_λ
π_n or η_n and p_9
Calculate: f, $F_n / \dot{m}_0$, $TSFC$, I_s, η_{th}, η_p and η_o

$T_{t0} = T_0\left(1+\frac{\gamma-1}{2}M_0^2\right) = T_{t2}$	Get flight total temperature
$p_{t0} = p_0\left(1+\frac{\gamma-1}{2}M_0^2\right)^{\frac{\gamma}{\gamma-1}}$	Get flight total pressure
$V_0 \equiv M_0.a_0 = M_0\sqrt{\gamma R T_0}$	Get flight velocity
$\frac{p_{t2}}{p_0} = \left\{1+\eta_d\frac{\gamma-1}{2}M_0^2\right\}^{\frac{\gamma}{\gamma-1}}$ or $p_{t2} = \pi_d . p_{t0}$	Get total pressure at diffuser exit
$p_{t4} = p_{t2} . \pi_b$	Get burner exit total pressure
$f = \frac{h_{t4} - h_{t0}}{Q_R\eta_b - h_{t4}} = \frac{T_{t4} - T_{t0}}{Q_R\eta_b / c_p - T_{t4}}$	Get fuel-to-air ratio in the burner
$\pi_n = \left\{\left(\frac{p_{t4}}{p_9}\right)^{\frac{\gamma-1}{\gamma}} - \eta_n\left[\left(\frac{p_{t4}}{p_9}\right)^{\frac{\gamma-1}{\gamma}} - 1\right]\right\}^{\frac{-\gamma}{\gamma-1}}$	Get nozzle total pressure ratio
$p_{t9} = p_{t4} . \pi_n$	Get total pressure at nozzle exit
$M_9 = \sqrt{\frac{2}{\gamma-1}\left[\left(\frac{p_{t9}}{p_9}\right)^{\frac{\gamma-1}{\gamma}} - 1\right]}$	Get nozzle exit Mach number
$T_9 = \frac{T_{t9}}{1+\frac{\gamma-1}{2}M_9^2}$	Get nozzle exit static temperature
$a_9 = \sqrt{\gamma R T_9}$	Get speed of sound at nozzle exit
$V_9 = a_9 . M_9$	Get nozzle exit velocity
$\frac{F_n}{\dot{m}_0} = (1+f)V_9\left(1+\frac{1}{\gamma M_9^2}\left(1-\frac{p_0}{p_9}\right)\right) - V_0$	Get specific thrust
$TSFC \equiv \frac{\dot{m}_f}{F_n} = \frac{f}{F_n / \dot{m}_0}$	Get thrust-specific fuel consumption
$I_s = 1/(g_0 TSFC)$	Get fuel-specific impulse
$\eta_p = \frac{2(F_n / \dot{m}_0)V_0}{(1+f)V_9^2 - V_0^2}$	Get propulsive efficiency
$\eta_{th} = \frac{(1+f)V_9^2 - V_0^2}{2fQ_R\eta_b}$	Get cycle thermal efficiency
$\eta_o = \eta_p . \eta_{th} = \frac{(F_n / \dot{m}_0)V_0}{fQ_R\eta_b} = \frac{V_0 / Q_R\eta_b}{TSFC}$	Get overall efficiency

Table 1.4 Summary of ramjet equations in terms of nondimensional parameters (for calorically perfect gas).

Given:
M_0, p_0, T_0 (or altitude), γ and R
η_d or π_d
π_b, η_b, Q_R and T_{t4} or τ_λ
π_n or η_n and p_9
Calculate: f, $F_n/\dot{m}_0$, $TSFC$, I_s, η_{th}, η_p, and η_o

$\tau_r = 1 + \frac{\gamma-1}{2}M_0^2$	Get ram temperature ratio
$\pi_r = \left(1+\frac{\gamma-1}{2}M_0^2\right)^{\frac{\gamma}{\gamma-1}} = \tau_r^{\frac{\gamma}{\gamma-1}}$	Get ram pressure ratio
$\pi_d = \frac{p_{t2}}{p_{t0}} = \left(\frac{1+\eta_d\frac{\gamma-1}{2}M_0^2}{1+\frac{\gamma-1}{2}M_0^2}\right)^{\frac{\gamma}{\gamma-1}}$	Get inlet total pressure ratio
$f = \frac{\tau_\lambda - \tau_r}{\frac{Q_R\eta_b}{c_pT_0} - \tau_\lambda}$	Get fuel-to-air ratio
$\pi_n = \left\{\left(\pi_b\pi_d\pi_r\frac{p_0}{p_9}\right)^{\frac{\gamma-1}{\gamma}} - \eta_n\left[\left(\pi_b\pi_d\pi_r\frac{p_0}{p_9}\right)^{\frac{\gamma-1}{\gamma}} - 1\right]\right\}^{\frac{-\gamma}{\gamma-1}}$	Get nozzle pressure ratio
$M_9 = \sqrt{\frac{2}{\gamma-1}\left[\left(\pi_n\pi_b\pi_d\pi_r\frac{p_0}{p_9}\right)^{\frac{\gamma-1}{\gamma}} - 1\right]}$	Get nozzle exit Mach number
$V_9 = M_9\sqrt{\gamma RT_0\frac{\tau_\lambda}{1+\frac{\gamma-1}{2}M_9^2}} = a_0M_9\sqrt{\frac{\tau_\lambda}{1+\frac{\gamma-1}{2}M_9^2}}$	Get exhaust velocity
$\frac{F_n}{\dot{m}_0} = (1+f)V_9\left(1+\frac{1}{\gamma M_9^2}\left(1-\frac{p_0}{p_9}\right)\right) - V_0$	Get specific thrust
$TSFC \equiv \frac{\dot{m}_f}{F_n} = \frac{f}{F_n/\dot{m}_0}$	Get thrust-specific fuel consumption
$I_s = 1/(g_0.TSFC)$	Get fuel-specific impulse
$\eta_p = \frac{2(F_n/\dot{m}_0)V_0}{(1+f)V_9^2 - V_0^2}$	Get propulsive efficiency η_p
$\eta_{th} = \frac{(1+f)V_9^2 - V_0^2}{2fQ_R\eta_b}$	Get thermal efficiency η_{th}
$\eta_o = \eta_p.\eta_{th} = \frac{(F_n/\dot{m}_0)V_0}{fQ_R\eta_b} = \frac{V_0/Q_R\eta_b}{TSFC}$	Get overall efficiency η_o

therefore, they are useful in computer-based calculations/simulation of ramjets. These are the same equations as in turbojets except we have set $\pi_c = 1$ to simulate a ramjet.

1.11.1 Supersonic Combustion Ramjet

Ramjets cannot produce static thrust. They require ram compression, i.e. some forward flight speed, before these simple air-breathing engines (or ducts with burners) can produce thrust. It is seemingly ironic that the same engines (i.e. ramjets) *cease* to produce thrust at very high ram compressions! Two aspects of ram compression are detrimental to thrust production at high speeds:

1) The inlet total pressure recovery is exponentially deteriorated with flight Mach number.
2) The rising gas temperature in the inlet cuts back $(\Delta T_t)_{\text{burner}}$ to eventually zero.

The worst offender in total pressure recovery of supersonic/hypersonic inlets is the normal shock, which incidentally is also responsible for the rising gas temperatures ahead of the burner. Therefore, if we could only do away with the normal shock in the inlet, we should be getting a super-efficient ramjet. But the flow in a supersonic inlet without a (terminal) normal shock would still be supersonic in the combustor! Despite the obvious challenges, supersonic combustion ramjets, or scramjets are born out of necessity. Scramjets hold out the promise of being the most efficient air-breathing engines, i.e. with the highest (fuel) specific impulse, at flight Mach numbers above ~6 to suborbital Mach numbers (i.e. M~20); although the upper limits in scramjet operational Mach number is still unknown.

Scramjet engines, more than any other air-breathing engine, need to be integrated with the aircraft. The need for integration stem from a long forebody that is needed at hypersonic Mach numbers to efficiently compress the air. In addition, a long forebody offers the largest capture area possible for the engine, A_0. Aft-integration with the aircraft allows for a large area ratio nozzle suitable for high-altitude hypersonic vehicles. Figure 1.57 shows a generic scramjet engine that is integrated in a hypersonic aircraft. The inlet achieves compression both externally and internally through oblique shocks. The series of oblique shock reflections inside the inlet create a shock train, known as the *isolator*. The flow that emerges from the isolator is supersonic, say Mach 3.0, as it enters the combustor. Achieving efficient combustion at supersonic speeds is a challenge.

Fuel injection, atomization, vaporization, mixing, and chemical reaction time scales should, by necessity, be short. If air is moving at Mach-3 where speed of sound is ~333 m s^{-1}, it traverses 1 m in ~1 millisecond. This is just an indication of the convective or residence time scale in the combustor. Hydrogen offers these qualities. For example, hydrogen offers about 1/10 of the chemical reaction time scale of hydrocarbon fuels. Additionally, hydrogen is in a cryogenic state as a liquid; therefore, it offers aircraft and engine structure regenerative cooling opportunities.

By accepting high Mach numbers inside the scramjet engine; the static temperature of the gas will be lower throughout the engine and thus the burner is allowed to release heat in the combustor that is needed for propulsion. The h-s diagram of the scramjet cycle is shown in Figure 1.58.

1.11.1.1 Inlet Analysis

Scramjet inlets are integrated with the aircraft forebody, involving several external and internal oblique shocks. In addition, the vehicle's angle of attack, α, impacts the inlet

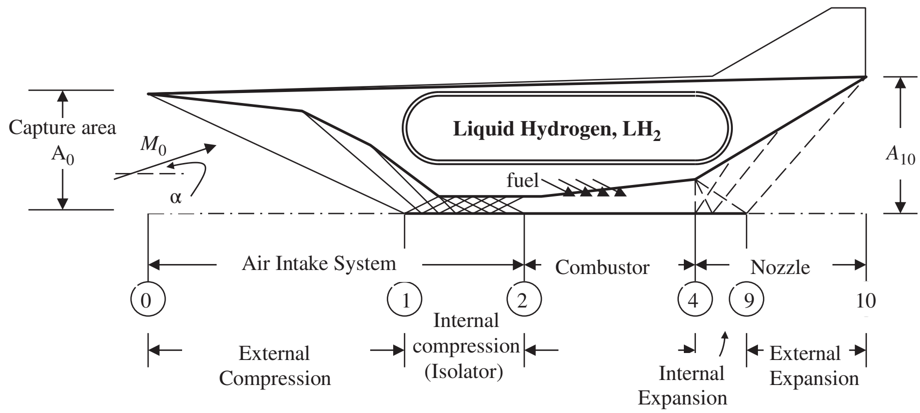

Figure 1.57 Typical arrangement of a generic scramjet engine on a hypersonic aircraft.

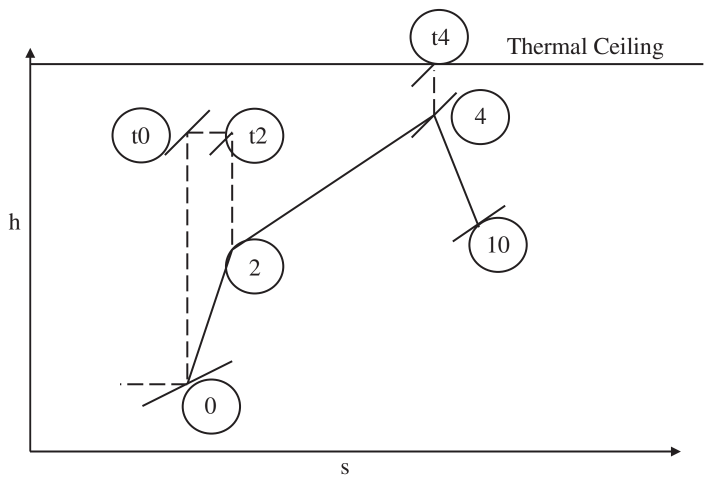

Figure 1.58 Static and stagnation states of gas in a scramjet engine.

recovery through oblique shock waves' angles. For a given forebody shape, we may use shock-expansion theory to calculate the waves' orientations and the associated total pressure recovery. In the absence of the detailed aircraft forebody geometry, or in the preliminary phase, we may assume an inlet recovery or resort to standards such as AIA or MIL-E-5008B (MIL-STD). We listed these here for convenience:

$$\pi_d = 1 - 0.1(M_0 - 1)^{1.5} \qquad 1 < M_0 \qquad \text{AIA} - \text{Standard} \tag{1.308}$$

$$\pi_d = 1 - 0.075(M_0 - 1)^{1.35} \qquad 1 < M_0 < 5 \qquad \text{MIL} - \text{E} - \text{5008B} \tag{1.309}$$

$$\pi_d = 800/\left(M_0^4 + 935\right) \qquad 5 < M_0 \qquad \text{MIL} - \text{E} - \text{5008B} \tag{1.310}$$

1.11.1.2 Scramjet Combustor

Although the detail design and analysis of supersonic combustion is beyond the scope of this book, we can still present global models and approaches that are amenable to closed-form solution. Supersonic branch of Rayleigh flow, i.e. a frictionless, constant-area duct with heating, is a possible (and the simplest) model for a scramjet combustor. The fact that the analysis was derived for a constant-area duct is not a major limitation, since we can divide a combustor with area change into a series of combustors with constant areas. Rayleigh flow is detailed in Chapter 2 of Farokhi (2014), and we will not review it here. However, we may offer to analyze a variable-area combustor that maintains a constant pressure. From cycle analysis viewpoint, constant-pressure combustion is advantageous to cycle efficiency, and thus we consider it here further. Figure 1.59 shows a frictionless duct with heat exchange but with constant static pressure. We assume the gas is calorically perfect and the flow is steady and one-dimensional. The contribution of fuel mass flow rate to the gas in the duct is small; therefore, combustion is treated as heat transfer through the wall. The problem statement specifies the inlet condition and heat transfer rate (or fuel-flow rate or fuel-to-air ratio) and assumes a constant static pressure in a duct with a variable area. The purpose of the analysis is to calculate the duct exit flow condition as well as the area, A_4.

We apply conservation principles to the slab of fluid, as shown. The continuity requires:

$$\rho AV = (\rho + d\rho)(V + dV)(A + dA) \quad \frac{dV}{V} + \frac{d\rho}{\rho} + \frac{dA}{A} = 0 \tag{1.311}$$

The balance of x-momentum gives

$$\dot{m}(V + dV) - \dot{m}V = pA - p(A + dA) + pdA \equiv 0 \quad dV = 0 \tag{1.312}$$

Equation (1.312) signifies a constant-velocity flow, i.e.

$$V_4 = V_2 \tag{1.313}$$

Therefore, continuity Eq. (1.311) demands ρA = constant; or area is inversely proportional to density.

The energy balance written for the duct gives:

$$h_{t4} - h_{t2} = \frac{\dot{Q}}{\dot{m}} = q = fQ_R\eta_b \tag{1.314a}$$

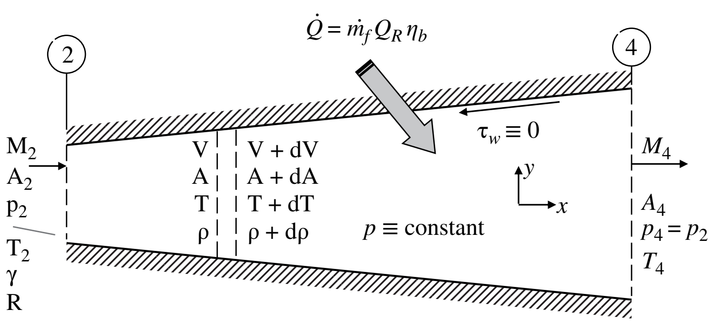

Figure 1.59 A frictionless, constant-pressure combustor.

Since with constant velocity, the kinetic energy (per unit mass) remains constant, then

$$h_{t4} - h_{t2} = h_4 - h_2 \tag{1.314b}$$

$$T_4 = T_2 + q / c_p = T_2 + fQ_R\eta_b / c_p \tag{1.315}$$

The RHS of Eq. (1.315) is known (as an input to the problem), which then establishes the exit static temperature, T_4. Since static pressure is constant, we can calculate the exit density, ρ_4. Also, the area ratio follows the inverse of the density ratio, i.e.

$$A_4 = A_2\left(\rho_2 / \rho_4\right) \tag{1.316}$$

which establishes the exit flow area. The exit static temperature calculates the exit speed of sound and Mach number (since V = constant).

We may calculate a critical heat flux, q^* (or critical fuel-to-air ratio, f^*), that will choke the duct at its exit. Eq. (1.315) is written as

$$\frac{T_4}{T_2} = 1 + \frac{q}{c_p T_2} \tag{1.317}$$

Also, Mach number ratio, M_4/M_2 is related to the ratio of speeds of sound following:

$$\frac{M_4}{M_2} = \frac{V_4 a_2}{V_2 a_4} = \frac{a_2}{a_4} = \sqrt{\frac{T_2}{T_4}} = \frac{1}{\sqrt{1 + \frac{q}{c_p T_2}}} \tag{1.318}$$

For a choked exit, $M_4 = 1$, therefore the critical heat flux, q^*, in terms of duct inlet flow conditions is expressed as:

$$\frac{q^*}{c_p T_2} = M_2^2 - 1 \tag{1.319a}$$

In terms of fuel-to-air ratio, we may express q^* as $f^* Q_R\eta_b$ to get:

$$f^* \approx \frac{c_p T_2}{Q_R\eta_b}\left(M_2^2 - 1\right) \tag{1.319b}$$

With calculated exit Mach number, we may arrive at the total pressure at the exit, following

$$p_{t4} = p_2\left(1 + \frac{\gamma - 1}{2} M_4^2\right)^{\frac{\gamma}{\gamma - 1}}$$

An input to this analysis is the burner efficiency, η_b. However, combustion efficiency in supersonic streams is not as well established or understood as the conventional low-speed burners. Mixing efficiency in supersonic shear layers, without chemical reaction, forms the foundation of scramjet combustion efficiency. A supersonic stream mixes with a lower speed stream (in our case the fuel) along a shear layer by vortex formations and supersonic wave interactions. These interactions require space along the (shear layer) or flow direction. Consequently, burner efficiency is a function of the combustor length and continually grows with distance along the scramjet combustor. Burrows and Kurkov (1973) may be consulted for some data and analysis related to supersonic combustion of hydrogen in vitiated air. Heiser et al. (1994) should be consulted for detailed discussion of hypersonic air-breathing propulsion.

1.11.1.3 Scramjet Nozzle

The large area ratios needed for high-speed, high-altitude flight prompted the use of aircraft aft-underbody as the expansion ramp for the scramjet nozzle (shown in Figure 1.57). For perfect expansion, we may approximate the area ratio requirements, A_{10}/A_9, by one-dimensional gas dynamic equations. Severe overexpansion at lower altitudes causes a shock to appear on the aft underbody of the vehicle. The complicating factors in the analysis of hypersonic air-breathing nozzles are similar to those in the rocket nozzles, i.e. continuing chemical reaction in the nozzle, flow separation, cooling, and flow unsteadiness, among others. Simple nozzle design based on the method of characteristics is a classical approach that students in gas dynamics learn. However, developing robust, high-fidelity computational fluid dynamics codes for direct numerical simulation of viscous reacting flows is the most powerful tool that researchers and industry are undertaking.

1.12 Rocket-Based Airbreathing Propulsion

Integrating rockets with ramjets has long been the solution of overcoming ramjets lack of takeoff capability. A ram-rocket may be a configuration similar to the one shown in Figure 1.60.

A fuel-rich solid propellant rocket provides the takeoff thrust. The air intake is sealed off until forward speed of the aircraft can produce the needed ram compression for the ramjet combustor to sustain stable thrust. The rocket motor serves as the *gas generator* for the ramjet, i.e. combustion gases from the fuel-rich solid propellant in the rocket motor mix with the air and the mixture is combusted in the ramjet burner to produce thrust. Variations of this scheme, such as a separate ramjet fuel, may be used in a gas generator ram-rocket. There is no new theory to be presented here, at least at the preliminary level, i.e. we have developed basic tools to analyze both components individually and combined. A ram-rocket configuration where the rocket provides takeoff thrust is shown in Figure 1.61. The ramjet fuel is injected in the air stream for sustained thrust, as shown.

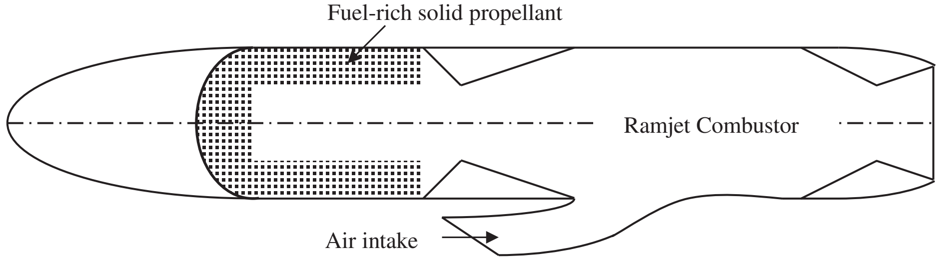

Figure 1.60 Schematic drawing of a gas generator ram-rocket.

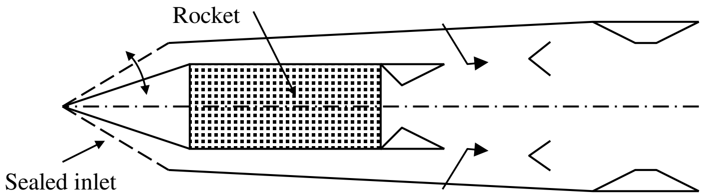

Figure 1.61 Ram-rocket configuration.

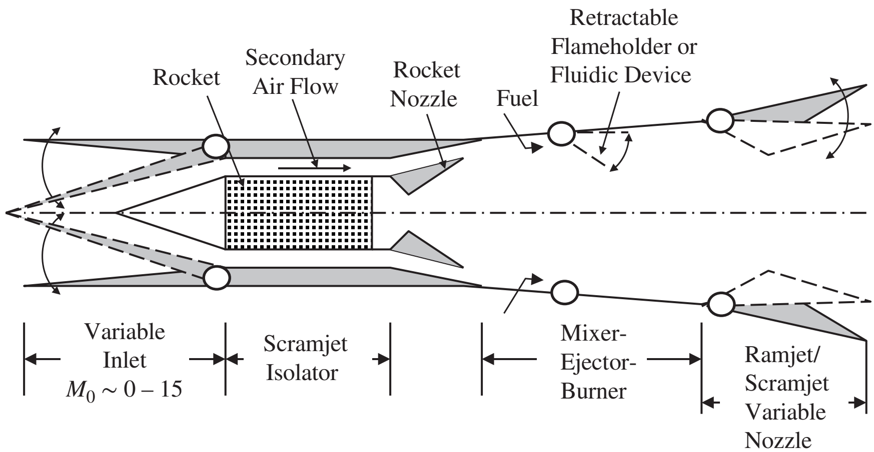

Figure 1.62 Concept in rocket-based-combined-cycle (RBCC) propulsion.

A rocket placed in a duct will draw air in and through mixing of the cold and hot gases will enhance its thrust level. This is the ejector principle. Since the propulsion is based on both the rocket and assisted by the secondary air mixing through an inlet, this may be referred to as an *air-breathing rocket*. The duct that follows the rocket nozzle is then the mixer-ejector, which may also serve as the combustor of a conventional or scramjet engine for combined operation. Now, we have clearly passed the air-breathing and rocket propulsion boundaries and entered into the realm of RBCC propulsion (see Figure 1.62). This is a promising approach to the future of hypersonic flight from takeoff to orbit. It clearly is an exciting time to be a propulsion engineer/researcher.

1.13 Summary

In this chapter, we reviewed air-breathing engine cycles and developed 1-D, steady solution methodology based on thermodynamics and conservation laws for their performance parameters. These were identified to be: specific thrust, specific fuel consumption, thermal, propulsive, and overall efficiencies. We had limited our approach to steady, one-dimensional flow and the "design-point" analysis. The gas was treated as perfect, but its properties were described in cold-hot-very-hot zones. Namely, the cold described inlet-fan-compressor, the hot described turbine and nozzle (if no afterburner was used), and the afterburner gas properties were used in the wet mode and in the nozzle. We included the effect of fluid viscosity and thermal conductivity in our cycle analysis empirically, i.e. through the introduction of component efficiency. The knowledge of component efficiency at different operating conditions is critical to their design and optimization. We always treated that knowledge, i.e. the component efficiency, as a "given" in our analysis, e.g. based on published data. RBCC propulsion system is introduced with the promise for hypersonic air-breathing propulsion.

We intentionally left the discussion of combustion-generated pollutants out of the current chapter, which is focused on cycle analysis. In three examples on separate-flow TF engine, mixed-flow TF engine, and a TP, we calculated cycle efficiencies, η_{th}, η_p, and η_o. All three examples revealed an inherent weakness in thermal efficiency of heat engines, or in our application, the Brayton cycle. The best thermal efficiency was about 50% and when combined with propulsive efficiency to produce the overall efficiency, we could only reach the peak overall efficiency of ~35%. This *inefficiency* to convert the thermal power in fuel–air combustion to thrust power in an aircraft is the *Achilles' heel* of the heat engines. We also learned that higher BPR, as well as higher OPR and TET, improve the cycle efficiency and reduce fuel burn. In addition to improved efficiency, higher TET reduces the core size; thus, engine weight is reduced. In the near-to-medium term (i.e. 2020–2035), these are the directions that the aircraft propulsion industry explores while developing practical hybrid and electric propulsion options for sustainable aviation. MacKay (2009) has addressed sustainable energy and energy conversion pathways/efficiencies, which is relevant to our discussion. David MacKay's book is on my highly recommended reading list.

Gordon and McBride (1996) address the composition of combustion gases in equilibrium reactions, which complement our discussions in primary combustor and afterburner. Archer and Saarlas 1998), Cumpsty (2003), Flack and Rycroft (2005), Hesse and Mumford (1964), Mattingly (1996), Mattingly et al. (2018), Oates (1988), Oates (1985), Oates (1989), Shepherd (1972), El-Sayed (2008), and Greitzer et al. (2004) are excellent aircraft propulsion textbooks and references that are recommended for further reading. On rocket propulsion and SSTO concepts, Sutton and Biblarz (2001), Varvill and Bond (2003), and Huzel and Huang (1992) may be consulted. Rolls-Royce (2015) and Pratt and Whitney (1980) have produced valuable reference manuals that are highly recommended (Anon. 2015, 1980).

References

Pratt & Whitney (1980). The Aircraft Gas Turbine Engine and Its Operation. Hartford, CT: Pratt & Whitney Aircraft Group/United Technologies.

Rolls-Royce (2015). The Jet Engine, 5e. New York: Wiley.

Anderson, J.D. (2003). Modern Compressible Flow, 3e. New York: McGraw-Hill & Co.

Archer, R.D. and Saarlas, M. (1998). An Introduction to Aerospace Propulsion. New York: Prentice Hall.

Asbury, S.C., and Yetter, J.A. 2000. Static performance of six innovative thrust reverser concepts for subsonic transport applications. Summary of the NASA Langley Innovative Thrust Reverser Test Program. NASA/TM-2000-210300, July.

Burrows, M.C. and Kurkov, A.P. (1973). Analytical and Experimental Study of Supersonic Combustion of Hydrogen in a Vitiated Airstream, *NASA TMX-2628*. Washington, D.C.

Cumpsty, N.A. (2003). Jet Propulsion: A Simple Guide to the Aerodynamic and Thermodynamic Design and Performance of Jet Engines, 2e. Cambridge, UK: Cambridge University Press.

Duong, L., McCune, M. and Dobek, L., 2009. US Patent 3, 0293278, December 2009.

El-Sayed, A. (2008). Aircraft Propulsion and Gas Turbine Engines. New York: CRC Press.

Farokhi, S. (2014). Aircraft Propulsion, 2e. Chichester, UK: Wiley.

Flack, R.D. and Rycroft, M.J. (2005). Fundamentals of Jet Propulsion with Applications. Cambridge, UK: Cambridge University Press.

Gordon, S. and McBride, S., “NASA Reference Publication 1311, Computer Program for Calculation of Complex Chemical Equilibrium Compositions and Applications, Vol. 1: Analysis,” October 1994 and “Vol. 2: User Manual and Program Description,” National Aeronautics and Space Administration, Washington, D.C, 1996.

Greitzer, E.M., Tan, C.S., and Graf, M.B. (2004). Internal Flow: Concepts and Applications. Cambridge, UK: Cambridge University Press.

Guynn, M.D., Berton, J.J., Tong, M.T., and Haller, W.J. August 2013. Advanced single-aisle transport propulsion design options revisited. AIAA Paper Number 2013-4330.

Hager, R.D. and Vrabel, D. 1988. Advanced Turboprop Project. NASA SP-495, Washington, DC.

Halliwell, I.2013. AIAA-IGTI Undergraduate Team Engine Design Competition Request for Proposal, 2010–2011. www.aiaa.org. Last accessed 24 November.

Heiser, H.W., Pratt, D.T., Daley, D.H., and Mehta, U.B. (1994). Hypersonic Airbreathing Propulsion. Reston, VA: AIAA, Inc.

Hesse, W.J. and Mumford, N.V.S. (1964). Jet Propulsion for Aerospace Applications, 2e. New York: Pittman Publishing Corporation.

Hill, P.G. and Peterson, C.R. (1992). Mechanics and Thermodynamics of Propulsion, 2e. Reading, MA: Addison-Wesley.

Huzel, D.K. and Huang, D.H. (1992). Design of Liquid Propellant Rocket Engines. Reston, VA: AIAA, Inc.

Kerrebrock, J.L. (1992). Gas Turbines and Aircraft Engines, 2e. Cambridge, Massachusetts: MIT Press.

Kurzke, J. (2017). A design and off-design performance program for gas turbines. *GasTurb* www.gasturb.de. Last accessed 19 December 2017.

Kurzke, J. and Halliwell, I. (2018). Propulsion and Power: An Exploration of Gas Turbine Performance Modelling. Cham, Switzerland: Springer International Publishing, AG.

Lotter, K. 1977. Aerodynamische Probleme der Integration von Triebwerk und Zelle beim Kampfflugzeugen. Proceedings of the 85th Wehrtechnischen Symposium, Mannheim, Germany.

MacKay, D.J.C. (2009). Sustainable Energy – Without the Hot Air. Cambridge (UK): UIT Cambridge Ltd.

Mattingly, J.D. (1996). Elements of Gas Turbine Propulsion. New York: McGraw-Hill.

Mattingly, J.D., Heiser, W.H., Pratt, D.T. et al. (2018). Aircraft Engine Design, 3e. Washington, DC: AIAA.

Oates, G.C. (ed.) (1985). Aerothermodynamics of Aircraft Engine Components. Washington, D.C.: AIAA Education Series.

Oates, G.C. (1988). Aerothermodynamics of Gas Turbine and Rocket Propulsion. Washington, DC: AIAA.

Oates, G.C. (ed.) (1989). Aircraft Propulsion Systems Technology and Design. Washington, D.C.: AIAA Education Series.

Shepherd, D.G. (1972). Aerospace Propulsion. New York: American Elsevier Publication.

Sutton, G.P. and Biblarz, O. (2001). Rocket Propulsion Elements, 7e. New York: Wiley.

Varvill, R. and Bond, A. (2003). A Comparison of Propulsion Concepts for SSTO Reusable Launchers. *Journal of British Interplanetary Society* 56: 108–117.

Vos, R. and Farokhi, S. (2015). Introduction to Transonic Aerodynamics. Heidelberg, Germany: Springer Dordrecht.